EUROPEAN COATINGS LITERATURE

VINCENTZ

Jochen Winkler

Titanium Dioxide

Jochen Winkler

Titanium Dioxide

Title: Sachtleben Chemie GmbH

Bibliografische Information Der Deutschen Bibliothek

Die Deutsche Bibliothek verzeichnet diese Publikation in der Deutschen Nationalbibliothek; detaillierte bibliografische Daten sind im Internet über http://dnb.ddb.de abrufbar.

Winkler, Jochen:
Titanium Dioxide
Hannover: Vincentz, 2003
(European Coatings Literature)
ISBN 3-87870-148-9

Vincentz Network, Postfach 6247, 30062 Hannover, Germany

Literature catalogue by:
Vincentz Network, Schiffgraben 43, 30175 Hannover, Germany
Tel.: +49 511 9910-033, Fax: +49 511 9910-029
e-Mail: books@coatings.de
http://www.coatings.de

Layout: Sperling Info Design GmbH, Gehrden, Germany
Print: Aalexx Druck, Großburgwedel, Germany
ISBN 3-87870-148-9

European Coatings Literature

Jochen Winkler

Titanium Dioxide

Acknowledgement

The German edition of this book appeared at the "European Coatings Show" in Nuremberg, Germany, in April 2003. Already at the exhibition, there were inquiries for an English version, which was a motivation not to take too long a time to translate the text into the English language. Simultaneously, this was taken as an occasion for a revision, so that literally in all the chapters, some changes – hopefully towards improvement - were made. References to relevant ASTM standards were added where appropriate, and literature citations were exchanged against English language sources where possible.

Originally, the idea for this book came from Mr. Lothar Vincentz, whom I would like to thank for that and for the trust he set in me as an author.

To begin with, I was a bit reluctant to consent, since a lot has been written and said about titanium dioxide. Furthermore, the internet furnishes a good deal of information dealing with titania upon a mouse click. Still, there is no newer treatise available that deals with the main properties, as well as colloid chemical aspects of using TiO_2 pigments, in a coherent fashion. This book is the manifestation of an effort to close this possible gap, at least partly.

Colleagues and coworkers have contributed to this book in different ways, be it by providing measurement protocols or figures, but also in conversations and technical discussions. Last but not least, partly also by mutual cooperation for years, whose results have found their way between these covers. Here, I would like to especially mention: Dr. Djamshid Amirzadeh-Asl, Gerd-Reiner Birnbaum, Dr. Ulrich Gesenhues, Bernd Hirthe, Andrea Holtbernd, Holger Jäger, Wolf Rüdiger Karl (†), Dr. Jürgen Kastner, Ilona Reinhard, Dr. Nicole Scotti, Ute Steinhaus and Martin Zilse.

I would like to especially highlight the contribution of Dr. Bernd Proft, who carried out the calculations of the Mie Theory and who provided figures in this context. At the same time, technical discussions concerning the topic "catalysis" and his proof reading of that chapter are gratefully acknowledged.

Likewise, my gratitude belongs to Mrs. Monika Heldt for typing the manuscript and for unburdening me from other, time consuming chores during the preparation of the book.

It was a special pleasure to have Dr. Ulrich Zorll as Editor and proof reader at my side. During some jointly spent years at the Paint Research Institute (Forschungsinstitut für Pigmente und Lacke) in Stuttgart, Germany, he was not only a paragon

with regard to his professionalism, but also a personal advisor at different occasions. Numerous valuable suggestions from him now entered this book.

The English version was also looked over by Gisela Gehrenkemper and by Peter Gribble and the manuscript was put into press by Birgit Seesing and Annegret Sperling. I am pleased to express my gratitude for the uncomplicated and professional assistance I got from all of them.

I would also like to thank the President of Sachtleben, Dr. Wolf-Dieter Griebler, for his support and his interest in the making of this book.

Finally, I would like to thank you as a reader for your interest and would be grateful to hear criticism and suggestions for improvement for a possible future edition of the book.

Successful Coatings

European Coatings Literature

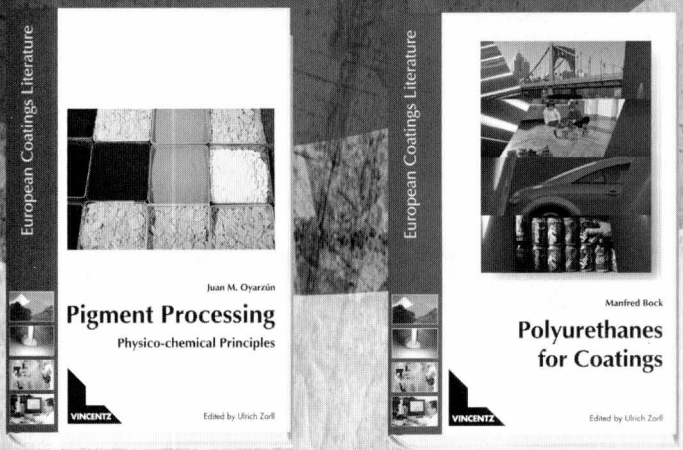

Pigment Processing
Physico-chemical Principles

This monograph is a practice-related exposition of the fundamental principles of pigment processing and a combination of the most important principles in a precise and comprehensive way. It offers the pigment technologist the possibility of informing himself adequately on the current state of the physico-chemical principles of pigment application technology without having to work through piles of the relevant magazines.

Juan M. Oyarzún, 2000, 236 pages,
hardcover, 69,– €
order no. 15127

Polyurethanes for Coatings

Polyurethanes are of great significance in a large number of industrial applications. These include adhesives, elastomers and foams, as well as raw materials for coatings which are the subject of this book. It starts by exploring the principles of polyurethane chemistry. This enables the reader to understand the current significance of the many applications and special developments and their future perspectives.

Manfred Bock, 2001, 232 pages,
hardcover, 69,– €
order no. 15317

Also published:

Waterbased Acrylates for Decorative Coatings – Schwartz / Baumstark
2001, 284 pages, hardcover, 69,– €
order no. 15130

Special Effect Pigments – Roman Maisch et al.
1998, 152 pages, hardcover, 69,– €
order no. 15335

Light Stabilizers for Paints – Andreas Valet
1997, 144 pages, hardcover, 69,– €
order no. 15392

Kontakt:
Vincentz Network
P.O. Box 62 47 · 30062 Hannover · Germany
Tel. +49 511 9910-025 · Fax +49 511 9910-029
books@coatings.de · www.coatings.de

VINCENTZ

Successful Coatings

Coatings Compendia

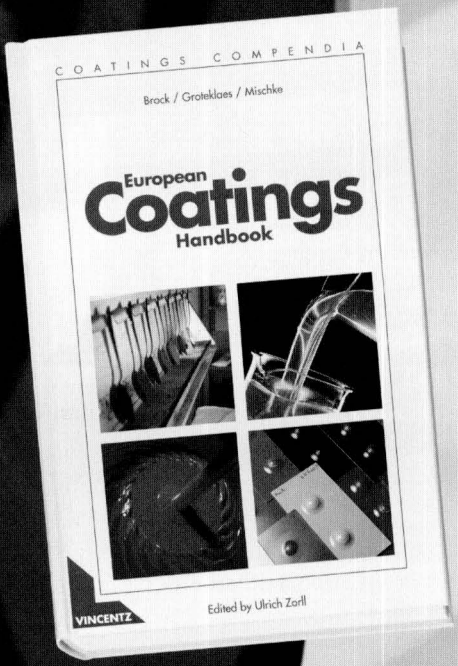

European Coatings Handbook – Brock • Groteklaes • Mischke

The reader will find not only a conventional account of how coatings are formed from their components (resins, pigments, fillers, solvents, additives), including the many different ways in which these interrelate, but also recent thinking on ecologically acceptable formulations using high-solids, water-based and powder coatings. Keeping abreast of the times, it also goes into methods of manufacture, application technology, quality testing and, not least, protection of the environment and safety in the workplace.
From this state of the art foundation it deals with all the central aspects of coatings manufacture and processing practice. This makes it equally useful to the reader whether for private study or as background reading to complement a formal course of instruction. The handbook will also help specialist practitioners wishing to update their knowledge.

2000,
410 pages,
hardcover,
98,- €,
order no. 15273

Kontakt:
Vincentz Network
P.O. Box 62 47 · 30062 Hannover · Germany
Tel. +49 511 9910-025 · Fax +49 511 9910-029
books@coatings.de · www.coatings.de

VINCENTZ

Contents

1 Introduction

Titanium dioxide pigments make up about 60 % of the global pigment production. In the year 2002, approximately 4.6 Million tons of production capacity were available. The annual increase of titanium dioxide pigment production averaged at about 2 to 5 % in the past. This growth rate is expected for the future as well. Whereas only twenty years ago, sulfuric acid was considered to be the indicator for economic growth, today this position is held by titanium dioxide.
Nonetheless, titanium dioxide is a fairly new industrial product that gained importance only after the second world war. Because of its high refractive index, it took the place of Lithopone, a co-precipitated product consisting of zinc sulfide and barium sulfate, as the standard white pigment.

This development was, however, not predetermined. Apart from having a high refractive index, it also has an undesirable property: titanium dioxide is a photo-semiconductor. It absorbs ultraviolet sunlight and transfers the energy of the absorbed photons into electrochemical reactions that lead to the disintegration of the medium in which it is embedded. The quest to overcome this problem led to the development of new technologies of pigment lattice doping and inorganic treatments of titanium dioxide surfaces. These techniques are today gradually utilized and refined in the context of problems concerning the production of other pigments, but also in heterogeneous catalyst development.

New developments make use of the particle size dependency of light scattering of titania to produce "transparent" titanium dioxide products. Nano-scaled TiO_2 particles scatter visible light far less than TiO_2 pigments, yet still have the intrinsic property of UV-light absorption. Today already, it is hardly possible to find a sun screen lotion with a high light protection factor that doesn't contain nano-scaled titania. Contrarily, the use of titania nanoparticles as a photocatalyst to avoid contamination by dirt or bacteria is still in an early stage.

For the practitioner, this book is conceived as a source of information on the properties and use of titanium dioxide pigments. At the same time, the current state of the development and use of nano-scaled titanias as UV-absorbers and effect pigments is outlined.

Whereas this can only be a momentary picture, the same is especially true for the last two chapters of this book that deal with the utilization of catalytic properties of TiO_2 as well as its use in photovoltaic cells. Since these topics may become important aspects in the near future, though, it was decided to include them in spite of the lack of resolved knowledge and established uses.

2 Physical, chemical and toxicological properties of titanium dioxide

2.1 Physical properties

Titanium dioxide exists in three modifications with different crystal lattice structures and therefore altering physical properties. These are rutile, anatase and brookite.

Stability

Rutile is thermodynamically the most stabile form. For that reason, anatase and brookite rearrange at elevated temperatures of 750 °C (brookite) or 915 °C (anatase), respectively, monotropically to rutile. This modification is stabile all the way up to its melting point at approximately 1830 °C to 1850 °C. The rearrangement from anatase to rutile is accompanied by a heat generation of 12.6 kJ/mol.

In all three crystal modifications, the titanium atoms are surrounded octahedrally in a distorted fashion by six oxygen atoms. The octahedra differ however in rutile, anatase and brookite with respect to their spacing relative to each other.

Of technical importance are only rutile and anatase, that differ from each other in some of their physical properties.

Crystal structure

One possibility to describe their crystal structures [1] is to start off with the placing of the oxygen atoms.

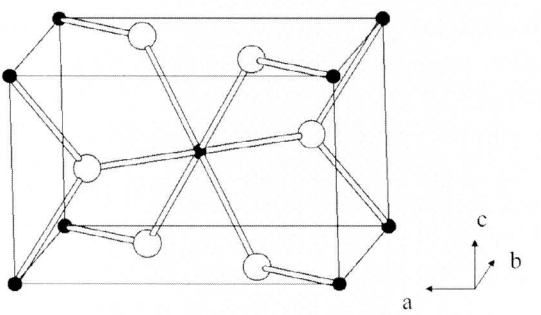

Fig. 2.1
Elementary cell of rutile; black spheres: titanium atoms; white spheres: oxygen atoms

rutile: hexagonal close packing of the oxygen atoms, in which half of the octahedral spaces are filled with titanium atoms.

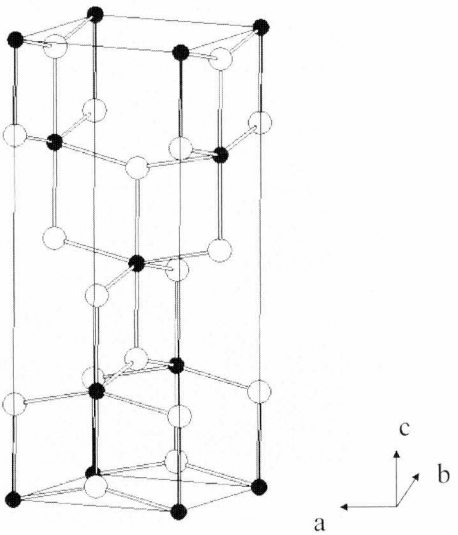

Fig. 2.2
Elementary cell of anatase; black spheres: titanium atoms; white spheres: oxygen atoms

anatase: cubic close packing of the oxygen atoms, in which half of the tetrahedral spaces are filled with titanium atoms.

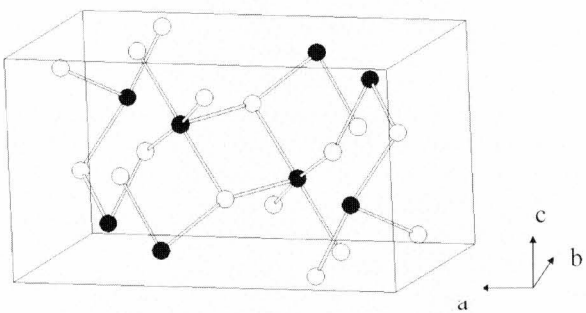

Fig. 2.3
Elementary cell of brookite; black spheres: titanium atoms; white spheres: oxygen atoms

Figures 2.1, 2.2 and 2.3 compare the elementary cells of rutile, anatase and brookite. The crystal structure is developed by extending one elementary cell by others in the front, back, left, right and above as well as below. When doing this, one will recognize that, in the case of rutile, the octahedra, which belong to the titanium atom in the center of the cell, form a chain of octahedra connected via two of their edges. These chains develop in the c-direction of the elementary cell.

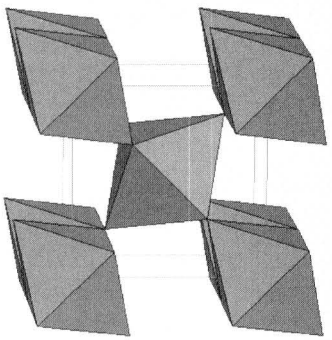

Fig. 2.4
Structure of rutile

Figure 2.4 shows a part of the crystal lattice of rutile as an arrangement of octahedra, viewed in the c-direction. On the outsides, the described rows of octahedra (two octahedra in this case) can be seen. The chain of octahedra in the middle connects the outer octahedra chains via mutually shared corners. The chain of octahedra in the middle is displaced by the length c/2 relative to the outer chains.

For anatase, the same procedure leads to a crystal lattice segment as shown in figure 2.5. In this case, the viewing direction runs along the b-axis of the elementary cell. It is seen that the octahedra of one layer are connected via four corners with each other. To the bottom and the top, every octahedra shares two edges with its neighbors. Finally, figure 2.6 demonstrates the circumstances for brookite.

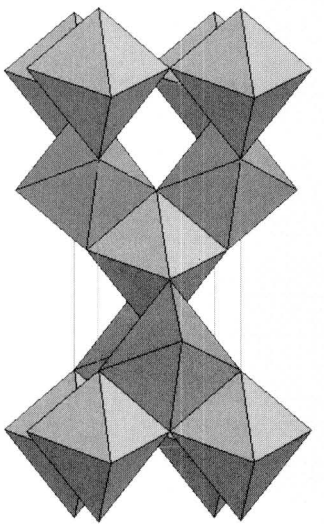

Fig. 2.5
Structure of anatase

Table 2.1 compares the crystallographic data of rutile, anatase and brookite as well as their Moh's hardness and densities.

Hardness

Compared with rutile, anatase has a lower Moh's hardness of 5.5 to 6 instead of 6.5 to 7. For that reason, anatase is predominantly used where the lower hardness leads to a technical advantage. This is especially the case in the textile industry, where anatase pigments are used for the

matting of synthetic fibers. But also in plastics, where weather stability may not be so important in all cases, anatase is used because of its lower level of wear on machinery; just as in the paper industry, where mostly the softer anatase is used as a white pigment, because it is abrasiveness easier on cutting tools. A further reason lies in its UV-absorption at lower wave-lengths than rutile – see below –, since optical fluorescence brighteners, that change UV-light into visible blue radia-tion, are often used in paper. Rutile absorbs the UV-light necessary for that to occur.

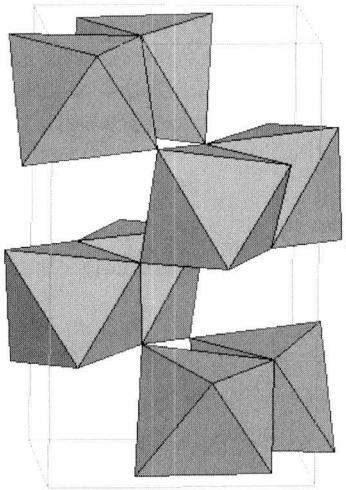

Fig. 2.6
Structure of brookite

Refractive indices

The high refractive index of titanium dioxide, in combination with a lack of absorption in the visible range of the spectrum between 380 nm and 700 nm wavelength, is the reason for its usefulness as a white pigment.

	Rutile	**Anatase**	**Brookite**
Chemical formula	TiO_2	TiO_2	TiO_2
Crystal system	tetragonal	tetragonal	orthorhombic
Point group according to Schönflies	D_{4h}	D_{4h}	D_{2h}
Point group according to Hermann-Mauguin	4 mmm	4 mmm	mmm
a (nm)	0.4594	0.3785	0.9184
b (nm)	0.4594	0.3785	0.5447
c (nm)	0.2958	0.9514	0.5245
Volume of the elementary cell (nm^3)	62.07	136.25	257.38
Molar volume (cm^3/mol)	18.693	20.156	19.377
Moh's hardness	6.5 - 7	5.5 - 6	5.5 - 6
Density (g/cm^3)	4.2 - 4.3	3.8 - 3.9	3.9 - 4.1
Melting point (°C)	1830 - 1850	transformation to rutile	transformation to rutile

Table 2.1
Crystallographic and physical properties of rutile, anatase and brookite

Both rutile and anatase form birefringent crystals, in which the refractive indices of the ordinary (n_o) and extraordinary (n_e) rays are wavelength-dependent. As

shown in figure 2.7 (values from [2]) the refractive indices rise in the direction towards the absorption edges. This is a completely normal behavior for a dielectric substance like titania (termed: " optical dispersion"). Whereas in rutile the extraordinary ray possesses higher refractive index values, the opposite is true for anatase. Rutile is called a "positive crystal" ($n_o < n_e$) and anatase a "negative crystal" ($n_o > n_e$). In the case of anatase, the refractive indices of both rays differ less than in rutile.

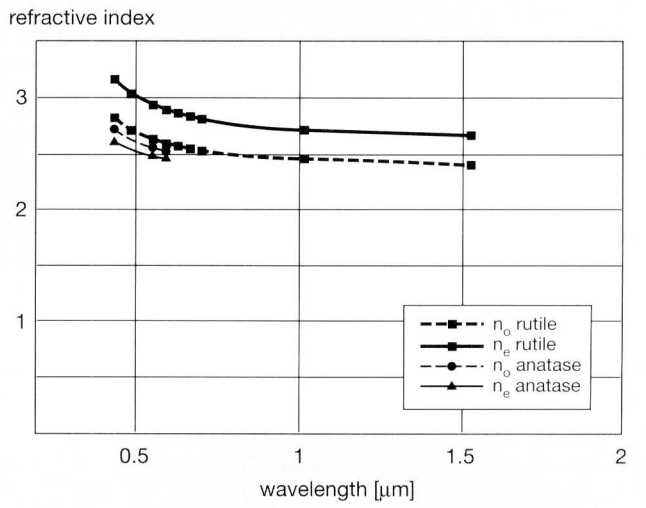

Fig. 2.7
Wavelength dependency of the refractive indices for the ordinary and extraordinary rays of rutile and anatase

Since titania pigments consist of submicroscopic particles of mean particle sizes between 0.2 µm and 0.3 µm, it doesn't make sense to distinguish between the refractive indices of the ordinary and extraordinary rays. Normally, a mean value of both refractive indices is therefore assigned to every wavelength. In practice, it has become customary to use one value for the whole visible range of the spectrum, taking 2.7 as the refractive index of rutile and 2.55 as that of anatase, respectively.

Polarisibility

The high refractive index is a consequence of the easy polarisibility of the binding electrons in the crystal lattice. These are mainly assorted around the oxygen atoms in the crystal. With the Lorenz-Lorentz equation:

$$a = \frac{3}{4\pi} \cdot \frac{M}{N_L \rho} \cdot \frac{n^2 - 1}{n^2 + 2} \qquad (2.1)$$

n = refractive index (rutile: 2.7)
M = molecular weight (titanium dioxide 79.9 x 10^{-3} kg/mol)
ρ = density (rutile: 4.2 x 10^3 kg/m^3)
N_L = Avogrado's number (6.0221367 x 10^{23} mol^{-1})

the polarisibility of rutile is calculated as being 0.51 x 10^{-23} m^3. This is five to six orders of magnitude higher than for common organic molecules [3].

Absorption spectra

There are characteristic differences in the UV-Vis spectra of rutile and anatase (see figure 2.8). To begin with, figure 2.8 shows the appreciable difference in the absorption of the two modifications in the near UV part of the spectrum. By

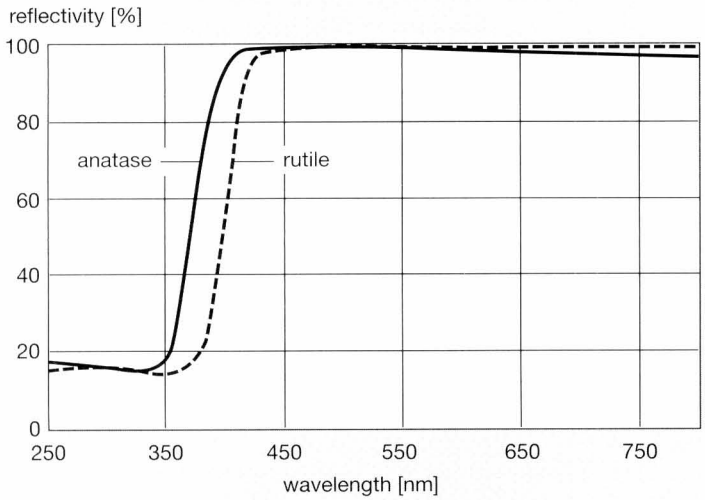

Fig. 2.8
UV-Vis spectra of pressed powder tablets of rutile and anatase

differentiation of the reflectance curves, their inflection points are found, that depict the exact location of the absorption bands. They lay at wavelengths of λ = 397 nm (rutile) or 377 nm (anatase), respectively.

With the equation

$$E = h \frac{c}{\lambda} \qquad (2.2)$$

h = Planck's constant (6.626×10^{-34} J s)
c = speed of light (2.99793×10^{8} m s^{-1})

the energies E of these absorption processes can be calculated: they are 50×10^{-20} Joule for rutile and 52.7×10^{-20} Joule for anatase.

These energies are often cited in the dimension electron Volt (1 eV = 1.602×10^{-19} J). A conversion from Joules to eV yields a "bandgap" of 3.127 eV for rutile and 3.289 eV for anatase[1]. The expression "bandgap" comes from the "energy band model" of chemical bonds [4].

Photoactivity

Due to light absorption in the near UV, electrons are hoisted from the energy level of the valency band of TiO_2 into that of the conductive band, thus leaving a positively charged hole in the valency band. The separated electron/hole pair is called "exciton". The generation of excitons is the cause for the light induced semiconductor properties of TiO_2. The photoactivity of titania is generally disliked, since the excitons can have an oxidizing influence on its surroundings (see chapter 5) and, for example, destroy a polymer matrix in which it is imbedded. Therefore, the titanium dioxide pigment industry goes through some efforts to diminish the photoactivity. On the other hand, this property is utilized purposefully in titania photocatalysts (see chapter 8.3).

Blue tint

The remission of anatase, taking place in the barely visible part of the spectrum (above 385 nm), leads to a slightly bluer appearance of an anatase in comparison to a rutile of comparable purity.

For enhancing the blue tint, other metals with higher oxidation states (e.g. Sb^{5+}, Mo^{6+}, W^{6+} or Ta^{5+}) can be added as dopants to the calcination step. They supposedly act in the way that they reduce some of the Ti^{4+} to Ti^{3+}, which is blue in color.

Reflectivity

Figure 2.8 also shows that anatase has a slightly lower remission in the red part of the visible spectrum than rutile.

Figure 2.9 exhibits the reflectance of anatase and rutile in the near infrared (NIR) from 700 nm to 2500 nm in addition to the UV-Vis region. In the NIR region, the

1 Often, a bandgap of 3.03 eV for rutile and 3.15 eV for anatase is reported. The corresponding absorption wavelengths are 415 nm and 385 nm, respectively. These wavelengths can be found by extrapolating the two "linear" parts of the remission curves to the left and right of the inflection point of the spectrum, where absorption takes place. Their crossing points yield these wavelengths.

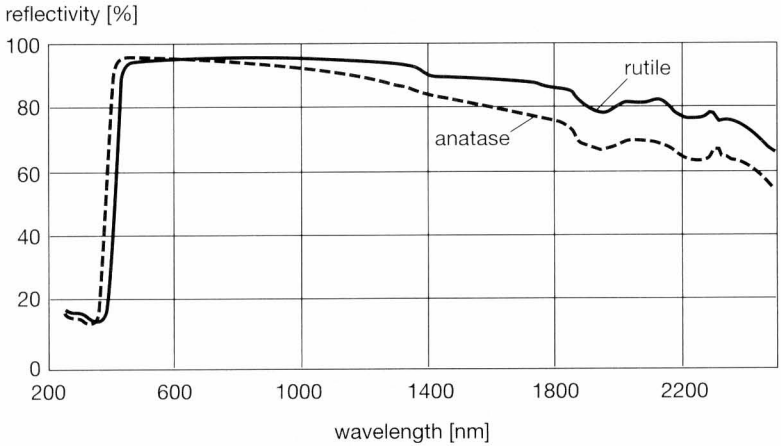

Fig. 2.9
UV-Vis/NIR spectra of pressed powder tablets of rutile and anatase

slightly enhanced absorption of anatase in comparison to rutile remains. Rutile itself starts to absorb at wavelengths exceeding 1300 nm. Neither of them, not anatase, nor rutile, have characteristic absorption bands in their NIR spectra.

The further course of the reflectance spectra of anatase and rutile in the wavelength region between 2.5 µm and 25 µm (Infrared, IR) is presented in figure 2.10. At 5 µm (corresponding to a wave number of 2000 cm^{-1}), approximately 27 per cent of the light is reflected. The next light absorption of approximately 100 per cent (equivalent to approximately 0 % reflection) is found at 10.75 µm (930 cm^{-1}) or 11.1 µm (900 cm^{-1}) for anatase and rutile, respectively. Following the reflectance curves to higher wavelengths from there on, both anatase and rutile again have higher reflectivities until wavelengths of approximately 20 µm.

Other properties

Rutile and anatase are clearly distinguished by their x-ray diffraction spectra. This is seen in figures 2.11 (rutile) and 2.12 (anatase), that show the diffraction signals up to 2-theta values of 70°. Table 2.2 offers detailed information on the location and the relative intensities of the x-ray diffraction signals based on the main peak (equivalent to 100 % intensity).

Titanium dioxide is basically an isolator. The dielectric constants of titanias are relatively high with values near 100. Dielectric properties found by measurements on titania powders are, however, not relevant for practical purposes.

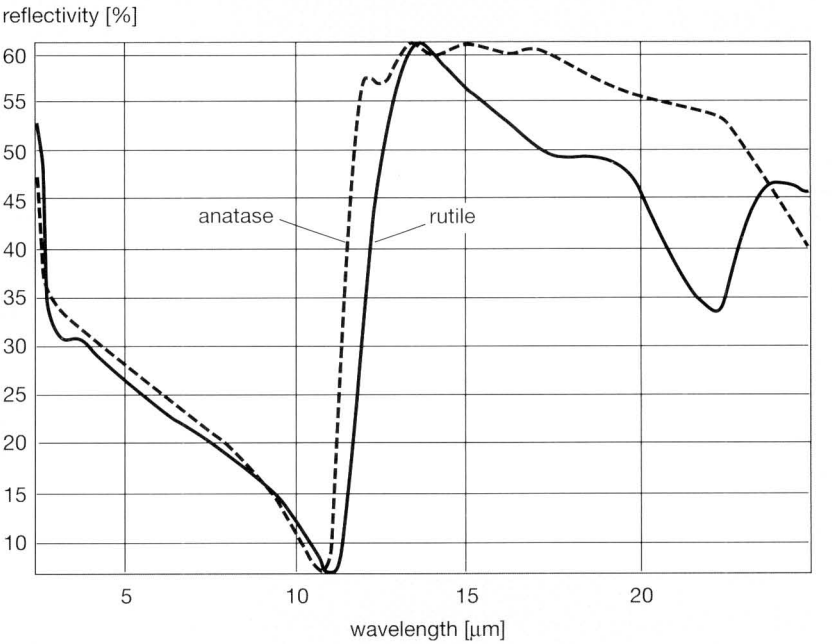

Fig. 2.10
IR-spectra of pressed powder tablets of rutile and anatase

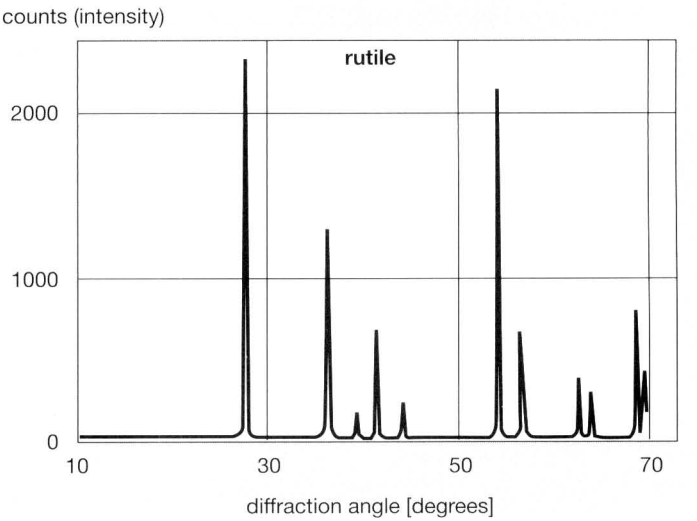

Fig. 2.11
X-ray diffraction spectrum of rutile

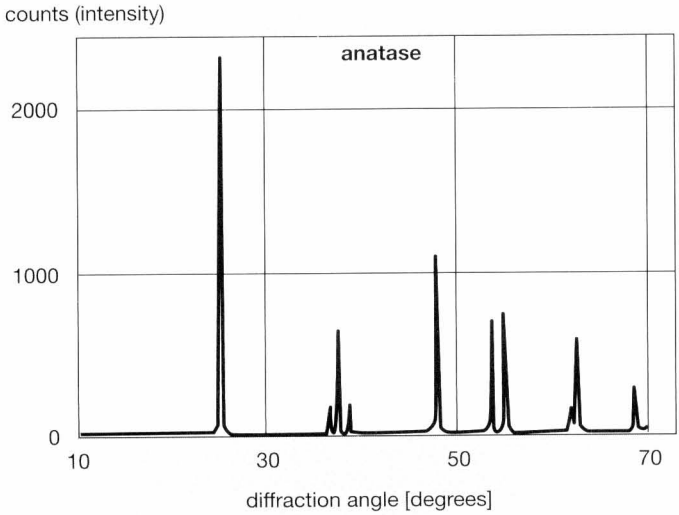

Fig. 2.12
X-ray diffraction spectrum of anatase

The heat capacity of TiO_2 is 0.69 J/g K. Titanium dioxide is weakly paramagnetic. This allows its separation from ferromagnetic ilmenite in a benefication process.

Titanium dioxide is thermally relatively stabile, although it easily releases small amounts of oxygen. At 100 °C, for example, this causes a slight gray color – due

Anatase		Rutile	
2-Theta (degrees)	**Rel. Intensity (%)**	**2-Theta (degrees)**	**Rel. Intensity (%)**
25.289	100	27.436	100
36.949	10	36.087	50
37.791	20	39.183	8
38.566	10	41.226	25
48.052	35	44.048	10
53.902	20	54.313	60
55.065	20	56.651	20
62.109	4	62.739	10
62.688	14	64.030	10
68.770	6	65.485	2
70.317	6	69.005	20
74.024	2	69.791	12
		72.413	2
		74.403	1

Table 2.2
Location and relative intensities of the 2-theta peaks of the X-ray diffraction spectra of rutile and anatase

to the generation of Ti^{3+} – which is however reversible. At 400 °C, titanium dioxide appears yellow, caused by the expansion of the crystal lattice. This is reversible as well. The melting point of rutile lies between 1830 °C and 1850 °C, as stated earlier.

2.2 Chemical properties of TiO_2

Titanium itself is a relatively unnoble metal which – similar to aluminum – is only stable in the atmosphere because of an oxide passivation layer. It has a pronounced tendency to form oxides, which are very stable. The far most preferred oxidation state is that of Ti^{4+}. Expectedly, titanium dioxide is chemically hardly reactive.

Solubility

Titanium dioxide is insoluble in water. Calcinated titania, especially in the rutile modification, is insoluble or only moderately soluble even in hot, concentrated acids. In acidic or basic melts, however, even rutile is dissolved.

Reduction reactions

Small amounts of oxygen are easily withdrawn from titanium dioxide. In that case, Ti^{3+} is generated, that leads to a grayish color of titania due to the fact that Ti^{3+} within the TiO_2 lattice is dark blue, almost black. This reduction on the surface is, however, reversible. Even the oxygen in the air suffices to recover Ti^{4+}, which is not colored. When illuminated with UV-light in the presence of reducing agents such as mandelic acid, glycerine or $SnCl_2$, yet in absence of oxygen, TiO_2 also obtains a blueish-gray color. Differences in their tendency to become gray under these conditions act as an indicator for the photostability of different samples. With glycerine, the reduction reaction leads to the formation of Ti_2O_3. Especially anatase pigments of lower purity exhibit some graying, even in the absence of reducing agents, when subjected to intensive illumination. This reversible behavior is known as "phototropy".

Yet, even under strongly reducing conditions, titania is not transformed into titanium metal. In the presence of nitrogen, carbon, halogen or sulfur, titanium nitride, titanium carbide, titanium halide and titanium sulfide are formed.

The reaction behavior against chlorine is utilized in the chloride process of titanium dioxide production, in which the titanium in the ore is transferred into $TiCl_4$. In iron production, ilmenite and other titanium bearing synthetic products help to extend the lifetime of blast furnaces. The titanium carbides and nitrides that are generated condense on the heat insulating refractory bricks inside the furnaces, thus regenerating them [5, 6].

Even the reaction with hydrogen under dramatic conditions (100 bar, 2000 °C) only leads to TiO in the oxidation state of Ti^{2+}. Only when TiO_2 is annealed in the presence of elementary silicium, calcium or magnesium, is titanium metal formed, along with the corresponding oxides of silicium, calcium or magnesium.

The reaction with magnesium is technically used for the production of titanium metal, whereby the starting titanium chemical is $TiCl_4$, though [7]. The reaction that is carried out under inert gas leads to a sponge of metallic titanium, along with $MgCl_2$, which is leached with hydrochloric acid. The titanium sponge is sintered to the final compact metal in an electric arc furnace.

Titanium metal is appreciated either by itself or as an alloy component for its low density (4.5 g m^{-3}) and its good mechanical properties (hardness, flexibility, heat fastness). Because of its high price, however, it is used reluctantly in many potential applications. Today, the main area of use are in ship building and airplane construction, in mechanical and chemical engineering (e.g. for chemically resistant heat exchangers) and other applications, such as for frames for glasses etc. Owing to its favorable biocompatibility, titanium metal is used as an implant material in medicine and dentistry. Of late, it is also increasingly used for the production of jewelry, namely for its grayish, matt gloss.

Reaction with peroxides

With hydroperoxide, the yellow colored structure unit – TiOOH is easily formed even at room temperature. When hydroperoxides come into contact with titanium dioxide pigments, this leads only to a slightly yellowish color due to the low specific area and the lightening effect of the pigment itself. Pigments that carry no inorganic surface treatment have approximately 5.6 (rutile) to 8 (anatase) OH-groups per nm^2 [8,9] that are capable of reacting with peroxide. With solid meta titanic acid [$TiO(OH)_2$], though, an intensively yellow colored product is formed, due to the high specific surface area of commonly more than 150 m^2/g.

Next to photo-oxidation reactions, in which the titanium dioxide itself is unchanged, the reaction with hydroperoxides is the only chemical reaction that plays a role in the application of TiO_2 pigments. Needless to say, the yellowing is normally disliked.

2.3 Toxicological properties of titanium dioxide

Table 2.3 lists the most important identification numbers, labels and legislative requirements for titanium dioxide pigments and UV-absorbers.

Material data sheet[1]	
Labels	
IUPAC Label	Titanium dioxide
Chemical Abstracts Name	Titanium dioxide
Chemical formula	TiO_2
Molecular weight	79,9
Registration numbers	
Chemical Abstracts Services register numbers	
Titanium dioxide	13463-67-7
Anatase titanium dioxide	1317-70-0
Rutile titanium dioxide	1317-80-2
Color Index Label	CI 77891; Pigment White 6
National Cancer Institute Number	NCI-15204
EINECS (European Inventory of Existing Chemical Substances)	236-675-5
Dye Code	E 171
TSCA (Toxic Substances Control Act; EPA Inventory)	13463-67-7
AICS (Australian Inventory of Chemical Substances)	13463-67-7
DSL (Canadian Domestic Substances List)	13463-67-7
ENCS (Existing and New Chemical Substances; Kashin Act of Korea)	KE 30681
PICCS (Philippinian Inventory of Commercial Chemical Substances)	522.5600
BAGT (Poison list of the "Bundesamt für Abfall und Gesundheitswesen" of Switzerland)	G 2950 gkf
MITI (Ministry of International Trade and Industry – Japan)	1-588
Registration Requirements	
BgVV (Bundesinstitut für gesundheitlichen Verbraucherschutz und Veterinärmedizin)	Limits according to IX are typically met.
EN 71/3; Safety of toys; leachable elements	No limits for titanium or other elements customarily used (e.g. in surface treatments)
AP 89/1; AP 96 (5) (EU-resolution about surface coatings intended to come into contact with food)	Listed in Ref.-Nr. 93440
TabakVO (Verordnung über Tabakerzeugnisse)	Permitted in the form of E 171 (dye code)
95/45/EC (Commission Directive on purity criteria for foodstuff colorants)	Permitted in the form of E 171 (dye code)
Verordnung über Tabakerzeugnisse (from 12.20.77; Directive concerning tobacco)	Permitted in the form of E 171 (dye code)
Arzneimittelfarbstoffverordnung (from 08.25.82) (Directive on colorants for pharmaceuticals)	Permitted in the form of E 171 (dye code)
XV Gefährliche Stoffe, Rechtsakt mit Bezug auf 67/548/EWG (Dangerous Substances)	No dangerous substance

Table 2.3
Identification numbers, labels and legislative approvements
(to be continued on following page)

XV Gefährliche Stoffe, Rechtsakt mit Bezug auf 67/548/EWG (Dangerous Substances)	No dangerous substance
1999/10/EC (Commission Directive on eco-label paints and varnishes)	Permitted
1999/178/EC (Commission Decision on eco-label textile products)	Permitted
76/768/EEC (The Cosmetics Directive)	Permitted
82/578/EWG (List of simulants used for testing the migration of elements from plastics in direct contact with food)	Inert against liquid simulants
95/3/EC (Amendment of 90/128/EWG; Plastics materials and articles intended to come into contact with foodstuffs)	Permitted
96/13/EC (Commission Decision establishing the ecological criteria for the award of the Community eco-label to indoor paints and varnishes)	Permitted
CEPE (First Supplement to Synoptic 7: Aufgelegt 15.05.1994. Materialien für Lebensmittelkontakt)	Listed under Ref.-No. 93440
2002/34/EC (26th directive adapting to technical progress, Annexes II, III and VII to Council Directive 76/768/EEC on the approximation of the laws of the Member States relating to cosmetic products)	Titanium dioxide as UV-absorber permissible up to 25 weight percent
Liste östrogenähnlicher Stoffe (List of estrogen-similar substances)	Not listed
Registration requirements in the USA	
FDA (Food and Drug Administration)	Listed in § 178.3297
CONEG (Coalition of the North-Eastern Governers)	Limits are typically met.
Clean Air Act Amendments 1990 (Controlled Ozone Depleting Substances; USA)	Not harmful to ozone layer
HAPS (Hazardous Air Pollutants; USA)	No pollutant.
Labeling	
GefStoffV (List of dangerous substances; Germany)	TiO_2 (rutile and anatase) are not dangerous substances according to German or European law and are therefore free from labeling.
Ecological notes	
WGK (Hazards for water)	Not hazardous to water according to appendix 1 VwVwS
Waste disposal	
EWC (European waste catalogue)	EWC 06 04 01, Metal oxide

[1] Largely identical to material data sheets on rutile and anatase from Sachtleben, compiled by P. Wetzig.

Table 2.3
Identification numbers, labels and legislative requirements

2.3.1 Oral intake

Long-termed feeding of rats and mice with up to 5 weight percent of titanium dioxide in the feed resulted in no detrimental effects [10]. Nano-sized titanium dioxide with a mean particle size of 30 nm was administered in a dose of 10,000

mg/kg body weight. This amount caused no health reactions [11]. The LD_{50} value (rats) for titanium dioxide lies above 10 g/kg.

Titania pigments are used in tablets, tooth pastes and also for the coloring of food. In the investigation of inflamed tissue in the region of the bowel ("Crohn's Disease"), titanium dioxide particles were found inter alia [12]. If these particles actually cause the disease, however, is judged differently. On the one hand, such granuloma[2] are only found in 35 % to 60 % of the cases [13]. On the other hand, there seems to be no connection between the degree of exposure and the probability for the illness [14].

2.3.2 Parenteral uptake

An uptake directly into the tissue, avoiding the gastro-intestinal system, is called "parenteral".

Intraperitoneal (going into the peritoneum) injections of titanium dioxide suspensions were detained by guinea pigs for a longer period of time, yet no changes were observed in the tissue [15]. Likewise, intraperitonael injections of up to 25 mg of TiO_2 resulted in no indications for the generation of tumors, whether in the area of the administration, nor in other places [16].

Weekly intratracheal (going into the trachea) administration of up to 3 mg of TiO_2 on hamsters over a period of 15 weeks again led to no tumors. Two cases of tracheal papilloma (papilloma = benign tumor – as a wart – due to overgrowth of epithelial tissue on papilla of vascular connective tissue – as of the skin) occurred in the unexposed population [17].

2.3.3 Percutaneous uptake

Percutaneous means "through the skin". Titanium dioxide pigments with particle sizes of 0.3 µm have been used in cosmetic preparations that are applied to the skin for a long time. Since about 1990, very fine particle sized titanias also find use, mainly as UV-absorbers in sun screens (see chapter 7.3).

Titanium dioxide caused neither inflammatory or sensitizing reactions of the skin, nor was its uptake by the skin found [18]. For "transparent" (i.e. very fine) titanias in particular, investigations of the permeation behavior through human cadaver skin, dissected human cadaver skin and mouse skin displayed only negligible

2 A special form of chronic inflammation. It is formed most often when either a foreign body or persistent microorganism, such as the tubercle bacillus, evades destruction by the unmodified chronic inflammatory response of the body. In its most classical form, a granuloma consists of concentric layers of cells that, together, form a distinctive lesion.

permeation, regardless of the pH-value of the TiO_2-suspension [19]. The dermal LD_{50} value (rabbit) lies at values[3] exceeding 10 g/kg.

2.3.4 Hypodermic injection

Forty rats received a single injection of 30 mg of titanium dioxides of different purities. After their natural death, none of the animals showed any signs of tumor development in places where the titanias were injected [20].

2.3.5 Inhalation

In animal experiments, the reaction upon the pulmonary uptake of TiO_2 dust depends largely upon the ability of the animals to clear their respiratory tract by natural means. There is decisive evidence that smaller particles in suspended dusts are generally more harmful to the health than coarser particles [21]. This seems also to apply to TiO_2, whereby titanium dioxide does not lead to inflammations by specific chemical interactions. Thus, 250 mg TiO_2 per m^3 of air cause a similar tumor occurrence as 1 mg SiO_2 per m^3 [23][4] .

TiO_2 dust

Rats were subjected to titanium dioxide dust over a period of two years, five days per week and six hours per day. At exposures of 10 mg/m^3 and 50 mg/m^3, no health effects were encountered. Only a dust concentration of 250 mg/m^3 led to an increase in tumors [25].

Nano-titanium dioxide

In a further investigation dealing especially with nano-scaled titanium dioxide, rats, mice and hamsters were exposed to dust eighteen hours per day for five days a week over a period of two years. TiO_2 dust concentrations were 7.5 mg/m^3 to 15 mg/m^3 [26]. Six months after termination of the exposure, the animals were sacrificed in order to access the results of this treatment. Whereas no tumors were generated in the mouse and hamster populations, the rats showed a statistically significant increase. The comparatively elevated susceptibility of rats for tumors is attributed to their longer snout, which makes it more difficult for them to free their respiratory system from inhaled dust. The authors concluded that titanium dioxide probably has no genotoxicity (poisonous effect on the genome in the cells) [26].

3 Nevertheless, one should avoid contact of the skin when working with titanium dioxide pigments, since they are difficult to rinse off, because of their tendency to dehumidify the skin upon lengthy exposures, and since organic surface treatments may be present.

4 Titanium dioxide is therefore often used as an inert comparative substance in animal experiments dealing with inhalation toxicity.

Occupational safety and health

In the area of human toxicology, there presently exists only one epidemiological study, in which 2477 workers, who were exposed to titanium dioxide pigments at their working place, were included [27]. No indications of health hazards with respect to lung cancer, chronicle respiratory passage affections, pleural diseases or fibrosis of the lungs (fibrosis = propagation of connective tissue growth) were found.

Still, for the purpose of a precautionary occupational safety, the limits for exposures to inorganic fine particle dusts were decreased in the past. In 1989, for example, their maximum allowable concentrations laid between 5 mg/m^3 and 20 mg/m^3 in the most important industrial nations, with a mean value of 9.5 mg/m^3 [28].

At the moment, the German "TRGS 900" (Technische Regeln für Gefahrstoffe) sets limit values that depend upon the particle size. It distinguishes between "respiratory dust" and "alveole active" dust. In the latter, particles having aerodynamic particle sizes between 0 and 10 µm are present. The maximum workplace concentration for respiratory dust lies at 10 mg/m^3, that for alveolus active dust at 3 mg/m^3. Other European countries still have their own national laws, and harmonization may still take some time.

In the United States of America, the Occupational Safety and Health Administration (OSHA) has set the Permissible Exposure Limit (PEL) for TiO_2 dust to 10 mg/m^3 with a respiratory fraction of 5 mg/m^3 at the most. The PEL values are legal limits, whereas the Threshold Limit Values (TLV) recommended by the American Conference of Governmental Industrial Hygienists (ACGIH) are not. In the case of TiO_2, the TLV is also 10 mg/m^3, though. Both PEL and TLV are to be understood as 8-hour time-weighted averages (TWA) per day . Both OSHA and ACGIH limits are based on assumptions concerning the risk of physical irritation associated with exposure to titanium dioxide dust.

References

[1] A. F. Wells, "Structural Inorganic Chemistry", 4th. Ed., Clarendon Press, Oxford (1975) p. 143, 146, 447 (Anatase); p. 14, 141, 158, 200, 447, 487, 488 (Rutile)

[2] Gmelins Handbuch der anorganischen Chemie, Band Titan, 8th Ed., Verlag Chemie, Weinheim (1951) p. 244

[3] G. M. Barrow, "Physikalische Chemie", Teil III, Aufbau und Eigenschaften der Kerne, Atome und Moleküle, 3rd Ed. (1976) p. 203

[4] Ullmann's Encyclopedia of Industrial Chemistry, 5th Edition, VCH Weinheim (1993), Vol A 23, p. 539

[5] J.-Ch. Dierich et al., Stahl und Eisen 119 (1999) No. 8, p. 85

[6] H.-G. Grabietz et al., 45th. International Colloquium on Refractories, October 16 and 17, 2002, Aachen, Congress Book, p. 56

[7] V. I. Evdokimov, V. A. Krenev, Inorganic Materials, 38, No. 5 (2002) 490

[8] T. Rentschler, Europ. Coatings J., 10 (1997) p. 939

[9] H. P. Boehm, M. Hermann, Z. Anorg. Allg. Chemie, 352 (1967) p. 156

[10] US National Cancer Institute, Bioassay of Titanium Dioxide for Possible Carcinogenicity, Tech. Rep. Ser. No. 97 (1979)

[11] H.S. Tichy, Seifen-Öle-Fette-Wachse 117, No. 10 (1991) 389, Citation No. 23

[12] J.J. Powell et al., Gut 38 (1996) 390

[13] D. Hollander et al., Intern. Med. 105 (1986) 883

[14] R.V. Heatley et al., Digestion 20 (1980) 307

[15] Documentation of the Treshold Limit Values, 4th Edition, American Conference of Governmental Hygienists, Cincinnati, Ohio, USA (1980) p. 399

[16] F. Bischoff, G. Bryson, Res. Commun. Chem. Pathol. Pharmacol. 38 (1982) 279

[17] F. Stenbäck et al., Oncology 33 (1976) 29

[18] H.E. Stockinger, Patty's Industrial Hygiene and Toxicology, 3rd Edition, Vol. 2A, G.D Clayton and F.E. Clayton Eds., J. Wiley, New York (1981), p. 1968

[19] H.S. Tichy, Seifen-Öle-Fette-Wachse 117, No.10 (1991); Citation No. 24

[20] C. Maltoni et al., in "Advances in Modern Environmental Toxicology", Vol. 2, A. Englund, K. Ringen, K. Mehlman, M. A. Mehlman Eds., Occupational Health Hazards of Solvents, Princeton, N.J., Princeton Scientific Publishers, p. 77

[21] H.E. Wichmann et al., Health Effects Institute, Cambridge, USA, Report 98 (2000)

[22] World Health Organization, "Environmental Health Criteria", 24, Titanium, WHO, Geneva, Switzerland

[23] P.M. Hext, Human & Experimental Toxicology 13 (1994) 700

[24] S. Diabaté et al., Nachrichten Forschungszentrum Karlsruhe 34, No. 1 (2002) 75

[25] K. P. Lee et al., Toxicol. Appl. Pharmacol. 79 (1985) 179

[26] U. Heinrich et al., Inhalation Toxicology 7 (1995) 533

[27] J. L. Chen, W.E. Fayerweather, J. Occup. Med. 30 (1988) 937

[28] JARC Monogr. Eval. Carcinog. Risks Hum., Volume 47 (1989) 313

3 Production of titanium dioxide pigments

3.1 Raw materials

Titanium is the fourth most abundant chemical element of the earth. In nature, titanium occurs only in the form of its oxides or mixed oxides with other elements. Mineable deposits are generally of volcanic origin. The titanium contents of these ores are higher, the higher the level of erosion by weathering is.

The titanium dioxide pigment industry uses between 90 % and 95 % of the global titania ore extraction. The rest is used for producing titanium metal, for the manufacturing of welding rods and, in pig iron production, to replenish the internal refractory bricks of the blast furnaces. Furthermore, titanium is a component in colored mixed metal oxide (MMO) pigments, such as Nickel Titanium Yellow and Chrome Yellow Titanium [1].

In DeNOx honeycomb catalysts for the purification of power plant tail gases, titanium dioxide catalyses the reduction of nitrogen oxides by a comproportionation reaction with ammonia or urea. Finally, extremely pure barium titanate is used in the electronic industry for the production of capacitors because of its high dielectric constant.

Table 3.1 lists a number of titanium containing ores. Only the first five raw materials are used for the production of titania pigments [2]. Ilmenite, leucoxene and naturally occurring rutile are found in nature, whereas synthetic rutile and titanium slags

Raw Material	% TiO_2 - Content	Usage in
natural rutile	92 - 98	chloride process
synthetic rutile	89 - 93	chloride process
leucoxenized ilmenite	55 - 65	chloride process
titanium slag	75 - 85	sulfate process
ilmenite	37 - 54	sulfate process
anatase	90 - 95	none
brookite	90 - 100	none
perovskite	40 - 60	none
sphene (titanite)	30 - 42	none
titanomagnetite	2 - 20	none

Table 3.1
Natural and synthetic raw materials for the production of titanium dioxide

are made especially for titanium dioxide production. Leucoxene is – similar to natural rutile – the erosion product of weathered ilmenite.

Titanium slags are made from ilmenite by the chemical reduction of its iron oxide content (Sorel process). This is done in a metallurgic process with anthracite coal in a carbon arc furnace, and along with the slag, pig iron is recovered. Titanium slags are mainly produced in Canada (Quebec Iron and Titanium Company, QIT) and South Africa (Richard Bay Minerals, RBM), and are traded under the name "Sorel Slag". In Norway, Tinfos slag is produced. These three slags make up about 30 % of the world's feedstocks for TiO_2 pigment production.

Synthetic rutile is processed either from ilmenite (Benelite process) or from leucoxene (Becher process) [3].

In the Benelite process, the ore is reduced with coal or another energy source – often with Na_2CO_3 of K_2CO_3 as a catalyst – in a rotary kiln to transform the iron from the trivalent to the divalent state. Subsequently, the iron is leached with 20 % hydrochloric acid. The emerging synthetic rutile has a TiO_2 content of approximately 96 %.

In the Becher process, leucoxene is first oxidized and then reduced. This "potentiation" [4] fulfills the function of creating pores and cracks in the surface of the ores, and simultaneously transforms the iron into an elemental state. The iron is then oxidized by air – with ammonium chloride as a catalyst – and leached from the ore in a further step ("rusting"). Under these conditions, a titania containing raw material with a TiO_2 content of typically 90 % is formed. The advantage of the Becher process definitely lies in the fact that the iron is gained in the form of

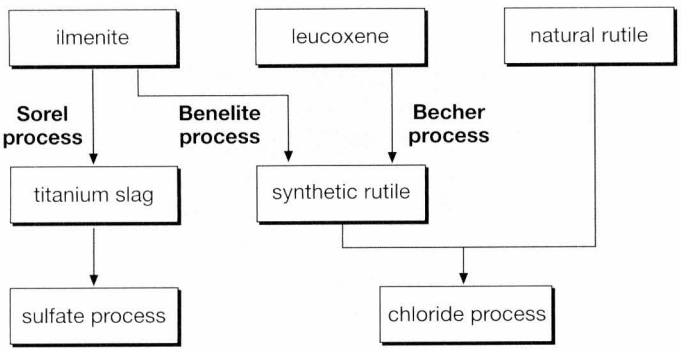

Fig. 3.1
Raw materials for the production of titanium dioxide pigments via the sulfate and chloride processes

an oxide, completely free of chloride ions, which facilitates its use in subsequent processes. Figure 3.1 shows the relationships in a flow chart.

New method developments for the benefication of titania ores predominantly aim at energy savings and finding environmentally more favorable production routes (see for example [5]).

Likewise, anatase (TiO_2), perovskite ($CaTiO_3$), sphene ($CaTi[SiO_4]O$; also called titanite), brookite (TiO_2) and titanium magnetite (TiO_2-FeO-Fe_2O_3 with up to 6 % TiO_2) are found in nature, however without being utilized as a raw material for titanium dioxide production as yet. Possibly, naturally occurring anatase or perovskite may gain some importance in the future. However, in both cases, the presence of calcium is detrimental, since it would always accrue in some unfavorable, non utilizable form.

The sulfate and the chloride processes do not compete for the same raw materials, since both production methods have different demands. In general, the chloride process relies on starting materials with a higher titanium content, since all metal atoms are converted into chlorides. On the one hand, this leads to a higher chlorine consumption, and on the other hand, more waste materials are generated. In general, the wastes that arise from the chloride process (mainly $FeCl_2$), although purer, present a greater problem compared to those from the sulfate process because of a lack of recycling alternatives.

Furthermore, the chloride process is sensitive towards the presence of calcium and magnesium in the ore, since $CaCl_2$ and $MgCl_2$ are non-volatile under the conditions of the chlorination reaction and therefore tend to distort and agglutinate the reaction bed. Zirconium silicate is also disliked for its low reactivity with chlorine and its tendency to accumulate in the chlorinator for the same reason.

In light of all this, the preferred raw material for the chloride process is natural rutile followed by synthetic rutile. Synthetic rutile is porous and this has a lower density than natural rutile. Hence, more care has to be taken that unreacted starting material is not carried out of the chlorinator when synthetic rutile is used.

Also, leucoxene and slags with especially low calcium levels can be handled in the chloride process. However, due to the low titanium content, this is only reasonable under special conditions.

3.2 Sulfate process

As said before, titanium dioxide pigments are manufactured today either by the sulfate process or by the chloride process.

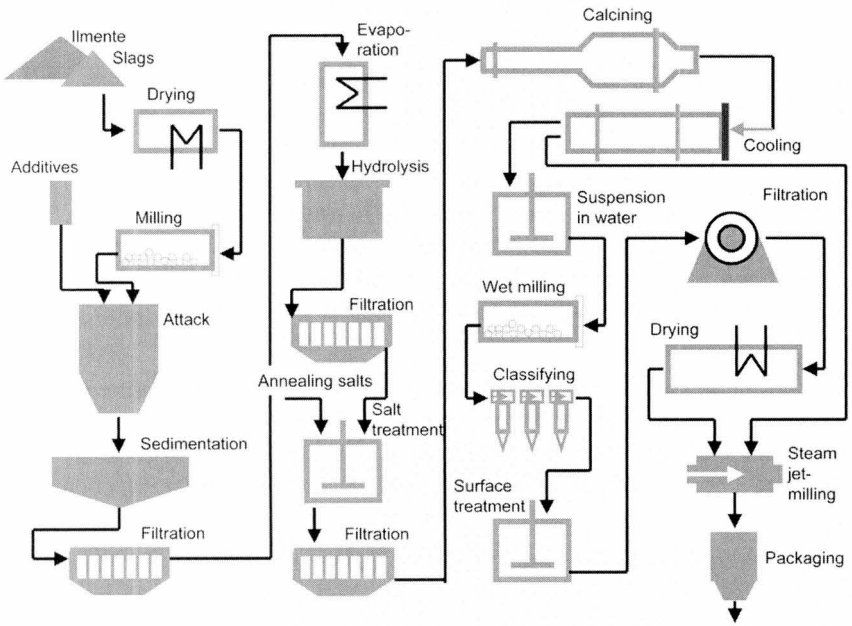

Fig. 3.2
Flow chart of the sulfate process for producing TiO_2 pigments

The sulfate process has been used for pigment production since 1919. In the sulfate process (viz. figure 3.2), the ilmenite or slags are first ground, dried and then air classified.

The dry ore with a specific grain size is then reacted with sulfuric acid and oleum in a very vigorous reaction ("attack") to form a solid fusion cake.

This cake consist of the sulfates of titanium, iron and other metal ingredients of the ore. After completion of the reaction, the cake is leached with diluted sulfuric acids that are recycled from the downstream part of the plant. By the addition of iron scrap metal, it is ensured that the iron is present as Fe^{2+} instead of Fe^{3+}. The ferrous ion, Fe^{2+}, is more soluble under the conditions present at the "hydrolysis" step later on in production (see below), compared to the ferric ion, Fe^{3+}, which would at latest precipitate at that stage of the production process.

Due to the addition of iron scrap metal, some of the Ti^{4+} is reduced to Ti^{3+}. The Ti^{3+}-ion, which is a deep violet, gives the solution a dark color. Therefore, and probably in light of its high viscosity, this solution is called "black liquor". In it, the titanium is present as titanyl sulfate, $TiOSO_4$.

Following the leaching process, the solution is freed from unreacted, solid components by flocculation, sedimentation and, finally, filtration steps. In some plants, the black liquor is cooled, whereby Fe^{2+} precipitates as a green colored hepta-hydrate ($FeSO_4$ x 7 H_2O, "copperas"), which is useful as a flocculant in water cleaning applications.

In the subsequent "hydrolysis", the solution is heated and diluted with water, so that metatitanic acid of the general formula $TiO(OH)_2$ precipitates ("pulp"). At this stage of the process, a decision can be made, if a rutile or an anatase pigment is to be produced. In the case that a rutile is aspired, separately produced rutilization seeds are added to the hydrolysis. Rutile seeds consist of $TiO(OH)_2$ made by the hydrolysis of $TiOCl_2$. They turn into rutile when heated.

Some sulfate pigment producers add the seeds together with annealing salts at a later stage of production, prior to calcination, though. The advantage lies in a higher degree of flexibility in production, the disadvantage being, however, that greater amounts of seeds are necessary to achieve the same results, which, in turn, is costly.

Anatase pigments can be hydrolyzed with or without seeds. When seeds are employed, they are precipitated from $TiOSO_4$ solutions, however. For this, the seeds are either produced by neutralization with sodium hydroxide ("Mecklenburg process"), or by heating of a titanyl sulfate solution ("Blumenfeld process").

After hydrolysis, the precipitated pulp is repeatedly filtrated and redispersed in water. At this stage, separately produced Ti^{3+}-solutions are added to make sure that metal ions of, for example, Fe, Cr, Cu, Mn, V etc., that would lead to discolorations if allowed to remain, are transferred into lower, more soluble oxidation states.

The thus purified pulp is then prepared for calcining by the addition of annealing salts. Their function is to ensure the formation of the desired particle size distribution of the pigment (alkali- and phosphate-ions) on the one hand, and, on the other hand, to impart weather resistance to the core pigment particle (in the case of rutile: aluminum-oxide or -hydroxide, historically also zinc oxide).

The aluminum ions penetrate into the crystal lattice of the TiO_2 by solid state diffusion during the calcination. This is referred to as "doping" of the titania. It has been found [6] that the aluminum oxide also has an effect on particle growth in the sulfate process.

At low concentrations, the aluminum atoms first take the place of titanium atoms in the crystal lattice and act as recombination centers for excitons (see chapter 5), that are generated when titania is illuminated with UV-light. At higher concentrations, the aluminum atoms also take up interstitial positions. Embedded

aluminum reduces the dimensions of the crystallographic elementary cell of rutile [7].

In the sulfate process, there is a limit to the amount of aluminum that can be added in the salt treatment, since otherwise the pigments turn yellow due to high aluminum concentrations in the outer shell of the core particles. The calcination itself is performed in rotary kilns at temperatures of around 1000 °C. After calcination, the TiO_2, which then has "pigment character" at this stage of production (it turns things white), falls into a cooling drum, where it loses access heat, so that the further steps in production (see chapter 3.4) may be performed.

3.3 Chloride process

The chloride process is the younger of the two industrial TiO_2 pigment production processes. It was developed in the 50's of the 20th century, significantly by chemists and technicians of the Company DuPont de Nemour.

In the chloride process [8] (see flow chart, figure 3.3) natural or synthetic rutile is reacted with chlorine gas and coke in a fluidized bed reactor (chlorinator) in the presence of oxygen according to the following equation.

$$TiO_2 + 2\,Cl_2 + C \longrightarrow TiCl_4 + CO_2$$

Carbon monoxide that is formed intermediately due to the Boudouard reaction

$$CO_2 + C \longrightarrow 2\,CO$$

extracts oxygen from the titanium ore, so that the reaction with chlorine may take place.

Apart from titanium, all other metal atoms react to form chlorides that are volatile under reaction conditions employed, with the exception of $MgCl_2$ and $CaCl_2$. After chlorination, the $TiCl_4$ is separated from most of the other reaction products by condensation. Subsequently, reducing agents are given to the condensed $TiCl_4$ in order to reduce both vanadium tetrachloride ($V^{4+}Cl_4$) and vanadyl chloride ($V^{5+}OCl_3$) to vanadium trichloride ($V^{3+}Cl_3$). Only this measure enables the separation of titanium and vanadium chlorides by destillation. Even the slightest traces of vanadium in the titania particles (approximately from 5 ppm onwards) already lead to discolorations, i.e. yellowing, of the titania.

The purified $TiCl_4$ is then reacted in a special burner under oxygen excess at temperatures ranging from 1400 °C to 1600 °C to yield TiO_2 according to the following reaction scheme:

$$TiCl_4 + O_2 \longrightarrow TiO_2 + 2\,Cl_2$$

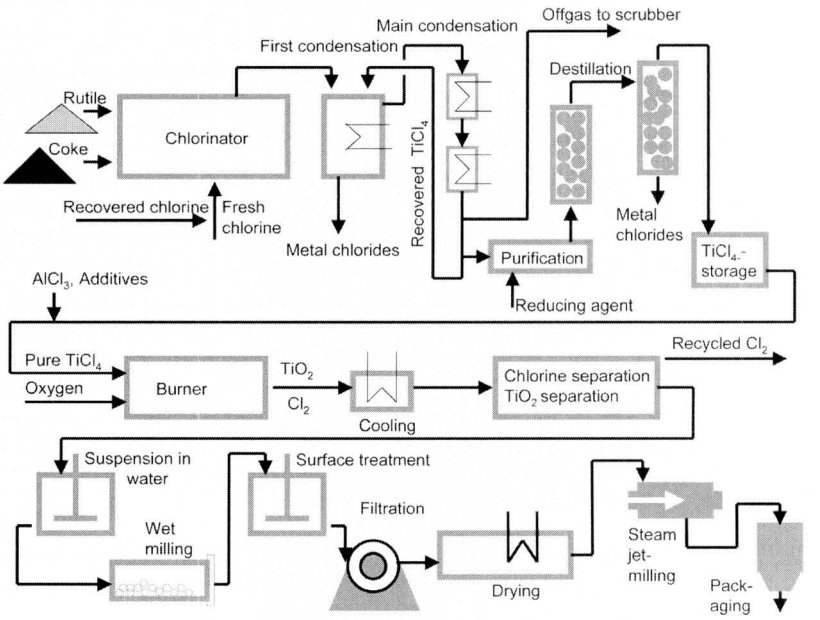

Fig. 3.3
Flow chart of the chloride process for producing TiO_2 pigments

For this, the reactants are preheated from 500 °C up to 1000 °C ($TiCl_4$), or 1000 °C (O_2), respectively. The TiO_2 produced in this reaction would be a mixture of rutile and anatase and would therefore hardly be suitable for industrial applications as a pigment. However, by the addition of approximately 0,5 % to 1,5 % of Al_2O_3 (as $AlCl_3$) to the $TiCl_4$ feed of the burner, the emerging TiO_2 turns into almost 100 % rutile. At the same time, the incorporated aluminum improves the photo- and weather resistance of the pigment, just as it does in the sulfate process (see chapter 5). A further effect of the Al_2O_3 addition is the promotion of finer particle sizes of the pigments. By the alternative addition of phosphor trichloride (PCl_3) or silicium tetrachloride ($SiCl_4$), it is supposed to be possible to suppress rutile formation and to come to a pure anatase [9]. An anatase produced in such a way is however presently not on the market.

Following the burner, the product must rapidly be cooled to temperatures lower than 600 °C and separated from the chlorine gas. This is done by quenching with air or nitrogen. In the further pneumatic conveyance of the TiO_2, a fine particle sized sand is added to the product stream. It prevents the TiO_2, which tends to agglomerate, from building up and clogging the pipings.

Naturally, the sand must be separated from the product again at a later stage. This is done by sieving after sand milling the TiO_2 pigment. Since at this stage of production, the pigment is inevitably in an aqueous slurry, almost all chloride pigment grades are surface treated in a further step, which is not necessarily the case with sulfate pigment grades.

3.4 Inorganic and organic surface treatments

After cooling, the core titania particles produced in the sulfate (rutile and anatase) and chloride processes (only rutile) are generally subjected to inorganic surface treatments. In this production step, the crude titania calciner- or burner-discharges are milled and subsequently covered with one or more layers of inorganic substances. Since the end of the second world war, approximately two thousand patents dealing with this special step of pigment production have been filed [10].

The principle of this method of pigment modification is to first add dissolved inorganic precursors to a milled suspension of the crude pigment. For this, it is necessary to adjust the pH value of the pigment slurry to a value where the precursors remain in solution. From this mixture, the inorganic substances are finely precipitated by gradual adjustment of the pH value towards neutral [11, 12, 13]. Due to the high ionic strength (see chapter 6.4.2) in solution, these precipitates are not stable against flocculation, but agglomerate and attach to the pigment's surface. The art involved in these surface treatments ("post-treatments") lies in the ability to achieve as complete a coating as possible around the TiO_2 core particles.

Surface treatments may be carried out either discontinuously in stirred, heated vessels, or otherwise, continuously in a number of consecutive tanks of a cascade. Both procedures lead to similar results, although the discontinuous procedure is easier to handle when the surface treatment is to be applied rather slowly for the sake of achieving a low specific surface area in the final product.

As surface treatments, the oxides or hydroxides, respectively, of aluminum, silicium, zirconium and even titanium are widely used. The amounts of post-treatments are normally denoted as weight percent of the oxide based on the titania amount deployed in the surface treatment step. So one would, for example, encounter an indication of "3 % Al_2O_3" as a surface treatment, although, in reality, the aluminum would be present as a mixture of oxides and hydroxides and, based on the final product, there would be less than 3% of Al_2O_3 in the surface treatment.

Typical reagents are $NaAlO_2$, $Al_2(SO_4)_3$, $ZrOSO_4$ and $TiOSO_4$. By mixing basic and acidic precursor solutions, it is possible to simultaneously precipitate two

different inorganic surface treatments, such as $Al_2(SO_4)_3$ and Na_2SiO_3, to form, for example, aluminum silicate.

As seen in this example, inorganic surface treatments do not necessarily have to be only of oxide nature, but may also consist of salts.

Thus, both aluminum and titanium, for example, form phosphates with low solubility that also coat nicely onto titania and fulfill certain objectives, depending on the intended use of the final product. Furthermore, next to co-precipitation, it is possible to cover the titania consecutively with layers of different or alike substances, leading to products with an onion skin type of architecture.

Following the inorganic surface treatments, the pigments are filtered, rinsed, dried and then further modified with an organic surface treatment, before being ground in a steam jet mill. The organic surface treatments are usually applied to an amount varying between 0.1 and 0.6 weight percent. Further information concerning their influence is give in chapters 6.2 and 6.3 of this book.

Inorganic surface treatments play a role in improving weather resistance and photostability, as well as colloid chemical and optical properties of titania pigments.

Table 3.2 [taken from 14] shows some examples of inorganic surface treatments in a laboratory experiment. In this series, one or two surface treatments, respectively, were applied one by one to a core titania taken from the sulfate process. The samples with only aluminum oxide (No. 1) or just silicium dioxide (No. 5) exhibit comparatively low relative scattering powers (see chapter 4.5). All other samples

	1	2	3	4	5	6	7
First treatment	3% Al_2O_3	1% TiO_2	3% Al_2O_3	1% TiO_2	0.5% SiO_2	0.5% SiO_2	3% Al_2O_3
Second treatment	-	-	1% TiO_2	3% Al_2O_3	-	3% Al_2O_3	0.5% SiO_2
Relative scattering power	98	106	105	107	98	107	108
CBU	13.7	14.8	14.8	14.8	13.4	14.9	15
20° Gloss	77	80	79	79	66	77	77
Spec. surface area m^2/g	11.1	8.4	16.0	13.9	8.0	13.1	13.1
60° Gloss after 36 months of natural weathering	12	9	34	46	2	10	10
Minutes of time required for washing 2 kg of TiO_2	63	180	55	48	>250	57	57

Table 3.2
Application properties of differently surface treated titania pigments

are more or less identical in this respect and also in respect to their carbon black undertone (color tint in combination with carbon black pigments. See chapter 4.9).

The 20° gloss (see chapter 4.10) was determined in a paint formulation at a PVC (pigment volume concentration)[1] of 17 %. Samples No. 1 and No. 5 were clearly less favorable in this respect as well. Whereas the surface treatment with silica from experience always leads to slightly diminished gloss values, in this case, the drastic slump in gloss of sample No. 5 is probably due to the fact that the overall coverage with 0,5 % silica is too low. It can be seen, however, that samples No. 6 and No. 7, both containing SiO_2, have the same tendency, compared with samples No. 3 and No. 4.

The samples again differ considerably in their specific surface area values. Compared to the untreated core titania with a specific surface area of approximately 8 to 10 m^2/g, inorganic surface treatments – when applied in customary amounts between 2 % and 4 % – normally enhance the specific surface area.

To point this out, figure 3.4 shows an electron microscopic picture of a titanium dioxide pigment particle coated with a combination of SiO_2 and Al_2O_3. Contrary to the crystalline titania core particle, which is distinguished by an interference pattern, the inorganic surface treatment is amorphous and more structured than the underlaying surface of the core. This results in a higher value of the specific surface area.

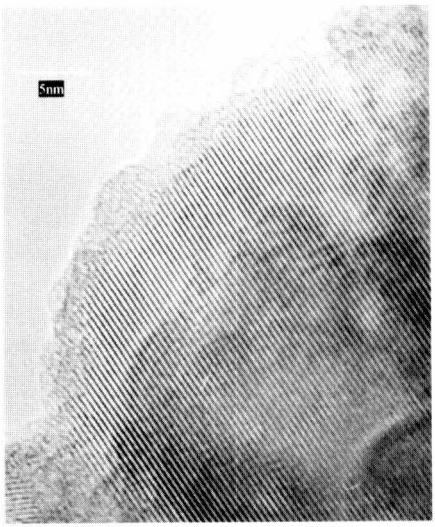

Fig. 3.4
TEM image of a titanium dioxide pigment particle with an inorganic surface treatment consisting of SiO_2 and Al_2O_3 (courtesy of T. A. Egerton)

Once again, large differences are seen in the gloss retention of painted panels after 36 months of natural weathering. In this respect, sample No. 4 shows the best result, and also regarding the ease with which salts were rinsed from the coated titania following the post-treatment. Conventional titanium dioxide pigments have a "conductivity" of less than 100 µS/cm (reciprocal value of the resistivity of a slurry of 20 g of pigment in 180 g of aqua dest., according to ISO 787, part 14). To

1 The PVC is the portion of the solid paint film volume which is made up of pigment.

reach this order of magnitude, the pigments must be rinsed on a filter with about five times their weight with deionized water. Sample No. 4 performed best with regard to its technical producibility, since it was the easiest to filtrate and wash. Aluminum oxide is certainly the most widely used surface treatment today, in the sense that it makes up always at least one of the components in any pigment coating.

Pigment application properties, however, do not only depend upon the manner in which the surface treatments were applied, but also upon the history of the core titania particles.

For this reason, products of different manufacturers usually have surface treatments that are chemically different from each other, even when they were developed for the same applications.

References

[1] Ullmann's Encyclopedia of Industrial Chemistry, 5th Edition, VCH, Weinheim, Volume A20, p. 276

[2] K. J. Stanaway, Mining Engineering, 46, No. 12 (1994) 1367

[3] P. N. Mohan Das et al., Metals Materials and Processes 13, No. 2-4 (2001) 205

[4] Patent WO 02/49964 A1, June 27, 2002

[5] D.E Moore, "Key strategic, economic and technical issues in the supply of titaniferrous feedstocks", TiO_2-93 Conference, Chicago, 14-15 September 1993, Intertec Conferences, Portland ME, p. 16

[6] U. Gesenhues, Solid State Ionics, 101-103 (1997) 1171

[7] U. Gesenhues, J. Solid State Chemistry 143 (1999) 210

[8] Ullmann's Encyclopedia of Industrial Chemistry, 5th Edition, VCH, Weinheim, Volume A20, p. 279

[9] Patent US 6444189 B1, September 3, 2002

[10] R. Davies et al., Advanced Materials 10, No. 5 (1998) 1264

[11] U. Gesenhues, J. Colloid Interface Sci. 168 (1994) 428

[12] U: Gesenhues; FARBE&LACK 94, No. 3 (1988) 184

[13] U. Gesenhues, 21st Fatipec Congress, June 14–18, 1992, Amsterdam, Congress Book, Vol. 1, p. 44

[14] J. Winkler, High Performance Pigments 2000, Berlin, September 11–13, 2000, Congress Book, Lecture No. 19., Intertec Conferences, Portland ME

Lost in the lab?

Formulation Center – the new online raw material database for the coatings and printing inks industry. Search, free of charge, for the right raw material: compare physical or chemical properties, download up-to-date product data sheets, point and click for product samples, tech support or sales contacts and browse our editorial archives for relevant information from FARBE & LACK and European Coatings Journal. **Register now, free of charge, at**

www.coatings.de/formulationcenter

formulation center

Search. Find. Formulate.

CENTZ

4 Optical properties of titanium dioxide pigments

4.1 Fundamentals of color measurement

In this chapter, the fundamental aspects of color measurement are only dealt with to the extent, that the reader is enabled to understand the optical parameters that are used to characterize titania pigments.

The aim of color measurements is to describe the sensation that human beings have, when viewing colored objects, with the help of numbers. In industry, this quantification plays an important part, since this allows delivery tolerances to be negotiated and followed.

Colored objects are separated into primary light sources, such as the sun or lamps, and secondary light sources or "*surface colors*". A surface color comes into being when, for example, "white" daylight, or any other visible radiation coming from a primary light source, hits an object. A part of the spectrum is absorbed and turned into heat, whereas the remaining parts are reflected. This reflected part of the spectrum meets the retina of the eye, where "rods" and "cones", which are sensitive towards red, green and blue light, transform this color stimulus into electrical signals that are passed on to the brain via the optic nerve. There, in the brain, the sensations of "color", "light" and "dark" are generated.

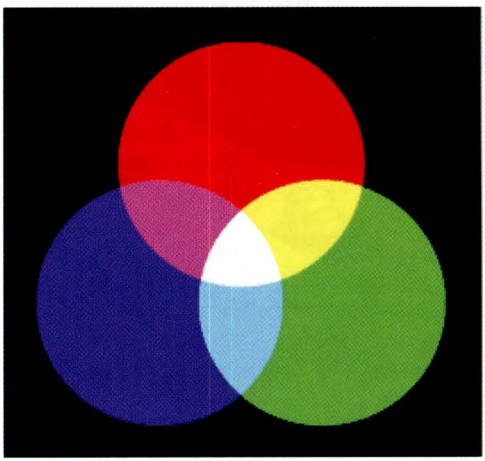

Fig. 4.1
The principle of additive color mixing

The measuring of colors using the additive color mixing according to the CIE (*Commission Internationale de l'Eclairage*) is based on the concept, that any color may be realized by mixing different proportions of red, green and blue. When a red, a green and a blue colored, transparent filter are illuminated by white light, and the three transmitted light cones are overlain (figure 4.1), white or "non-colored" light is recovered once again.

Naturally, this is only true for certain, well defined colored filters.

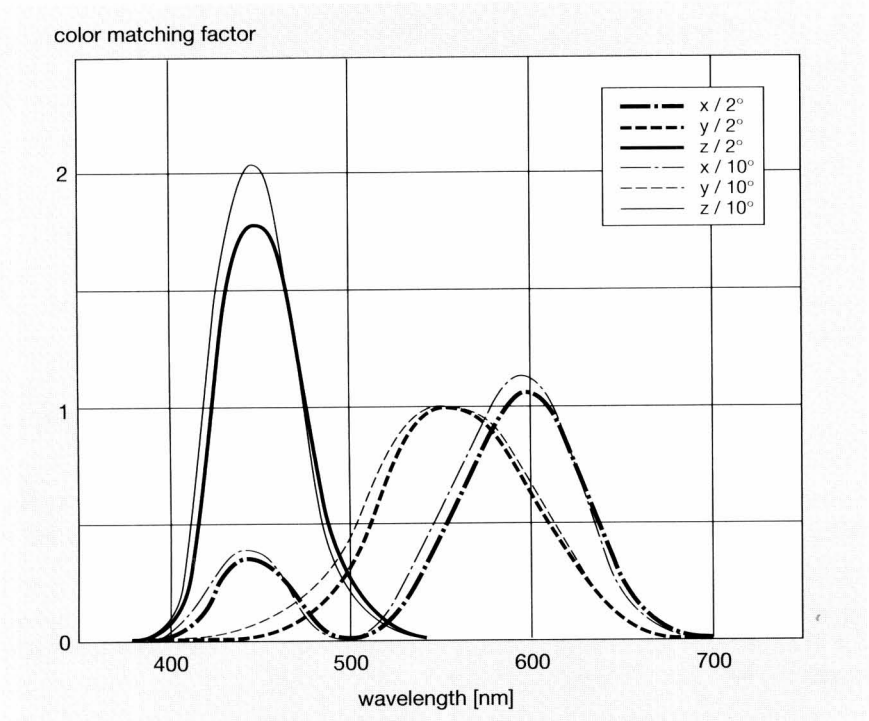

Fig. 4.2
The color matching functions according to ISO 7724-1

Also shown in figure 4.1 are the well known colors obtained when mixing red with blue (= violet), blue with green (= blue-green) and green with red (= yellow).

Figure 4.2 shows the transmittance spectra of such colored filters as defined in ISO 7724, part 1, for the 2° and 10° *CIE standard observer*. The 2° (10°) standard observer looks onto a circular area with 1.4 cm (7 cm) diameter from a distance of 40 cm. The "*RGB color matching functions*" red $\bar{x}$, green $\bar{y}$ and blue $\bar{z}$ for the two observers are different from another because, depending upon the area that is covered by view, different parts of the retina are involved. The human retina is not equally sensitive in all places.

From the *remitted irradiation R* (reflectance factor) and the CIE color matching functions, the *XYZ tristimulus values* are calculated using the following equations

$$X = \int_{\lambda = 380\ nm}^{720\ nm} (\bar{x}_\lambda \times R_\lambda)\, d\lambda \tag{4.1}$$

$$Y = \int_{\lambda = 380\ nm}^{720\ nm} (\bar{y}_\lambda \times R_\lambda)\, d\lambda \tag{4.2}$$

$$Z = \int_{\lambda = 380\ nm}^{720\ nm} (\bar{z}_\lambda \times R_\lambda)\, d\lambda \tag{4.3}$$

From these, the so called *chromaticity coordinates* are easily calculated

$$x = \frac{X}{X + Y + Z}, \quad y = \frac{Y}{X + Y + Z} \text{ und } z = \frac{Z}{X + Y + Z} \tag{4.4}$$

Since x, y and z add up to 100 %, any color is completely characterized by any two of the three chromaticity coordinates. It is, however, customary to choose x and y.

"Achromatic", i.e. lacking any hue, is the surface color of an object that remits equal portions of red, green and blue light. As figure 4.3 shows, this is the case for $x = 0.33$ and $y = 0.33$. At this point, z is automatically 0.33 (rounded figures, of course).

When following a straight line, extending from the achromatic point of the color space (figure 4.3; "*color shoe*") into any direction outwards, one moves along a line of colors having identical hue. The colors do, however, become more saturated, the farther one moves along this line. At the edge of the color space, the color is completely saturated, due to the fact that the object absorbs the corresponding light that matches its color to 100 %. A further increase of color intensity (= saturation) is physically not possible.

The numbers along the outskirts of the color space denote the wavelength of the corresponding light (spectral wavelength) that, when suitably mixed with achromatic light stimulus, would result in all the colors along the line coming from the achromatic point. They are only defined for the region from red, over green to blue colors. The so called "purple line", as the direct connection between red and blue, has no corresponding wavelengths listed, since purple is not a spectral color, but a mixture of red and blue.

Perpendicular to the *x/y* plane, going right through the achromatic point, there is another axis describing lightness. Thereby, a three dimensional color space is opened, that embodies all colors (= tints, hues), saturations and lightnesses that are visible to the human eye.

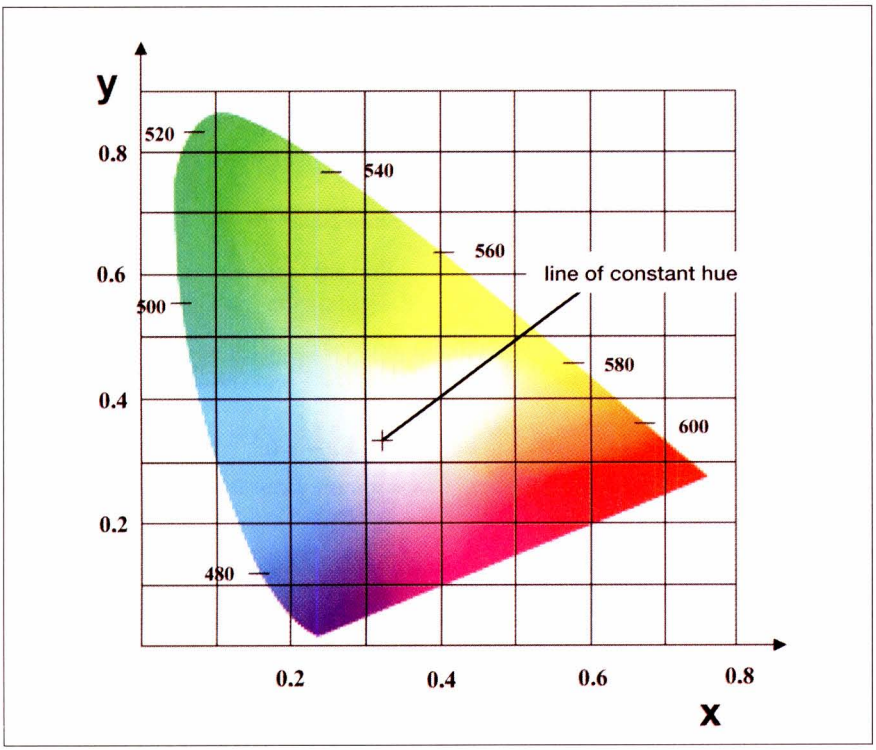

Fig. 4.3
The "color shoe" according to DIN 6162, part 1

A drawback of the color shoe is, however, that colors take up differently large areas. Whereas red and blue occupy relatively small fields, the color green makes up a large portion of the color shoe. Whereas in the red area, small changes in x- and y-values already change the hue considerably, similarly large changes in the green field may not even be noticed by an observer.

For the sake of negotiating color tolerances, this is of course unfavorable, and therefore, efforts were made to define a new color space that does not have this drawback (or at least less of it) by stretching or compressing the color axes. The result is laid down in ISO 7724, "Paints and Varnishes, Colorimetry; part 3: Calculation of color differences". This standard is based upon DIN 6174 and uses the "*CIELAB-formula*" of the CIE.

The CIELAB-formula defines a color space (figure 4.4) that is characterized by an a^*-axis, that goes from green to red, and by a b^*-axis, extending from blue to yellow, as well as a lightness axis L^*, that is perpendicular to the other two. Just as in the color shoe, a ray in the a^*/b^*- plane, leaving the achromatic point in the

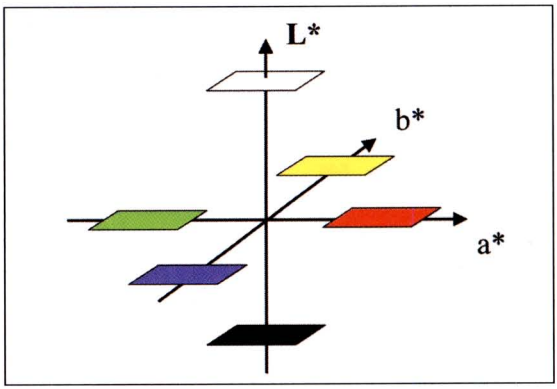

Fig. 4.4
The color space of ISO 7724-3; CIELAB formula

center of the space, defines a hue that becomes more saturated, the farther outside it goes. The lightness axis extends from $L^* = 0$ (black) to $L^* = 100$ (white).

Two points in the CIELAB color space have a color distance (separation distance in CIELAB units) of

$$\Delta E_{ab} = \sqrt{(\Delta L^*)^2 + (\Delta a^*)^2 + (\Delta b^*)^2} \tag{4.5}$$

if ΔL^*, Δa^* and Δb^* are the differences of the corresponding coordinates in the color space. Irrespective of the position in the color space of the CIELAB-system, colors with the same ΔE_{ab} values are normally felt to be "similarly different". Generally, color differences ΔE_{ab} of $\pm$ 1 are tolerated as color fluctuations from delivery to delivery.

4.1.1 CIELAB-values of titanium dioxide pigments

In trade as a whole, the lightness L^* and the yellow tint b^* according to ISO 7724, part 3, is part of delivery specifications of titanium dioxide pigments. To find these values, tablets are pressed from the powders and normally then measured with spectral photometers. It is important to specify measuring geometry, light source and often even the photometer model when negotiating specifications, since the values found depend, or may depend, upon these parameters.

Anatase pigments may obtain a yellow tint and lose lightness when placed under persistent, strong illumination.

Thus, it makes sense to use so called "flash photometers", by which only a short light flash is used to illuminate the sample, instead of using a simple remission photometer.

4.2 Electromagnetic waves ("radiation")

Two basic relations (equations 4.6 and 4.7) characterize electromagnetic waves.

The speed of electromagnetic radiation in vacuum c is a constant (2.992×10^8 m/s). It is the product of the wavelength λ and the frequency ν of the radiation.

$$c = \lambda \cdot \nu \tag{4.6}$$

The corresponding energy of the radiation is directly proportional to the frequency ν. The proportionality constant is h, also called Planck's constant (6.626×10^{-34} Js).

$$E = h \cdot \nu \tag{4.7}$$

When an object absorbs radiation, it uptakes exactly this energy quantum for each photon.

The energy of an electromagnetic wave is carried by its electrical field. The electrical field of an electromagnetic wave runs sinusoidal along its propagation direction. The corresponding magnetic field vector runs perpendicular to the plane of the electrical field and with a phase difference of 180° relative to it. If the electrical field vector is confined to one single plane, then this is referred to as "polarized" light.

Light which is visible for the human eye covers the wavelength range between approximately 380 nm and 700 nm.

All pigments principally undergo two types of interactions with light: light absorption and light scattering. In composite materials, pigments also contribute to the appearance by structuring the surface of the materials. This leads to a further optical phenomenon, the surface gloss, that, with respect to perception, is similarly significant as color.

4.3 Light absorption, light scattering, reflection and diffraction

All of the interactions between matter and light that are listed in the title above are based upon interactions of the electrons of the substance with the electric field of the light. When light waves fall on matter, the electrons in it are incited to oscillate. If the frequency of the light wave coincides with the "natural frequency" (= "eigenfrequency") of an electron transfer from a lower to a higher energy level, the energy of the light wave is absorbed and (usually) deactivated without any further radiation processes by being turned into heat.

When non-polarized light falls on a transparent object, that is an object which does not absorb light, then the oscillating electrons - which act as oscillating dipoles - emit radiation. Since an oscillating dipole never sends radiation out into the direction of its line of vibration, but only perpendicular to it, the "scattered" light is completely or partially polarized, depending on the viewing direction.

Figure 4.5 shows this context for a "scattering center" that is much smaller than the wavelengths of the incident light ("Raleigh scattering"). Non-polarized light falls on the scattering center (e.g. a particle) from the front (in the direction of the

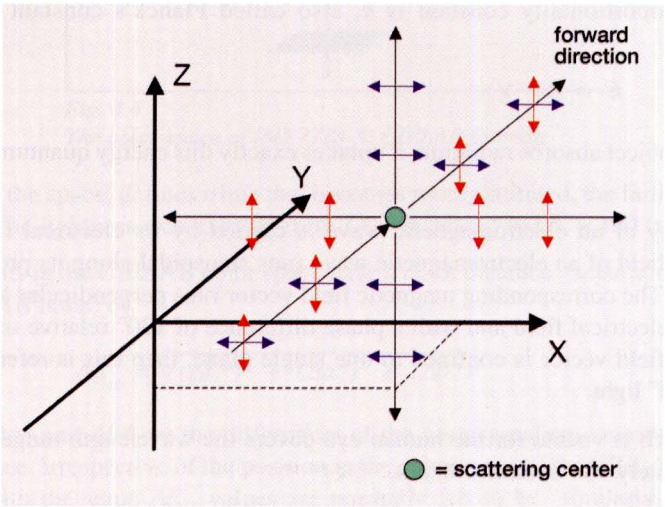

Fig. 4.5
Directional dependency of the polarization of light scattered by a scattering center

y-axis). In this light ray, the double-arrows depict two electric field vectors that are perpendicular to each other. (Both are colored differently in figure 4.5 for easier distinction). The electrons in the scattering center are incited to oscillate in the planes of the two field vectors of the incident light. As oscillating dipoles (Hertz-dipoles), they send – like transmitter antennas – radiation perpendicular to their vibrating directions.

The light scattered in the forward direction (along the *y*-axis in figure 4.5) is therefore non-polarized. The light scattered in a 90° angle upwards, downwards, to the left and the right are polarized in the way as shown. All other rays (not shown) are partially polarized.

Figure 4.6 shows the intensities of two polarized scattered light rays, for example from the (horizontal) *x*/*y*-plane around the particle in figure 4.5, which were

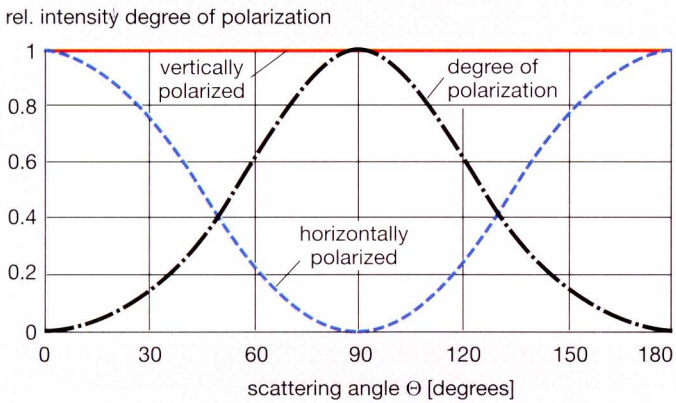

Fig. 4.6
Angle dependency of the intensities of the scattered, polarized light from the horizontal x/y-plane of figure 4.5 and the resulting degree of polarization

calculated using the Mie theory (see chapter 4.4). In this figure, 0° depicts the forward direction, 90° the sideways direction and 180° the back scattered light in relation to the illuminating ray.

The intensity of the ray which is polarized perpendicular to the *x/y*-plane (colored red, like in figure 4.5) is independent of the viewing angle. The horizontally polarized ray (colored blue, like in figure 4.5) decreases gradually, starting from 0°, and has a minimum value of zero at 90°. From there on, the intensity increases again until 180° is reached.

Likewise, the degree of polarization is shown. It is zero for non-polarized light and one, when the light is completely polarized.

In the case that the scattering center is an atom in an ideal crystal, that is to say, if it is surrounded regularly by other scattering centers, then all rays, except those scattered in the forward direction, are annihilated by interference[1]. What remains, is the ray scattered in the forward direction, along with the parts of the incident ray not having interacted with the electrons in the crystal, and the ray that is scattered in the backward direction.

1 Strictly speaking, this is only true if the electromagnetic rays do not have too short a wavelength. Since in this example, we are dealing with the transmission of visible light through a crystal, this condition is met, though.

The rays that are scattered from the borders of particles are not completely nullified. They are termed as "diffracted" or "deflected" light rays[2]. In a microscope, for example, this phenomenon enables even sub-microscopic particles to be seen. The images seen in this case are called "*deflection patterns*" of the particles.

If the scattering centers are not regularly spaced, then the scattered light rays are not annihilated by interference. If, furthermore, the material has no absorption in the visible region of the spectrum, then the scattered light appears to be white. An example for this case is the clouds in the sky that obtain their white color from the scattering of light from the micrometer-sized droplets of fog. But, also white pigments operate exactly by the same principle.

When colored pigments are considered, the color impression results from the not absorbed, but scattered wavelengths. A green pigment, for example, absorbs blue and red light and scatters the medium-wavelength green light.

From all that was said until now, it can easily be understood why colored dye molecules, that hardly scatter light at all, but instead, are merely capable of light absorption, only achieve to color a paint or a plastic when viewed in transmission of the incident light. When viewed "from the top" (only reflection effective), such surfaces only show a color if, for example, titanium dioxide as a light scattering pigment is additionally present. The dye (or "transparent", very fine particle sized colored pigment) filters certain wavelengths away by absorption, whereas the remaining spectral wavelengths are scattered out of the material by titanium dioxide.

Light absorption as well as light scattering are particle size dependent.

4.3.1 Particle size dependency of light absorption

Light absorption can be characterized by measuring "in transmission" the intensity of the passing light I and comparing it to the intensity of the incident light I_0. Lambert-Beer's law can be applied:

$$\ln \frac{I}{I_0} = -\varepsilon \cdot c \cdot d \tag{4.8}$$

c = concentration of dye or pigment
d = layer thickness
ε = absorption coefficient

As a result of the method of measurement, the absorption coefficient depends upon the spatial distribution of the color bestowing substance. Since colored

2 By evaluating the patterns of diffracted rays, the sizes of small particles can be determined (Fraunhofer diffraction).

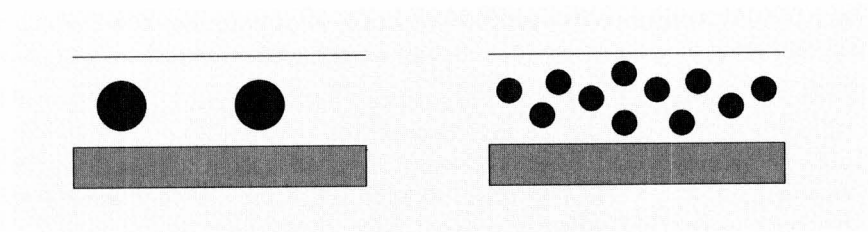

Fig. 4.7
Influence of the particle size on the screening effect. Left: coarse titanium dioxide particles with little screening ability. Right: fine titanium dioxide particles with high screening ability

pigments consist of small particles, their absorption coefficients are particle size dependent.

As exemplified in figure 4.7, the "*surface coverage*" (the ability to "cast a shadow") of coarser particle is much worse than that of the same mass of finer particles. (The smaller particles in figure 4.7 have approximately 57 % of the diameter of the larger particles. Accordingly, eleven small particles have about the same volume as two large particles.) Light passing through a pigmented film has far less probability of making contact with a particle if these are coarser. The absorption coefficient therefore has a particle size dependency as shown schematically in figure 4.8.

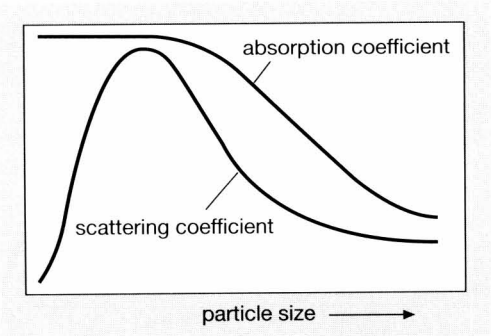

Fig. 4.8
Particle size dependency of the absorption coefficient and the scattering coefficient (schematically)

4.3.2 Particle size dependency of light scattering

The light scattering ability of particles depends incredibly upon their size relative to the wavelength of the light. This pertains not only to the intensity of the scattered

light, but also to its direction dependency and to its polarization. For molecules and very small particles, the information given in figures 4.5 and 4.6 applies.

In this case (Raleigh scattering), the scattered light intensity increases proportionally to the volume of the particles, i.e. proportional to the third power of their diameters. This holds true up to particle sizes of approximately one tenth of the length of the incident light waves. Next to this, "Raleigh scattering" is very wavelength dependent, namely inversely proportional to the fourth power of λ.

$$\frac{I}{I_0} \sim \frac{d^3}{\lambda^4} \tag{4.9}$$

Blue light, with a wavelength of 400 nm, is thus scattered ten time as efficiently as red light with 700 nm.

With these relationships, the color of the sky (blue at daytime, red-yellow at sunset, etc.) can be explained with light scattering processes by gas molecules in the atmosphere.

One example for the light scattering behavior of titanium dioxide pigment particles of 0.2 µm diameter in a resin matrix with a refractive index of 1.5 for (green) light of 550 nm wavelength is shown in figure 4.9. The figure shows that, in this case, the amount of backscattering is very small (approximately 3 to 5 %) and that the polarization is no longer highest at a 90° angle to the incident light (compare

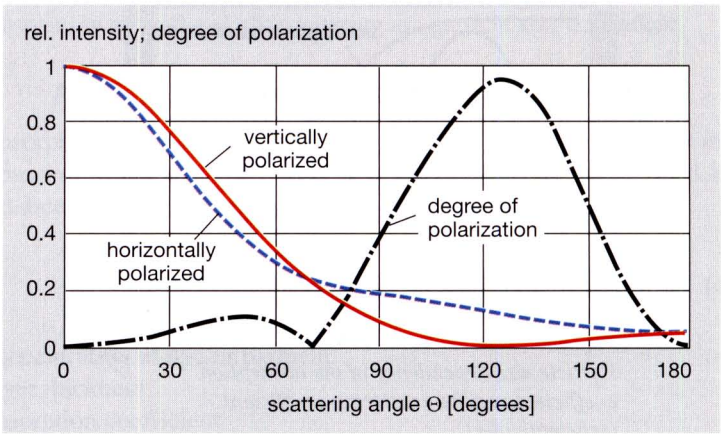

Fig. 4.9
Angle dependency of the intensities of the scattered, polarized light (horizontally and vertically polarized) in the horizontal plane surrounding a titanium dioxide pigment particle in a resin and the degree of polarization that results from that. (Analogous to figure 4.6 under the conditions stated in the text.)

figure 4.6), but at an angle of approximately 125°. From figure 4.9 it becomes clear, that even titanium dioxide must rely on multiple scattering in order to scatter the light out of a material. Once again, the illustration in figure 4.9 is a (foreclosed) result of the Mie theory of light scattering (see next chapter 4.4). In this theory, the angle dependence of the scattered light intensity allows the calculation of a scattering coefficient. It is a measure for the ability of a particle to scatter light backwards. The scattering coefficient is small both for very small, and for large particles. In between, it runs through a maximum. The reason for this is that scattering becomes more efficient when, ideally, all dipoles, i.e. electrons, of a particle are activated to oscillate by one single photon. At first approximation, this is the case if the particles have a diameter about half the size of the incident wavelength. From this results the dependency of the scattering coefficient on particle size, as is also shown schematically in figure 4.8.

4.4 Mie theory

The interaction of light with dielectric particles of sizes beyond the applicability of the Raleigh theory was first described by Gustav Mie [1]. The mathematics involved are, however, somewhat difficult and exceed the scope of this book. Therefore, only the main aspects and most important results that arise from this theory are presented here. The more ambitious reader should turn to the relevant literature [2, 3].

When a particle is located between a light source and an observer, it may both absorb and scatter light. The particle therefore has a shadow effect. Following the Mie theory, this can be expressed by the extinction cross section C_{ext} which is the sum of the absorption cross section C_{abs} and the scattering cross section C_{scat}.

$$C_{ext} = C_{abs} + C_{scat} \tag{4.10}$$

For white pigments, C_{abs} is ideally zero.

By dividing C_{ext}, C_{abs} and C_{scat} by the geometric cross section G of the particle, the *efficiencies* for extinction Q_{ext}, absorption Q_{abs} and scattering Q_{scat} are defined.

$$Q_{ext} = \frac{C_{ext}}{G} \qquad Q_{abs} = \frac{C_{abs}}{G} \qquad Q_{str} = \frac{C_{str}}{G} \tag{4.11}$$

It is important that the scattering efficiency can obtain values greater than one. In that case, the pigment particle scatters light from a volume larger than its own spatial dimension. This, at first glance maybe baffling circumstance, becomes

understandable when it is brought back to mind, that light scattering is based on the interaction between dielectric materials and electromagnetic waves. Thus, it is a *field interaction.*

The scattering cross section C_{scat}, and thereby the scattering efficiency Q_{scat}, is related in a complicated manner to the differences in the refractive indexes of the particle and its surroundings on one hand, and to the ratio of particle diameter to wavelength of the light, on the other hand. Light scattering is only possible, if the refractive index of a particle is different from that of the surrounding medium. If the refractive indexes become identical, light scattering ceases. Light scattering increases continuously with increasing differences of the refractive indexes. As far as the ratio of the particle size to the wavelength of the light is concerned, there exists an optimum in light scattering ability (at a ratio of approximately 1:2).

So called "Bessel functions" are used recursively to compute scattering cross sections. This is to say, that one uses the result of a calculation as the starting point of a second calculation and continues this process until the result has converged to a final value.

Not only the *degree* of light scattering changes with the quoted parameters, but also the *directional distribution* of the scattered light in space (see chapter 4.3.2). This behavior, which depends largely upon the particle size, may be expressed by the asymmetry parameter g. A particle that scatters the same amount of light forwards as it does backwards, has an asymmetry parameter of zero. g is positive, if the particle scatters light predominantly in the forward direction (in extension of the direction of the incident light), and negative, when it is mainly scatters light backwards. According to Bohren [4] the *light scattering coefficient* S_B is given[3] by:

$$S_B = \frac{3}{2} \int_d \frac{Q_{scat}}{d} \cdot (1 - g) \cdot q(d) \qquad (4.12)$$

with

$q(d)$ = particle size distribution function
d = particle diameter

The particle size distribution of TiO_2 pigments is normally approximated well enough by a logarithmic normal distribution:

3 The term S_B is different from the *spectral scattering coefficient* of the Kubelka-Munk theory (see chapter 4.5).

$$q(d) = \frac{1}{d \cdot \ln \sigma\sqrt{2\pi}} \cdot e^{\frac{1}{2}\left(\frac{\ln d / d_{50}}{\ln \sigma}\right)} \qquad (4.13)$$

In equation 4.13, d_{50} depicts the mean diameter of the log-normal distribution. For a standard deviation value of the distribution of $\sigma = 1.3$, the scattering coefficients of anatase and rutile are plotted as a function of particle diameter d and the light wavelength λ in figures 4.10 and 4.11.

The following results may be summarized:

- Anatase and rutile have a maximum scattering coefficient for $\lambda = 550$ nm at a particle size of approximately 0.22 µm[4]
- The scattering coefficient for short wavelengths (blue light) is higher than for long wavelengths. This results from the fact that the refractive index of titanias increase towards the absorption edge (see figure 2.7 in chapter 2.1).
- Rutile has a higher scattering coefficient at any particle size and wavelength than anatase at the corresponding sizes and wavelengths.

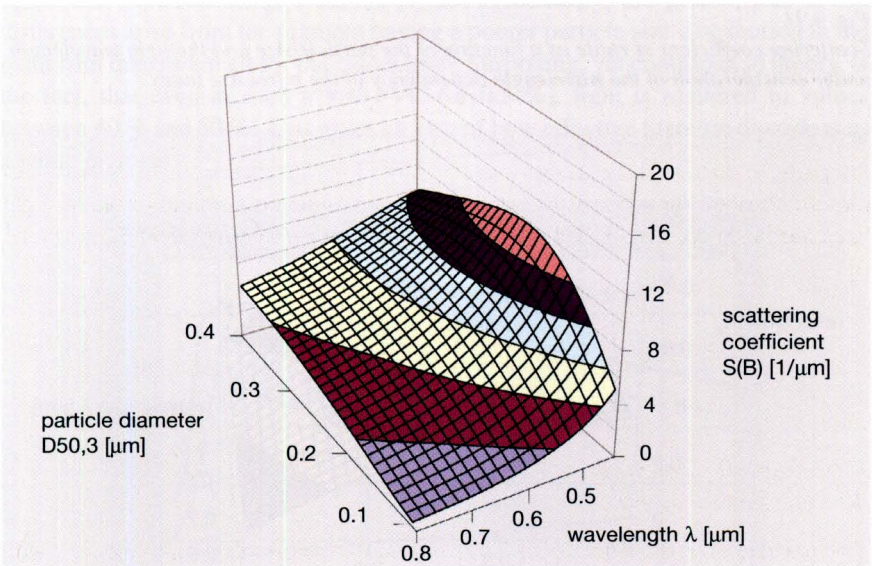

Fig. 4.10
Scattering coefficient of anatase as a function of the particle size and the light wavelength under consideration of the wavelength dependency of the refractive index.

4 Although 0.22 µm is the optimal particle size for the light scattering, the best scattering efficiency is found in an actual pigment sample if the weight average of the particle size is approximately 0.28 µm.

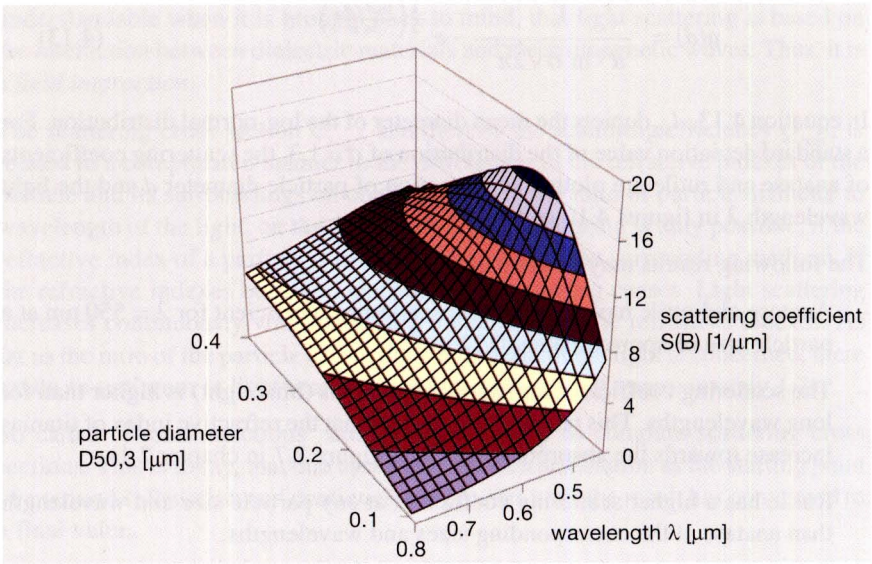

Fig. 4.11
Scattering coefficient of rutile as a function of the particle size and the light wavelength under consideration of the wavelength dependency of the refractive index

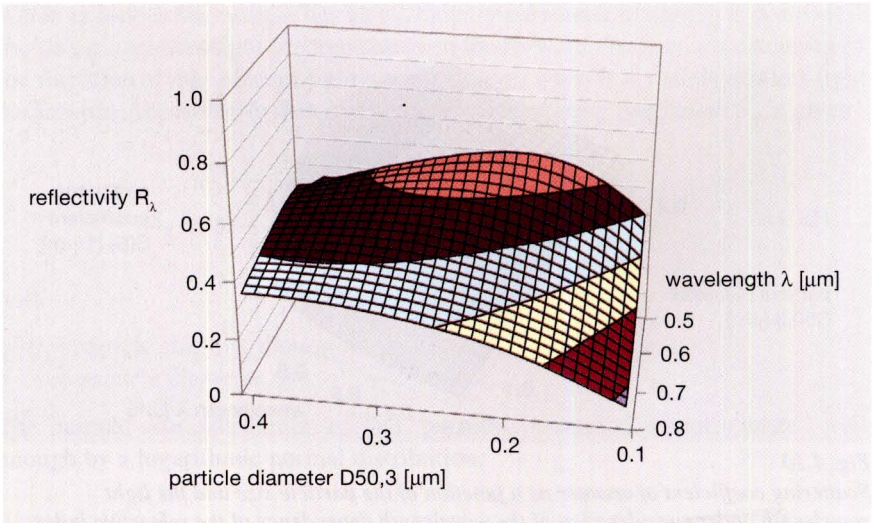

Fig. 4.12
Reflectivity of rutile (PVC 0.5%) as a function of the particle size and the light wavelength and under consideration of the wavelength dependency of the refractive index

Because of the lower scattering coefficients, anatase pigments have lower hiding power (see chapter 4.7) than rutile. Their use is therefore normally limited to applications, in which their lower Moh's hardness presents an advantage.

Following Palmer [5], the *reflectance* R_λ of light from a paint film can be calculated as a function of the pigment volume concentration *PVC* and the layer thickness h of the paint film, if the scattering coefficient S_B is known:

$$R_\lambda = \frac{S_B \cdot PVC \cdot h}{2 + S_B \cdot PVC \cdot h} \tag{4.14}$$

An example is shown in figure 4.12 as the result of a calculation for a rutile pigment with a PVC of 0.5 % and a layer thickness of 50 µm.

Figure 4.13 shows a comparison of measured and calculated results. Next to the experimentally accessed remission curve of a standard rutile pigment in an alkyd paint at that PVC and a paint film thickness of 53 µm, the calculated remission curve of a (weight average) particle diameter of 0.33 µm is presented. The agreement between the two curves is fair. Presumably, the greater part of the differences arise from the pigment having a poorer particle size distribution in the paint film than assumed for the calculation. Surprising, yet compliant to theory, is the fact, that even at such a low PVC (of 0.5 %), light is scattered to values between 40 % and 50 %! This gives an idea of how effective titanium dioxide is as a white pigment.

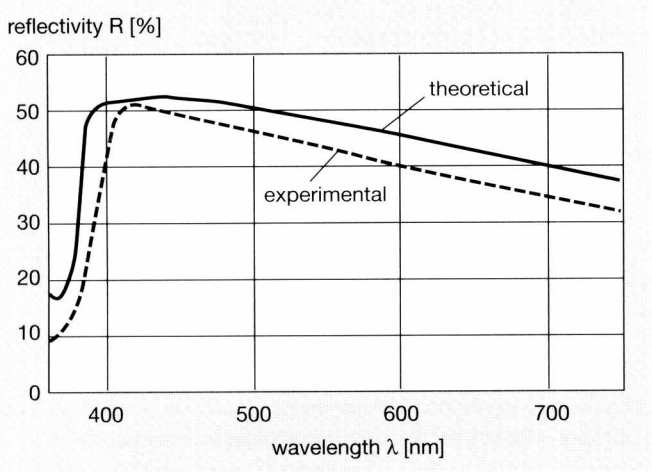

Fig. 4.13
Reflectivity of a rutile-pigmented coating, measured and calculated (conditions as stated in the text)

4.4.1 PVC-depency of light scattering

As said before, an important result of the Mie theory is that pigment particles scatter light out from a space that exceeds their own geometrical volume. When pigments are separated to a distance of, say, more than twice or thrice their own diameters, every particle is able to scatter light without interfering with its neighbors.

So, when the spectral scattering coefficient (see chapter 4.5) of a paint film is determined as a function of the PVC of titania in the formulation (figure 4.14), there is at first a linear relationship. But at a PVC of approximately 10 to 15 % upward, the pigment particles by chance come to rest so close to each other, that the scattering volumes begin to overlap.

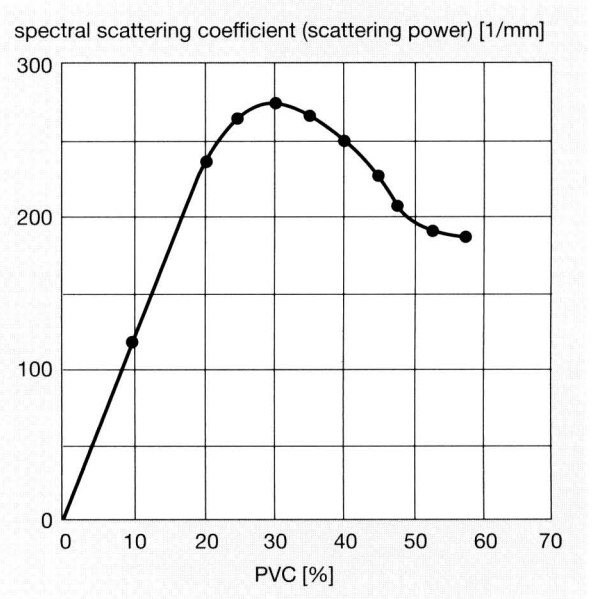

Fig. 4.14
Dependency of the spectral scattering coefficient on the pigment volume concentration (experimental values for a commercial rutile pigment)

The particles effected by this no longer contribute a 100 % share to light scattering efficiency, but less. The scattering coefficient therefore no longer increases linearly, but less than proportional to the increasing pigment load.

At a PVC of about 30 %, it comes to the point where further pigment additions not only contribute less to scattering themselves, but also abate the scattering power

of the particles already present. As a result, the *spectral scattering power* (see chapter 4.6) and, with it, *hiding power* (see chapter 4.7) actually decrease with a further increase in PVC. The paint film really becomes more transparent!

This reduction in scattering power continues until, at the critical PVC, not enough resin is present to completely coat the pigment's surface. From the critical PVC onwards, more interfaces between pigment and air come into being, so that the relative refractive index rises appreciably. Coatings that are over-critically pigmented have what is called "dry hiding". In this type of paints, fillers with refractive indexes of about 1.6 can act as white pigments. This is, for example, the case in emulsion paints, where calcium carbonate, with its refractive index of 1.6, is extensively used for that reason[5].

From these findings, it is immediately clear that titania pigments can only display optimal optical behavior, if the pigment particles are not attached to each other due to poor dispersion or flocculation. Instead, it is desirable for titanium dioxide pigments to be well dispersed and stabilized against flocculation, regardless of the system in which they are used.

4.5 Kubelka-Munk theory; relative scattering power

The Kubelka-Munk theory enables the description of general light absorption and light scattering properties of paints, plastics and other pigmented systems with the help of measurements of their reflectivities. The Kubelka-Munk theory is a so called "phenomenological" theory. This means that it is only descriptive and makes

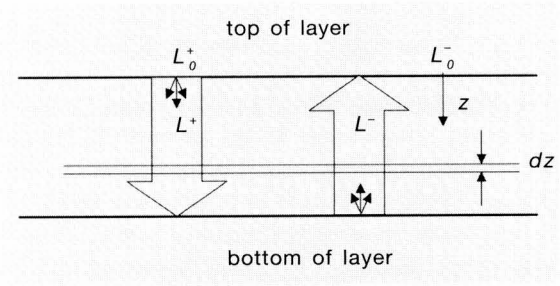

Fig. 4.15
Principle scheme for the deduction of the Kubelka-Munk function; 2-channel theory; balancing of light fluxes

5 The same phenomenon is in effect when writing on a blackboard with a wet piece of chalk. Only when the water has dried off does the writing become visible.

no assumptions concerning the physical reasons for light absorption or light scattering.

Its result, the Kubelka-Munk equation, is one of the most important colorimetric relations in pigment technology, since it allows the determination of both the coloring ability of colored pigments and the scattering power of white pigments in pigmented materials. The theoretical approach consists in the definition and the balancing of radiation fluxes that occur when light penetrates a pigmented object.

In the simplest case, the so called "two-flux-theory", only diffuse radiation is considered that falls on a pigmented layer and penetrates it. The radiation (light in this case) is characterized by its "flux density", i.e. its energy distribution.

The ray moving in the forward direction gets the index plus (variables used as in [6]). The one moving in the backward direction gets the index minus. The *spectral absorption coefficient K* is defined as the relative decrease of the flux density due to absorption while passing through the film;

$$K = \frac{1}{L} \cdot \frac{dL}{dz} \Big/_{abs} \tag{4.15}$$

Analogously, the *spectral scattering coefficient S* is defined as the decrease in flux density due to light scattering:

$$S = \frac{1}{L} \cdot \frac{dL}{dz} \Big/_{scat} \tag{4.16}$$

K and S therefore carry the dimension of a reciprocal length.

The ray moving in the forward direction (into the film) suffers a loss of flux density both by absorption and by light scattering, but is intensified by backscattering of the radiation flux that is leaving the film, $S \cdot L^-$

$$\frac{dL^+}{dz} = -(K + S) \cdot L^+ + S \cdot L^- \tag{4.17}$$

For the ray moving in the backward direction (out of the film), an analogous balance arises.

$$\frac{dL^-}{dz} = (K + S) \cdot L^- + S \cdot L^+ \tag{4.18}$$

By dividing equation 4.17 by $S \cdot L^+$ and equation 4.18 by $S \cdot L^-$, one gets:

$$\frac{1}{SL^+} \cdot \frac{dL^+}{dz} = -\frac{(K+S)L^+}{SL^+} + \frac{SL^-}{SL^+} \tag{4.19}$$

and

$$\frac{1}{SL^-} \cdot \frac{dL^-}{dz} = \frac{(K+S)L^-}{SL^-} - \frac{SL^+}{SL^-} \tag{4.20}$$

The quotient SL^- / SL^+ is the *reflectivity* ρ_∞ that an optically completely hiding film has due to light scattering. Within the film, there is a balance between both flux intensities, the one in the forward and the one in the backward direction. So, by equating 4.19 and 4.20 and substituting SL^- / SL^+ by the reflectivity ρ_∞ of the completely hiding paint film, the Kubelka-Munk function is obtained:

$$\frac{K}{S} = \frac{(1-\rho_\infty)^2}{2\rho_\infty} \tag{4.21}$$

This equation is used to both determine relative color strengths as well as relative scattering powers of pigments. For that, it is customary to assume that absorption processes in materials may be ascribed completely to the colored pigments, whereas scattering phenomena are due to the presence of white pigments. So, by leaving the pigmentation level of colored pigments constant, but using different white pigments in a formulation, the relative scattering power S_{rel} is determined by the quotient of the two K/S values. Multiplication with 100 yields results in percent.

$$S_{rel} = \frac{(K/S_{reference})}{(K/S_{sample})} \cdot 100 = \frac{S_{sample}}{S_{reference}} \cdot 100 \tag{4.22}$$

This value is commonly employed by TiO_2 pigment producers as a specified product property in delivery certificates and in product brochures. Relative scattering powers are based on randomly selected reference TiO_2 pigments and are therefore unsuited for the direct comparison of pigment grades from different suppliers. The standard ISO 787, part 24, only requires the reference pigment to have a TiO_2 content of at least 95 %. Furthermore, it is to be kept in mind that light scattering depends upon pigment loading. ISO 787, part 24, recommends a PVC for the white pigment of 17 %. This value is above the PVC at which the spectral scattering coefficient is still proportional to pigment loading (see chapter 4.4.1).

The relative scattering power may also be ascertained following the "*gray paste method*" (DIN 53165), which coincides with DIN ISO 787, part 24, in its main aspects.

Finally, it should be emphasized that, when evaluating the performance of a pigment by these methods, care has to be taken that no flocculation takes place. Flocculated systems are sub-optimal both in view of light absorption (effected by colored pigments) and light scattering ability (effected mainly by white pigments).

If the colored pigment flocculates, the absorption coefficient is reduced and the color of a pigmented material becomes less saturated. The opposite happens when a selective white pigment flocculation takes place; the color becomes more saturated.

Equation 4.21 is especially interesting, since it renders the impression that an observer has when viewing a colored object. With this knowledge, it is not surprising that, in pigmented systems, the colors remain unchanged if the relation between the amounts of colored and of white pigments are kept constant. So when, from an esthetic point of view, the right color has been found (or matched), the hiding power (see chapter 4.7) can easily be lowered or increased just by putting in a lower or greater amount of pigment mixture, thereby leaving the relative ratio of the different pigments unchanged.

4.6 Determination of the spectral scattering coefficient

Absolute values of the spectral scattering coefficient can also be ascertained. For that, one needs either a completely hiding paint film and a non-hiding film over a randomly colored substrate, or a non-hiding paint film over a black and a white substrate [7]. The procedures are partially fixed in industrial standards.

Thus, DIN 55 984 describes the determination of the spectral scattering coefficient from measurements on a hiding and (at least) three non-hiding layers of paint. For the algorithms, the standard itself should be referenced.

All methods employed have in common that they require some experience in order to yield reliable and meaningful results.

Whereas titanium dioxide pigment producers may be especially interested in the scattering power of their pigments, for the pigment user, the hiding power (in paints) or the lightening power (in plastics) is of greater interest.

4.7 Hiding power

4.7.1 Standardized methods for determining hiding power

The hiding power of a paint is defined as its ability to cover the color or color differences of substrates, on which they are applied.

Both light absorption and light scattering contribute to hiding. Light absorption is, as a matter of fact, a very efficient contribution to hiding. Hiding is expressed as square meter per liter, or square meter per kilogram of dry paint. In American standards (e.g. ASTM D 2805), square feet per gallons is used alternatively.

According to DIN 55 984, hiding power is determined from the spectral scattering coefficient (of equation 4.21) and the reflectivity of an optically completely hiding paint film.

$$D = (c_1 \cdot \rho_\infty^{\,2} + c_2 \cdot \rho_\infty + c_3) \cdot S \qquad (4.23)$$

The factors c_1 to c_3 depend upon ρ_∞ and are listed in tables of the cited standard. The factors are such, that the term in parenthesis of equation 4.23 becomes larger when the remission decreases. Therefore, the hiding power D increases with increasing scattering coefficient and decreasing reflectivity (= increasing light absorption of a completely hiding paint film).

In reflectivity measurements, the reflectivity ρ is always corrected for the inherent surface reflection of 4 % (Saunderson correction) if the measurement was not taken with a gloss trap that blocks the specular beam from the detector in the photometer sphere. The Saunderson correction, that is deducted from the measured reflection, takes into account that, according to the Fresnel equation, every material with a refractive index n exhibits a reflection R of

$$R = \frac{(n-1)^2}{(n+2)^2} \qquad (4.24)$$

If a value for n of 1.5 is set into equation 4.24 – which is accurate enough for almost all polymeric materials – R becomes 0.04 or 4 %.

In the United States of America, hiding power is referred to as "spreading rate" and is mainly determined by the procedure described in ASTM D 2805. A paint is applied to black and white paper charts or black and white glass panels. The film thickness is calculated by the density of the applied paint film and its weight. As a criterion for hiding, the contrast ratio C is determined, which is defined as the quotient of the reflectivity over the black substrate R_B and the reflectivity over the white substrate R_W.

$$C = \frac{R_B}{R_W} \tag{4.25}$$

The spreading rate H of a paint is calculated using the formula

$$H = \frac{A \cdot N \cdot D}{10 \cdot M} \tag{4.26}$$

by inserting the following variables in the physical dimensions listed:

H = spreading rate corresponding to a contrast ratio; m^2/l
A = template (= covered substrate) area; cm^2
N = nonvolatile content of the paint (decimal fraction)
D = paint density; g/ml
M = dry film weight; g

For complete hiding, the contrast ratio should be 0.98 (or 98 %). The corresponding spreading rate can be calculated from equation 4.26, using the appropriate input data for that paint.

So, ASTM D 2805 answers the question, with what dry paint film thickness complete hiding can be obtained. This is a measure for the cost effectiveness of a paint (and a pigment).

In Europe, two standards are mainly used to determine hiding power: DIN 55 987 and DIN 55 601.

As far as the experimental procedure is concerned, DIN 55 987 is very similar to ASTM D 2805. Paint films of varying film thickness are applied to black and white paper cards, and the color distance ΔE_{ab} between black and white is determined (ISO 7724, part 3). ΔE_{ab}-values are then plotted against the reciprocal dry film thickness (in mm) or against the reciprocal surface weight of the paint (in m^2/kg) [9]. By extrapolation, the value of the hiding power is found, at which $\Delta E_{ab} = 1$ (or another value agreed upon by the parties involved).

By experience, however, at least in the case of TiO_2, color differences of $\Delta E_{ab} = 1$ are easily detected by the eye, so it may be wiser to use $\Delta E_{ab} \leq 0{,}5$ as a better criterion for complete hiding.

In the standard DIN 55 601, hiding power is accessed with the help of a metal block, in which a path is tapered lengthwise, similar to a Hegman gage (ASTM D 1210), only that there are two parallel black and white glasses placed on the bottom of the channel. One drop of the liquid paint is placed in the deep end of the groove and drawn with a scraper (like with a Hegman gage, ASTM D 1210, or a Grindometer, DIN 53 203) through the channel. Afterwards, the paint is allowed

to dry and then, by visual means, the place along the channel is detected, where the contrast ratio appears to be one. At that point, the film thickness is determined using a light section microscope. Hiding power H is calculated from the reciprocal value of the dry film thickness X_D.

$$H = \frac{1000}{X_D} \tag{4.27}$$

If in equation 4.27, X_D is inserted with the dimension µm, then H comes out as m^2/l. (Example: for X_D = 100 µm the hiding power is 10 m^2/l).

The procedure according to DIN 55 601 is, however, less in use, since in practice, it has turned out that its accuracy is not as good, and because the bedding of the glass inlays tends to change due to swelling by solvents and because of the influence of heat, for example when baking enamels are tested. A comparison of the different methods to access hiding power is given in [8].

4.7.2 Hiding power of sulfate and chloride grade pigments

Table 4.1 shows in an exemplary fashion that – as said in the preceding chapter – hiding power (= "spreading rate") depends not only on scattering power, but also on the absorption of the pigments. The absorption is physically expressed with the aid of the reflectivity at infinite film thickness ρ_∞ (i.e. at complete hiding). Another sensible measure is also the yellow tint b* (see chapter 4.1).

Generally, titanium dioxide pigments produced via the sulfate route tend to have slightly lower scattering power than pigments from the chloride process. The reason for this is that the control of particle size distribution is more difficult in the sulfate process because of sintering of the particles during calcination and, maybe, because the primary particles are less spherical than those from the chloride process. On the other hand, sulfate pigments are somewhat more yellow than chloride pigments (compare b* values in table 4.1), which is due to impurities by other metal ions in the crystal lattice of the titania.

With regard to hiding power, chloride and sulfate grade pigments are therefore usually comparable. Because of their (hardly noticeable) higher yellow tint, sulfate pigments with up to 10 % less scattering power than chloride pigments nevertheless reach the same hiding power. Table 4.1 shows that even the products of the producer "E", which have extremely low scattering powers, are at least in the midfield in terms of hiding power due to their considerable yellow tint b*.

Not in principle contradiction to these statements is the fact, that a number of sulfate pigment producers offer very well milled special grades of pigments for

Producer	Type	S /mm^{-1}	L*	b*	D / m^2/l
A	sulfate	182	95.98	1.14	18.4
B	sulfate	174	95.99	1.16	18.2
B	sulfate	169	95.90	1.21	17.2
B	sulfate	157	95.89	1.33	16.3
C	chloride	193	96.54	0.50	18.1
C	chloride	180	96.41	0.39	17.4
D	chloride	171	96.29	0.51	16.4
B	chloride	169	96.37	0.28	15.7
E	sulfate	135	93.84	4.65	17.1
E	sulfate	125	93.64	4.74	16.1

Table 4.1
Scattering- and hiding-power of some sulfate- and chloride-grade titanium dioxide pigments of different producers. (All samples in the rutile modification.)

use in printing inks. Printing inks require high hiding even at lower film thickness. On the other hand, the abrasiveness is an important issue in order to avoid extensive wear of the print rollers. In that sense, sulfate pigments have a competitive edge.

In colored formulations, sulfate and chloride pigment grades are undistinguishable as far as b* values are concerned. Even the "purest" white colors are generally slightly buffed in order to be able to correct color shades in production. Only on rare occasions is the "cold", blue-tinted white of a pure chloride grade pigment sought for. (But see chapter 4.9 on the topic of carbon black undertone).

4.8 Lightening power

Lightening power is the tinting strength of a white pigment. It is the ability of a pigment to increase the lightness of a colored, gray or black medium.

In the German standard DIN 55 982, lightening power AV (Aufhellvermögen) is defined as the mass ratio of sample pigment to reference pigment put to a colored paste, at which both mixtures have the same lightness L*.

$$AV = \frac{m_r}{m_s} \cdot 100 \qquad (4.28)$$

In equation 4.28 m_s is the weight of sample pigment and m_r is the weight of the reference pigment.

Especially in plastics, where the aim is not to obtain high hiding in thin layers, lightening power is an important pigment property.

Theoretically, lightening power and relative scattering power should run parallel. (The ASTM standard D 2745, "Relative tinting strength of white pigments by reflectance measurements" actually uses the Kubelka-Munk function to calculate relative scattering power, which is there called "tinting strength"). In practice though, AV and S_{rel} do not always correlate. This may have to do with different pigment particle distributions of the pigments in the different resins suggested in the quoted standards. Pigments for plastics and pigments for paints will vary both in their inorganic and organic surface treatments and can therefore perform relatively better in one or the other system.

4.9 Color tint

When different white pigments are dispersed into a paste of colored pigments or carbon black, the resulting colors can be different. This phenomenon is referred to as "color tint" or "*carbon black undertone*" (CBU) of the white pigment.

The reason for the different color tints lies in the particle size dependency of the light scattering of longer and shorter wavelengths by white pigments like TiO_2. The greater the fine sized fraction of the particle distribution is, the more blue light is preferentially scattered.

Figure 4.16 shows the case of a dispersion of carbon black with a titanium dioxide that scatters blue light relatively better than green or red light. In this example, the green and red light rays cover a longer distance within the film before they leave it again. Because of this, they suffer a greater loss in intensity via absorption by the carbon black particles. Therefore, more blue, less green and an even lesser

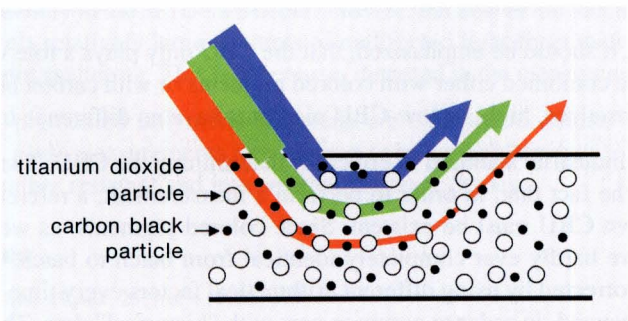

Fig. 4.16
Light scattering from a pigment with a high CBU (schematically)

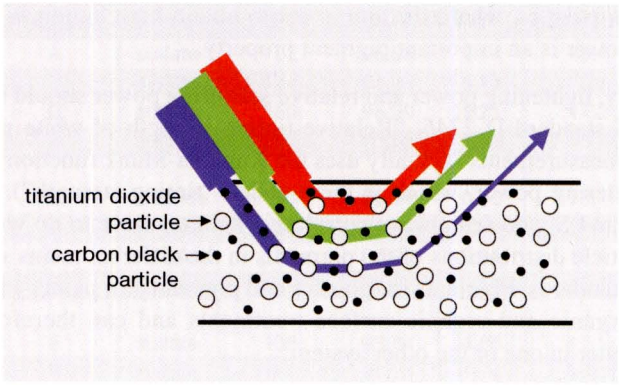

Fig. 4.17
Light scattering from a pigment with a low CBU (schematically)

amount of red light leaves the film. An observer then has the sensation of viewing a blueish-gray color.

A titanium dioxide pigment that has a coarser particle size distribution conversely scatters red and green light preferentially. In this case, the blue light with its shorter wavelength passes a longer distance through the material and is therefore absorbed to a greater extent (compare figure 4.17); the gray paste appears yellowish-gray.

A gray color with a blue tint appears fresher to the human eye than one with a yellow tint. Yellow tinted colors have a "stained" appearance. For this reason, standard TiO_2 pigment grades do not fall below a certain CBU value.

Although the particle size distribution is more or less easily controlled to get a fine particle size and, thus, a higher CBU, this leads at some point to a loss of scattering power for longer wavelengths and, thereby, to reduced hiding power.

Once again, it should be emphasized, that the CBU only plays a role when white pigments are combined either with colored pigments or with carbon black. When used by themselves, high- or low-CBU pigments have no difference in color tint.

There is no industrial standard in effect for determining the CBU. The reason for this lies in the fact that, in order to perform a measurement, a reference sample with a known CBU must be existent. Since colored pigments, as well as white pigments, are hardly ever completely identical from batch to batch, differences have to be corrected by using different arithmetical factors every time a reference sample is changed, in order to compare new with "historical" data. This is barely possible within an enterprise, but impossible in industry as a whole.

4.10 Gloss and haze

The gloss of titanium dioxide pigmented coatings is – just like with other pigments and fillers – strongly dependent both upon the particle size distribution and the state of dispersion of the pigment.

A conventional, high quality TiO_2 pigment has a mean particle diameter (weight average) of approximately 0.3 µm. The particle size distribution should not exceed the 1 µm limit in order to be useful for high gloss coatings.

Standardized gloss measurement instruments named "reflectometers" illuminate surfaces at incident angles of 20°, 60° and 85° and detect the reflected light intensities at the corresponding angles of reflection (DIN 67 530, ISO 2813). High gloss surfaces exhibit a 20° gloss value of more than 95 %, based on a polished black glass as a reference. In the high gloss region, coatings will differ in the so called haze [10, 11,12]

Haze is a measure for how much of the flux of the incident light is reflected just barely outside the angle of reflection in relation to that reflected ideally. A larger haze manifests itself in such a manner, that the image of an object mirrored on the surface does not have clear contours. (Very nice pictures of this phenomenon are found in the ASTM standard D 4449 "Visual Evaluation of Gloss Differences Between Surfaces of Similar Appearance", especially figures 2 and 3 therein). The name "haze" is more or less self explanatory. Haze measurements are standardized in ASTM E 430 and ASTM D 4039.

Newly developed instruments on the market determine surface roughness and corrugation of surfaces by laser-optical means and calculate a DOI-value (*distinctness of image*) that is supposed to correlate with 20° reflectometer values.

A paint film with titanium dioxide will never achieve such low hazes as, for example, a paint film with a finely divided carbon black. The reason for this is to be sought not only in the difference in particle size, but also in the fact that titanium dioxide expels relatively large amounts of undirected light from materials due to (diffuse!) light scattering. This is, of course, detected in the measurement of haze.

When TiO_2-pigmented polymeric materials are exposed to natural or artificial weathering, gloss measurements have proven to be a reliable means to distinguish between weather resistant and less weather resistant grades.

References

[1] G. Mie, Ann. Physik, 25, No. 4 (1908) 377

[2] M. Kerker, "The scattering of light and other electromagnetic radiation", Volume 16 of Physical Chemistry, E. M. Loebl Editor, Academic Press Inc., New York, 1969

[3] C. F. Bohren, D. R. Huffman, "Absorption and Scattering of Light by Small Particles", John Wiley & Sons, New York, 1983

[4] C. F. Bohren et. al., Am. J. Physics 55, No. 6 (1987) 524

[5] B. R. Palmer et al., J. Coatings Technol. 61 (1989) 41

[6] H. G. Völz, "Industrielle Farbprüfung", Verlag Chemie, Weinheim, 1990, p. 55 .

[7] H. G. Völz, "Industrielle Farbprüfung", Verlag Chemie, Weinheim, 1990, p. 71 .

[8] M. Cremer, Progress in Organic Coatings, 9 (1981) 241

[9] H. G. Völz, FARBE&LACK 71 (1965) 725

[10] H. Becker et al., FARBE&LACK 74 (1968) 145

[11] U. Zorll, FARBE&LACK 79 (1973) 191

[12] F. Fensterseifer, Metall-Oberfläche 42 (1988-1989) 3

5 Photocatalytic properties of titanium dioxide

5.1 Chalking cycle

As stated in chapter 2.1, "Physical properties", titanium dioxide is a photosemiconductor both in the anatase and the rutile modification. To describe electrical properties of semiconductors, the band model [1] is usually used.

When titanium dioxide is thought of as an ionic crystal, the binding electrons are ascribed completely to the oxygen atoms. Following this formalism, the crystal matrix consists of O^{2-}-ions and Ti^{4+}-ions. At the surface, the crystal lattice terminates with OH-groups, that are consequently seen as OH^--ions.

In the band model of chemical bonds, the oxygen atoms occupy the lowest energy levels in the crystal lattice and therefore hold the electrons with them. These binding electrons are located in the so called "valence band".

The absorption of UV-light by titanium dioxide leads to a charge separation within the crystals. By this absorption, binding electrons are hoisted into a higher energy level, where – similar to the conditions in a metal – they can move freely. That's why this energy band is termed "conductive band" or "conduction band". In the event of such a charge separation, a positively charged "hole" remains in the valence band, that can carry current by taking an electron from one of the neighboring ions.

The separated electron/hole pair is called "exciton" (from Latin: excitare = excite, stimulate) [2], and – in the case of titanium dioxide – is chemically a very reactive state. The reactions that evolve from excitons in titania lead to the degradation of the polymeric materials, in which the pigments are normally embedded. This again results in gloss reduction and "chalking" of the materials. The expression "chalking" comes from the fact, that in such weathered materials, the TiO_2 pigment particles are no longer firmly fixed in the polymer matrix and are therefore easily wiped off, leaving a trace on, for example, the hand, as if chalk had been wiped from a blackboard [3].

The chemical reactions that lead to chalking were satisfactorily explored only in the seventies of the 20th century. This was made possible by utilizing electron spin resonance spectroscopy (ESR, with which radicals can be identified) in artificial weathering experiments under selective exclusion of oxygen and/or water molecules [4].

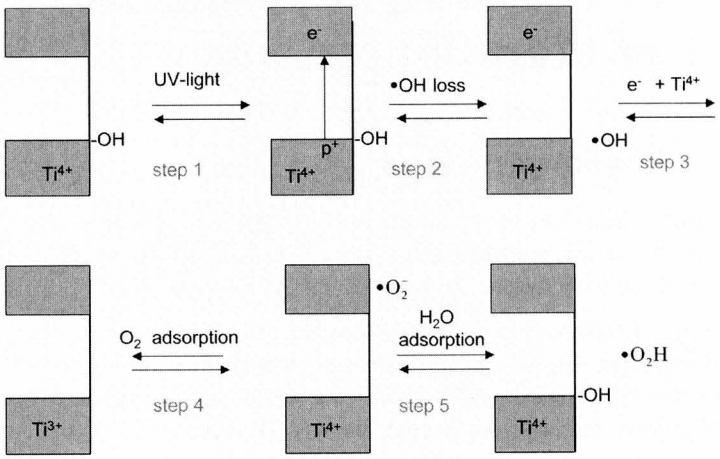

Fig. 5.1
The chalking cycle

Figure 5.1 shows a graphical representation of the four separate steps involved in the chalking cycle. In the first step (step 1) the charge separation - as explained earlier - takes place in the titanium dioxide particle. The exciton is formed with an electron e^- in the conductive band and a positive hole p^+ in the valance band.

$$TiO_2 + h \cdot v \rightleftarrows TiO_2(e^- + p^+) \qquad \text{(step 1)}$$

In the next step (step 2), the hole oxidizes a hydroxyl ion at the surface, thereby generating a hydroxyl radical:

$$p^+ + OH^- \rightleftarrows \bullet OH \qquad \text{(step 2)}$$

Hydroxyl radicals are viciously reactive and attack polymer molecules easily. Normally, this first leads to the abstraction of hydrogen radicals from the polymers under the formation of H_2O and a polymer radical R•.

The R• radical further reacts, for example, with oxygen atoms to peroxy radicals R–O–O•, or by decomposition into a further, different radical (R• $\rightarrow$ R_1• + R_2•). Through the annihilation of the hole by the electron of the hydroxyl anion at step 2, there remains a surplus of one electron in the conductive band of the titanium dioxide crystal. This electron can reduce Ti^{4+} to Ti^{3+} in the next step (step 3).

$$Ti^{4+} + e^- \rightleftarrows Ti^{3+} \qquad \text{(step 3)}$$

The Ti^{3+} cation can be oxidized again in a further step (step 4) either by already present, or by freshly adsorbed oxygen, yielding Ti^{4+} and an oxygen anion radical.

$$Ti^{3+} + O_2 \rightleftarrows Ti^{4+} + \bullet O_2^- \qquad \text{(step 4)}$$

The oxygen anion radical generated in such a way is adsorbed to the titania surface. Only in the presence of moisture can the then following step (step 5) take place. In this step, by the reaction of $\bullet O_2^-$ with H_2O, a hydroperoxy radical is formed, that can desorb and again attack the polymer, and a hydroxyl anion, that reacts with the titanium dioxide and restores the terminating surface hydroxyl group that was extracted in step 2.

$$Ti^{4+} + \bullet O_2^- + H_2O \rightleftarrows Ti^{4+} + OH^- + \bullet O_2H \qquad \text{(step 5)}$$

Thus, the chalking cycle is completed. All in all, two radicals were formed according to the following reaction scheme, using UV-light and TiO_2 as a catalyst:

$$H_2O + O_2 \xrightarrow{TiO_2 + h\nu} \bullet OH + \bullet O_2H \qquad \text{(step 6)}$$

Materials are not always stressed both by sunlight *and* moisture. For that reason, the photostability and weatherability of TiO_2 pigments are generally distinguished from each other, and appropriate tests are used. Photostability is referred to when only UV-light was active in the test. For testing weatherability, the joint influence of UV-Light and moisture, either in the form of (artificial) dew or (artificial) rain, is determined.

The difference is easily understood with the aid of the chalking cycle. The reaction scheme highlights that in the absence of oxygen and, in particular, water, the chalking cycle proceeds only up to step 3, the generation of Ti^{3+}. Ti^{3+} can be detected using ESR spectroscopy [4]. The additional electron in Ti^{3+} in comparison to Ti^{4+} has its energy level between the valence band and the conductive band of TiO_2, namely pretty close to the conductive band. The excitation energy into the conductive band corresponds (according to equation 4.7) to an absorption of green light. This leads to the intensive violet color of Ti^{3+}. That is the reason why materials pigmented with TiO_2 obtain a blueish-gray color when Ti^{3+} is formed. This behavior is made use of in accelerated tests for monitoring photoactivity. Normally, the discoloration is taken as a measure for that property [5].

When testing the weatherability, light, oxygen and moisture must be present so that steps 4 and 5 of the chalking cycle may take place. If either of the two atmospheric molecules are absent, the titanium dioxide protects the polymer from degradation instead of attacking it photocatalytically, regardless of the quality of its stabilization by crystal lattice doping or inorganic surface treatments [4].

In that case, only the O_2 and H_2O present at the beginning can react according to the steps 4 and 5. When these are used up, the reaction comes to a halt at step 3. As a consequence, steps 1 and 2 are discontinued, since all steps are equilibrium reactions that can only progress if the cycle is allowed to reach its end.

The degradation of the polymer under the influence of light, oxygen and water is normally not accompanied by a discoloration, since the intermediately evolving Ti^{3+} is constantly re-oxidized. Yet, the gloss is reduced due to increased surface structuring during polymer degradation and, with progressing destruction, the surfaces begin to chalk. Some polymers turn yellow, as chromophores, such as conjugated double bonds, are formed in the polymer.

Chalking can be determined by a number of different methods. Either a transparent tape is applied to the surface of the chalking item, which is then pulled off and the transparency loss of the tape is measured (DIN 53 223) or, otherwise, a black photographic paper (photographic paper exposed to light and then developed) is pressed onto the surface and the lightening effect on the paper is measured. (DIN 53 159). In DIN 53 159, the photographic paper is pressed to the surface with a defined force using a lever apparatus ("Kämpf Stempel").

ASTM D 4214 recommends a number of different tests. First, the "wet finger test" where a finger tip is moistened and rubbed on the surface for 2 to 2.5 inches (50 to 65 mm) and the rub off on the finger is compared with a reference given in the standard. Secondly, the "transparent tape method", where the tape is pressed onto the surface to be tested, then removed and adhered to black masking tape, before measurements of lightness are performed. Thirdly, a set of five different test methods, depending on the substrate used. Four of these are comparative, i.e. the surface is rubbed either with a moist finger, a black velvet cloth or, otherwise, a transparent tape is used to gain a sample. The results are then visually compared with photographic references given in the standard. One procedure also uses transparent tape, but evaluates chalking quantitatively by measuring the reflectance R_λ over a black background.

5.2 Photoactivity of anatase and rutile

From experience, anatase pigments are generally much less photo- and weather-resistant than rutile pigments. At first glance this is surprising. In figure 5.2, the spectrum of the sunlight as it reaches the surface of the earth is shown [6]. The absorption edges of rutile (415 nm) and anatase (385 nm) are also denoted in the graph. As for the location of the absorption edges, anatase should develop a lot less excitons (step 1 of the chalking cycle) in natural weathering than rutile, because there are less photons of higher energy on their way.

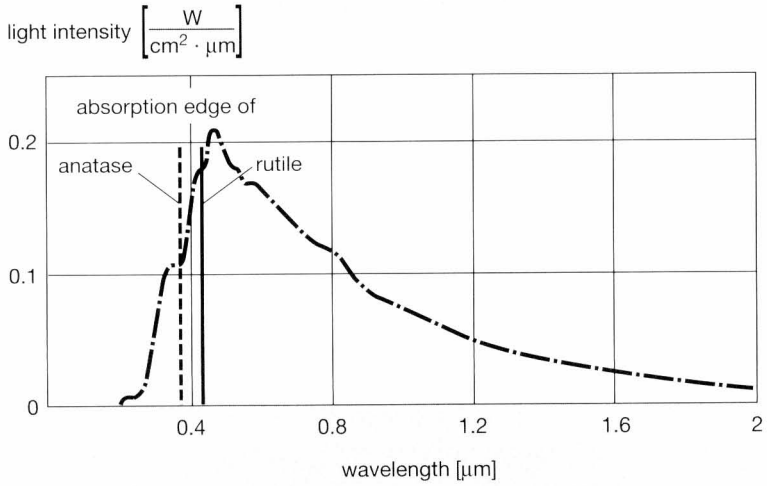

Fig. 5.2
Global solar radiation on the surface of the earth and absorption edges of rutile and anatase

The puzzling about the role of the OH-groups on the surface of the pigments in this context is certainly not over. Anatase and rutile do differ somewhat in the OH-group density of their surfaces. One finds approximately 6 hydroxyl groups per nm^2 on rutile and about 7 to 8 hydroxyl groups on anatase [7]. Yet, it has been reported that the photoactivity of anatase decreased with increasing hydroxyl-group density [8, 9], whereas in rutile it was just the opposite [9]. The fact that TiO_2 surfaces possess acidic as well as basic hydroxyl groups that might behave differently in step 2 of the chalking cycle [10, 11] complicates matters further.

Not only TiO_2 core particles, but also surface treated titanias usually have acidic next to basic hydroxyl groups as well [12]. By the way, inorganic surface treatments, that generally enhance weather resistance, tend to slightly increase the OH-group density to approximately 8 to 9 OH-groups per nm^2.

The momentarily probably most plausible explanation for the enhanced photoactivity of anatase was proposed by Gesenhues [14]. The difference between the absorption edge of anatase (3.15 eV) and rutile (3.02 eV) is 0.13 eV. According to Gesenhues, the energy levels of the conduction bands of rutile and anatase are approximately the same, so that the energy level of the valence band of anatas should lie lower by that value. Therefore, the hole that is generated when an exciton is formed should have a lower potential (approximately -215 mV) than the hole in the case of rutile. Due to general interrelations [15], the hydroxyl

radicals formed in step 2 of the chalking cycle also have a lower potential in the case of anatase and are therefore more oxidizing, i.e. more electron drawing, than in rutile.

5.3 Accelerated and natural weathering

It would be desirable to generally always test the fastness of pigments or of pigmented materials, respectively, under natural conditions, i.e. using the same influences that they would be exposed to in practical use. Unfortunately, for durable, long lasting systems, for which especially this property is important, there is normally not the time to do this.

Furthermore, there is no such a thing as an "absolute weather resistance".

For example, in natural weathering, the order of weather resistance found for a set of samples can be different from location to location. Well known exposition sites are Arizona (desert climate, dry, with large temperature changes) and Florida (maritime climate, humid and warm, with high solar irradiation). But, by experience, even in Germany, the home of the author, there are often differences, depending on the location of the exposure (at the North Sea coast, at the lower Rhine area or in the Black Forest), even though the climates in these areas are a lot more alike than, say, that of Arizona and Florida.

Furthermore, the fate of a coating during natural weathering depends not only on paint preparation and its ingredients, but also on the time of year when the weathering was initiated. Finally, even at the same place, the weather is different from year to year.

Although it is well known that illumination, oxygen concentration and moisture have a large influence on the chalking cycle, it is hardly possible to either predict the effect of each parameter, nor is it possible to later on explain exactly which influence caused which reaction. (This is naturally only correct with this stringency when "comparable" pigments are tested, so not, for example, an anatase against a rutile).

Therefore, accelerated weathering is widely employed. In this connection, the illumination used should match the relative intensity distribution of solar radiation, at least in the UV-region. This is the case when, for example, either high pressure xenon arc lamps or xenon- or mercury-vapor lamps in combination with adequate optical filters are used [16]. Degrees of freedom exist in the selection of the succession of irradiation and moisturizing, though, either as rain or dew. Bedewing is more aggressive than sprinkling water [17], since isolated water molecules can

penetrate a paint film or a plastic part more easily. The temperature also plays a significant role. Elevated temperatures have an accelerating effect [17]. This is, however, generally true, and not only in the presence of TiO_2 [18].

Highly durable systems (e.g. isocyanate crosslinked acrylates) need approximately 2000 hours (6 weeks) in an accelerated weathering cabinet in order to obtain relevant results. Less durable systems (e.g. air drying alkyds) are finished after about 500 hours. In any case, a standard should be tested in every weathering series, since – especially because of fluctuations in illumination intensity – different runs normally cannot be compared directly with each other.

It is generally accepted that for the testing of titanium dioxide pigments, natural weathering cannot be completely substituted by artificial weathering. A number of influences, starting from lamps over the temperature up to humidity and pollution, make it difficult to match both methods completely.

If a titanium dioxide pigment acts more as UV stabilizer, or if its photocatalytic properties overwhelm, depends highly upon the durability of the embedding medium.

Even without the presence of pigments, polymers also absorb UV-light, which may lead to their deterioration. Especially weather resistant resins are so by virtue of their transparency for UV-light. In a durable resin, even a highly stabile titanium dioxide pigment will much sooner act as a photocatalyst and enhance degradation, than to offer protection.

Not so in non-durable resins. In this case, titanium dioxide will sooner protect than destroy the resin matrix. If one or the other prevails can be exploited by testing at different TiO_2 PVCs. If the weather resistance (normally expressed as gloss retention) is better or just as well as with a higher PVC, then the protective action overwhelms.

All this leads to the conclusion that – in view of the testing method – it makes sense to test durable TiO_2 grades in durable resins. In non-durable polymers, the differences in durable and less durable titanias are less clear, at least with respect to gloss retention. With regard to chalking, a distinction is more probable in this case, although this only comes into effect at the end of the exposure, when the polymer is already heavily affected.

In the case of plastics, the criterion does not necessarily have to be gloss retention or discoloration (although the latter is commonly used), but the change in mechanical properties may be of interest. An example was reported in [10], where a polyethylene film lost its elongation at break, which was dependent upon the TiO_2 grade used. In the case of coatings, an embrittlement takes place too that eventually leads to cracking (see figure 5.3) of the surface [20].

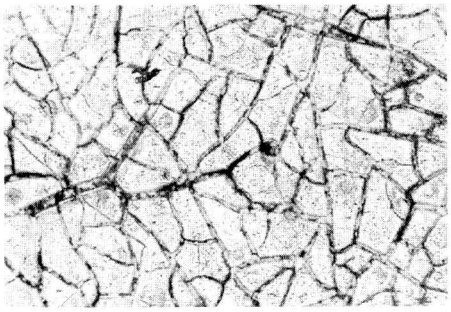

Fig. 5.3
Light-microscopic image of a weathered paint surface

Not only the photoactivity, but also the particle size distribution and the dispersibility of titanium dioxide pigments have a large influence on gloss retention during weathering [21]. The degradation proceeds in the course of weathering from the surface downwards into the polymer. Thereby, in any case, the imbedded pigments will sooner or later protrude the surface. If the pigment particle distribution is finer when this happens, then the surface will be less structured and the gloss will be considerably better. Titanium dioxide particles with sizes exceeding 1 µm in diameter will already have a negative effect on the gloss retention.

5.4 Accelerated tests for monitoring photoactivity

These tests can be distinguished into those, in which a discoloration takes place due to the generation of Ti^{3+}, and those, in which a chemical reaction is catalyzed and the reaction product is detected.

The "lead carbonate test" belongs to the former group. In this test, a mixture of lead carbonate, titanium dioxide and glycerine is illuminated with UV-light, while being kept free of oxygen [5]. The glycerine reduces Ti^{4+} to Ti^{3+}.

In the "isopropanol test", belonging to the second group, isopropanol is oxidized to acetone by UV-irradiation in the presence of TiO_2 [22]. The acetone is easily determined by gas chromatography.

Although both tests yield results within only a few hours, these are to be interpreted with caution. Especially different moisture contents and the presence of traces of oxygen influence the measurements.

References

[1] Ullmann's Encyclopedia of Industrial Chemistry, 5th Edition, VCH, Weinheim, (1993) Vol. A 23, p. 539

[2] Ch. Kittel, "Einführung in die Festkörperphysik", 7th Edition, Oldenbourg Verlag, Munich, (1988), p. 347

[3] H.G. Völz et al., FARBE&LACK 86 (1980) 1047

[4] H.G. Völz et al., FARBE&LACK 82 (1976) 805

[5] U. Gesenhues, FARBE&LACK, 94 (1988) 184

[6] Handbook of Chemistry and Physics, 56th Edition, 1975-1976, CRC Press, Cleveland, F196

[7] T. Rentschler, European Coatings J. 10 (1997) 939

[8] Y. Oosawa, M Grätzel, J. Chem. Soc. Faraday Trans. I: 84 (1988) 197

[9] K. Kobayakawa et al., Ber. Bunsenges. Phys. Chem. 94 (1990) 1439

[10] J. A. Davies et al., J. Colloid Interface Sci. 63 (1978) 480

[11] U. Gesenhues, FARBE&LACK 101 (1995) 7

[12] U. Gesenhues, 19th FATIPEC Congress, Aachen, September 18–24, 1988, Congress Book, Vol. 1, p. 237

[13] T. Rentschler, FARBE&LACK 106 (2000) 62

[14] U. Gesenhues, FARBE&LACK 100 (1994) 244

[15] F. Beck, "Elektroorganische Chemie", Verlag Chemie, Weinheim, (1974) , p. 21-25 and p.63-66

[16] J. Lamaire et al., Kunststoffe 76 (1986) 149

[17] W. Miehlke, P. Trubiroha, Materialprüfung 30 (1988) 10

[18] P. Schutyser, D.Y. Perera, Industrie-Lackierbetrieb 60, No. 11 (1992) 382

[19] R. Wolny, Kunststoffe 76, No. 2 (1986) 145

[20] D. Corless, Surface Coatings Australia, 26, No. 6 (1989) 18

[21] A. Mackor et al., 19th FATIPEC Congress, Aachen, September 18–24, 1988, Congress Book, Vol. 1, p. 197

[22] J. R. Brand, Plastics Compounding, July/August (1987) 27

6 Dispersing of titanium dioxide

6.1 Steps taking place during dispersion

Like all pigments and fillers, titanium dioxide pigment powders consist of primary particles, agglomerates and aggregates (see figure 6.1, DIN 53 206).
By definition, primary particles are the smallest single particles, whereas agglomerates are particles that are associated via their corners and edges. Aggregates, on the other hand, are made up of facially sintered particles.

Agglomerates differ from aggregates in the sense that their surface area is as large as the sum of the surface areas of the primary particles from which they are made up of. Aggregates, contrarily, have a lower surface area.

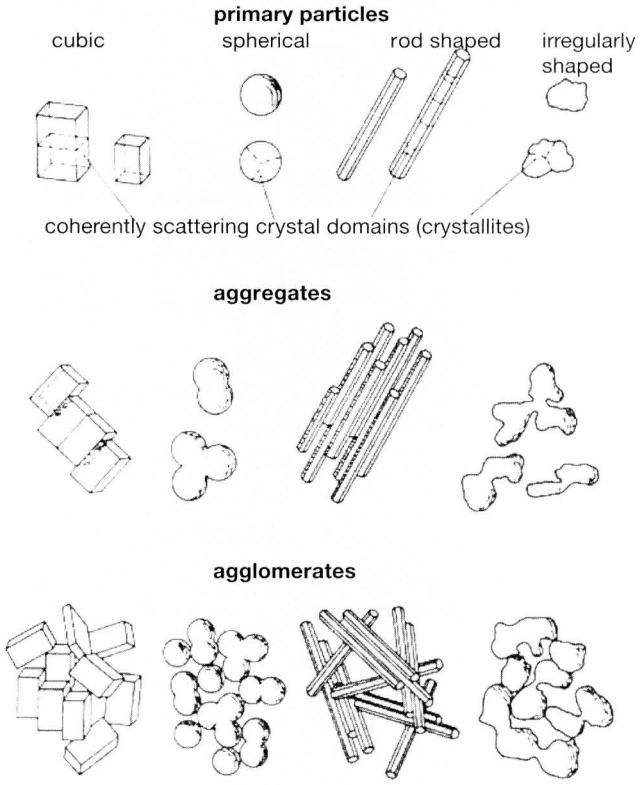

Fig. 6.1
Pigment model of DIN 53 206, part 1

The correct term for the rupturing of agglomerates, for which only adhesive forces have to be overcome, is "dispersing", whereas the disintegration of aggregates, which involves breaking of chemical bonds, is termed "milling".

Agglomerates are always formed when pigment or filler particles meet each other and no repulsive forces are active that save them from staying together. Agglomerates formed in liquid suspensions are called "flocculates". Aggregates, on the other hand, develop by sintering processes during pigment production, either during calcination (such as in the sulfate process) or during gas phase reactions (such as when titanium tetrachloride reacts with oxygen in the chloride process).

The generation of agglomerates is primarily due to London-van der Waals ("dispersive") forces between the particles[1]. When particles the size of TiO_2 pigments touch each other, the dispersive force is far greater than the gravitational force acting on them. Titanium dioxide, like all other pigments, would also be suspended in air without this attractive force because of the Brownian motion of the molecules in the air.

Titanium dioxide particles, however, only present the best hiding power, lightening power and the desired mechanical properties in the systems they are used in (e.g. coatings, plastics, man made fibers etc.), if they are optimally separated into primary particles. That's why dispersing is a critical step in the production of composite materials.

Upon dispersion, three separate steps simultaneously take place next to each other:

1.) the wetting of the pigment surface by liquid components of the mill base,
2.) the mechanical separation of agglomerates into smaller agglomerates and primary particles,
3.) the stabilization of primary particles and smaller agglomerates and aggregates against flocculation.

Even if only one of these steps does not take place adequately enough, then the total dispersion result is in question.

In comparison to many other pigments and fillers, titanium dioxide pigments are generally easily dispersed in liquids. Still, there are differences from one grade to the other, partially based on the fact that TiO_2 particle surfaces may be differently modified with inorganic and organic post treatments.

With regard to colloidal chemistry, a titanium dioxide with an Al_2O_3 surface treatment behaves completely different from one having an SiO_2 surface treatment.

1 Dispersive forces are a blessing for life on planet earth because, without them, the air would be full of dust, so that neither could sunlight penetrate the atmosphere, nor would it be possible for living creatures to breathe.

Both of these, again, are different from a pure, untreated TiO_2. For that reason, the most important aspects of the three crucial steps in dispersion are addressed in this chapter.

6.2 Wetting

Figure 6.2 shows a drop of liquid on a flat surface. The droplet is characterized by its contact angle Θ, also shown in figure 6.2. At the nadir of the sessile drop, several forces act that originate from free surface energies (= surface tensions) of

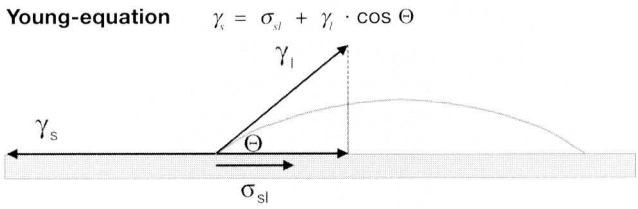

Fig. 6.2
Drop of liquid on the surface of a solid

the solid γ_s and the liquid γ_l as well as from the interfacial tension between the solid and the liquid σ_{sl}.

γ_s, γ_l and σ_{sl} are free energies that must be brought up in order to create interfaces between the solid and air, between the liquid and air and between the solid and the liquid, respectively. As the force scheme in figure 6.2 exemplifies, $\gamma_l \cdot \cos \Theta$ is the projection of the vector γ_l onto the plane of the interface solid-liquid.

The free surface energy of the solid has the tendency to spread the droplet, whereas the surface tension of the liquid, as well as the interfacial tension lead to forces that try to hold the drop together. At equilibrium, Young's equation applies:

$$\gamma_s = \sigma_{sl} + \gamma_l \cos \Theta \tag{6.1}$$

By rearranging equation 6.1, equation 6.2 is obtained, that connects the contact angle Θ with exactly these free energies:

$$\cos \Theta = \frac{\gamma_{sl} - \sigma_{sl}}{\gamma_l} \tag{6.2}$$

In principle, equations 6.1 and 6.2 also hold for the of wetting of pigment surfaces, although in this case, the contact angle can only be determined indirectly (see below).

When an agglomerate is placed into a liquid (e.g. a solvent or a resin solution), the liquid at first enters the agglomerate from all sides. The capillary pressure, with which the liquid tries to penetrate the agglomerate, is greater the larger γ_s, the free surface energy of the solid, the smaller σ_{sl}, the interfacial tension between solid and liquid, and the smaller γ_l, the surface tension of the liquid, are. A cross check with equation 6.2 verifies that the contact angle Θ also becomes smaller then.

The best and, thus, fastest wetting occurs, when the contact angle Θ is zero ($\cos \Theta = 1$). This is seen from the Washburn equation that describes the rate of entry of a liquid into an agglomerate:

$$\frac{m}{\sqrt{t}} = K \cdot \rho \cdot \sqrt{\frac{\gamma_l \cdot \cos \Theta}{\eta}} \qquad (6.3)$$

where m is the mass of liquid that penetrates the agglomerate within the time t (which enters the equation as a square root), K is a capillary term, ρ is the density and η the dynamic viscosity of the liquid.

However, the liquid only proceeds into the agglomerate until the state is reached, when the capillary pressure is equivalent to the counter-pressure of the entrapped air. If the agglomerate is weak, then the internal pressure of the compressed air can be large enough to cause the agglomerate to break. If not, then complete wetting of the agglomerate will only occur in the course of time, when the gas molecules are eventually dissolved in the liquid. In former times, it was customary to stir the pigments into the liquid and let them rest over night ("soaking the pigments"), and then disperse them the next day. Today, this patience is seldom brought up and so, instead, it is preferred to disperse them immediately with effective dispersion machinery such as high speed attritors [1] or sand mills [2] (see below).

Completely soaked agglomerates or parts of agglomerates can more or less just decompose (like a pharmaceutical tablet) in water.

The wetting of titanium dioxide pigment agglomerates can be sufficed by using appropriate inorganic and organic surface treatments, provided these improve the interaction between the pigment's surface and the liquid used for wetting. This can be achieved by taking advantage of acid/base interactions, or by covering the pigment's surface with an organic substance that is chemically similar to the dispersing liquid. Both measures act by reducing the interfacial tension σ_{sl} (see equations 6.1 and 6.2). Furthermore, organic surface treatments reduce the packing density of the primary particles in the agglomerates. This will be dealt with in the following chapter.

Another way to enhance wetting is to apply a vacuum to the mill base (=the mixture that is supposed to be dispersed). If the depression value is higher than

the capillary pressure of the liquid in the agglomerates, then the air escapes from them and the liquid can flow in freely. The vacuum is normally applied directly to the dispersing vessel (e.g. a vacuum high speed impeller). When using this machinery, though, care has to be taken that the boiling points of the liquid components at these reduced pressures are not exceeded.

6.3 Mechanical deagglomeration

6.3.1 Mill base formulation

The mechanical breaking of the agglomerates is performed in dispersion machinery. In most applications of titanium dioxide pigments, a dispersion with a high speed impeller equipment is sufficient [3]. Generally, a fineness of grind of less than 10 µm can be achieved with an impeller apparatus (measured e.g. with a "Grindometer" or "Hegman gage" according to DIN EN 21 524, DIN 53 203 or ASTM D 1210).

Ideal for this is a highly pigmented mill base [4], so that a slight degree of dilatant flow results (dilatancy: the shear stress and, with it, the viscosity increase more than linearly with increasing shear rate). It is also completely sufficient, if the dilatancy occurs only within a certain range of the shear rate. If, however, particularly high gloss is demanded, then the dispersion of TiO_2 pigments should be carried out in high speed attritors or sand mills. Both pieces of equipment consist of vessels that are filled with grinding media (pebbles of different materials and sizes or sand, respectively) and have some kind of an agitation device, such as a shaft, that keep these, as well as the "mill base" (= the mixture that is supposed to be dispersed), in motion. The dispersing takes place in this agitated bed of "grinding" media. In this case, the mill base should possess either Newtonian flow (the viscosity increases linearly with the shear rate) or pseudoplastic flow (The liquid has a yield point and the viscosity increases less than proportionally with the shear rate).

6.3.2 Agglomerate strength

It is not surprising that dispersion results depend upon the strength of the agglomerates.

In the case of titanium dioxide pigments, their agglomerate strength is widely influenced by organic surface treatments and by steam jet milling. Compared to a non-treated material, the compressive strength (expressed as the quotient of the work of compression and the agglomerate volume) can be reduced by one hundred-fold [5].

Organic surface treatments are normally added to the TiO_2 pigments just before steam jet milling. In doing so, the organic molecules spread evenly on the pigment's

surface and reduce the dispersive attractive force between the particles [6]. This leads to agglomerates that are less densely packed after milling, and therefore have fewer contact sites of the primary particles. Furthermore, every contact site has less adhesive force. As a consequence, though, some pigment properties may change to the worse, such as a lowering of the bulk density, free flow of the powders (even when packed in sacks) and higher dust development [6].

An important property of the organic substance used as a post-treatment is its *Hamaker constant A*. It is an energetic constant that determines the London-van der Waals interaction [7]. If the Hamaker constants are available, the attractive energies E_{att} and forces between molecules, but also between colloidal particles, can be calculated as a function of the particle to particle distance x by simply multiplying them with a distance function $H(x)$.

$$E_{att} = -\frac{A}{12} H(x) \tag{6.4}$$

Figure 6.3 shows the principle course of E_{att} as a function of the particle separation distance x for two larger and two smaller particles. The larger particles attract each other stronger than the smaller ones.

The Hamaker constant depends, on the one hand, on the high frequency polarizability α of the substance and, on the other hand, on the characteristic frequency

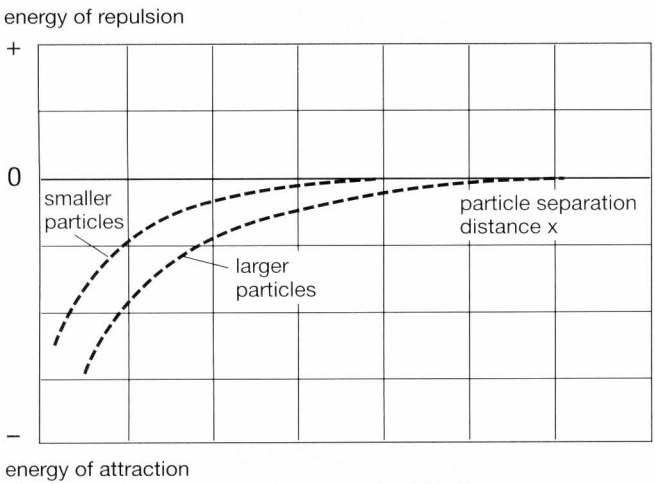

Fig. 6.3
Principle dependency of the attractive energy of particles as a function of their separation distance

ν_v (eigenfrequency, resonance frequency) of the electrons in the molecule. The high frequency polarizability is connected to the refractive index n, as is shown in the following formula:

$$A = \left(\frac{3}{4}\right)^3 \cdot h \cdot \nu_v \cdot \frac{n^2 - 1}{n^2 + 2} \tag{6.5}$$

In equation 6.5, is Planck's constant (6.626 x 10^{-34} J s).

It is also possible to calculate attractive energies between particles that are covered with an inorganic and organic surface treatment, provided that their Hamaker constants are known. [8]. The smaller the Hamaker constant of an organic post-treatment is, the better is its ability to reduce agglomerate strength [6].

Because of their low Hamaker constant, silicone oils, for example, are very well suited as post-treatments for titanium dioxides for use in plastics. Since plastic melts have poor wetting properties and relatively high viscosities, it is especially important in this case, that the agglomerates disperse easily from a mechanical point of view.

If organic substances with higher Hamaker constants are used, then higher amounts of them are required to obtain similar agglomerate strength reductions.

If the use of the pigment is well known, then it is possible to optimize the organic surface treatment exactly for that application. In the case of titanium dioxide pigments for paints, however, the products are expected to be universally applicable. Therefore, the organic surface treatments chosen tend to be more of a compromise.

6.3.3 Relationship between time length of dispersion, mechanical power input and dispersion success

When considering the mechanical rupture of pigment agglomerates, it is necessary to distinguish between time dependent and mechanical influences [9].

Pigment agglomerates in a mill base are not constantly exposed to mechanical stresses sufficiently high enough to cause their dispersion. This only takes place in certain parts of the dispersing vessel, and that means, only at the times when the agglomerates are located there. The time length of the dispersion determines the probability p_t with which the agglomerates reach such a mechanical stress situation in the first place. This can, for example, be in the gap between two milling beads that stream next to each other, where the agglomerate can either come into the shear field of the liquid or, otherwise, be directly hit by these grinding media. At that instant, enough energy density must be present to overcome the solidity of the agglomerates. (Both agglomerate strength and energy density have the same physical dimension of "energy per volume".) The probability p_e for an effective dispersion step to occur at that instance is higher, both when more mechanical

power is introduced into the dispersing vessel, and when the agglomerate strength is low.

The total probability p_T for dispersion to take place is the product of the single probabilities [9]:

$$p_T = p_t \cdot p_e \tag{6.6}$$

This means that a lack of dispersing time can not be compensated by a higher power input. Conversely, the absence of sufficient mechanical power cannot be overcome by dispersing for a longer period of time, either. Figure 6.4 is the

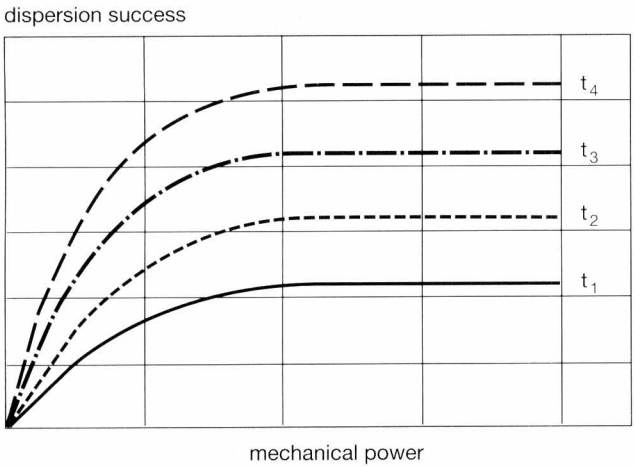

Fig. 6.4
Dispersion result as a function of the mechanical power at different lengths of dispersion (schematically; $t_1<t_2<t_3<t_4$)

schematic representation of the development of dispersion success (= deagglomeration) as a function of the mechanical power at different time lengths of dispersing. Figure 6.5 is the analogous plot of dispersion success as a function of dispersing time at different mechanical powers.

Experimentally accessible values suited to express dispersion success can be any property that changes as a function of deagglomeration. Especially the color strength (for colored pigments), and the gloss of a cured coating offer themselves to be used in this sense [10].

When a dispersing machine with a rotating shaft is utilized, the mechanical power can be calculated from its rotational speed n and from its torque τ:

$$P = 2\pi \cdot n \cdot \tau \tag{6.7}$$

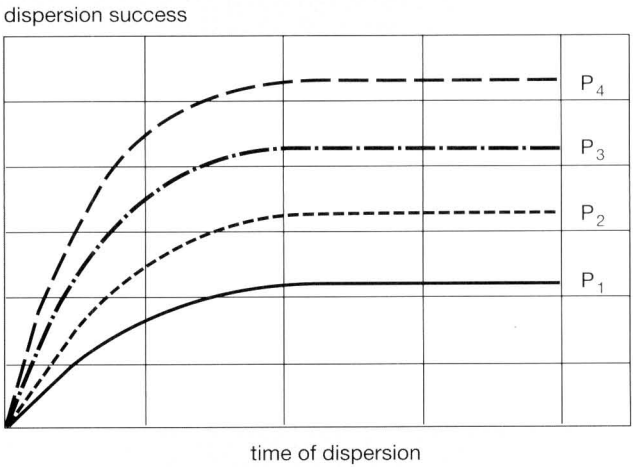

Fig. 6.5
Dispersion result as a function of the dispersion time at different mechanical powers (schematically; $P_1<P_2<P_3<P_4$*)*

For pigments like titanium dioxide, whose agglomerates can be dispersed both by impingement and by exposure to shear stress, dispersion success depends – from an energetic point of view – upon the absolute value of the mechanical power, regardless of the partial contributions of n and τ [9, 10].

If, in the course of a dispersion, the desired dispersion success isn't reached, then equation 6.6 points out how the reason for this can be easily accessed: If the degree of deagglomeration is not improved when dispersing for a longer period of time, then more mechanical power – for example by increasing the rotational speed of the shaft – must be introduced. If that doesn't lead to an improvement either, then the system is either optimally dispersed, or flocculation is taking place.

6.4 Stabilization against flocculation

Without any stabilizing force, all particles in a colloidal suspension would flocculate due to the attractive London-van der Waals interaction.

The stabilization of pigments against flocculation can be achieved by three different mechanisms:

1) electrostatic stabilization
2) steric (entropic) stabilization
3) stabilization by adsorbed inorganic nano-particles, carrying an electrostatic charge

The particles are stabilized against flocculation if, at each separation distance, repelling forces overcompensate the attractive dispersive force.

6.4.1 Electrostatic stabilization

The principle of electrostatic stabilization is based upon an electrostatic charge of the same sign on the pigment particles that therefore repel each other. Colloidal particles can gain electrostatic charges by a number of different mechanisms:
1) dissociation of surface groups
2) adsorption of (large) polyelectrolytes
3) adsorption of (small) ions

In aqueous systems, 1) and 2) overwhelm, whereas in organic phases, 3), the adsorption of ions, predominates (next to steric stabilization, see chapter 6.4.5). In all cases, the demand for charge neutrality, i.e. that exactly the same number of positive as negative charges must be present in the system as a whole, has to be fulfilled. Such charges are only distributed unevenly.

6.4.2 Zetapotential

Inorganic oxides carry OH-groups on their surfaces that differ in number [11, 12] and acidity [13, 14].

Figure 6.6 presents a schematic representation of the reactions that occur on such a surface in the presence of acids or bases, respectively. The addition of protons leads to a positive charge on the particles, whereas, at the same time, the pH-value does not fall to the same extent as it would have, if the particles weren't there. By the addition of hydroxyl ions, the particles obtain a negative charge and the pH-buffering action is also bestowed.

Such a behavior is characteristic for oxides, nitrides and sulfides that carry surface groups of –OH, =NH and –SH, respectively. These substances are termed "amphoteric" (Greek: amphoteros: each of two) since they are capable of reacting either as acids (with bases) or as bases (with acids).

The electrostatic charge of the particles is the reason why they migrate to the oppositely charged electrode when an electrical field is applied to the suspension. This phenomenon is utilized to explore the state of particle charge by measuring their speed of migration. Their velocity per unit of electrical field strength is called "electrophoretic mobility" μ. It has the dimension $\mu m\ s^{-1}/V\ cm^{-1}$. It is connected to the so called "zetapotential" ζ by the Smoluchowski equation (for aqueous systems) or by the Hückel equation (for organic systems), respectively, in which ε is the dielectric constant of the medium and η is its dynamic viscosity:

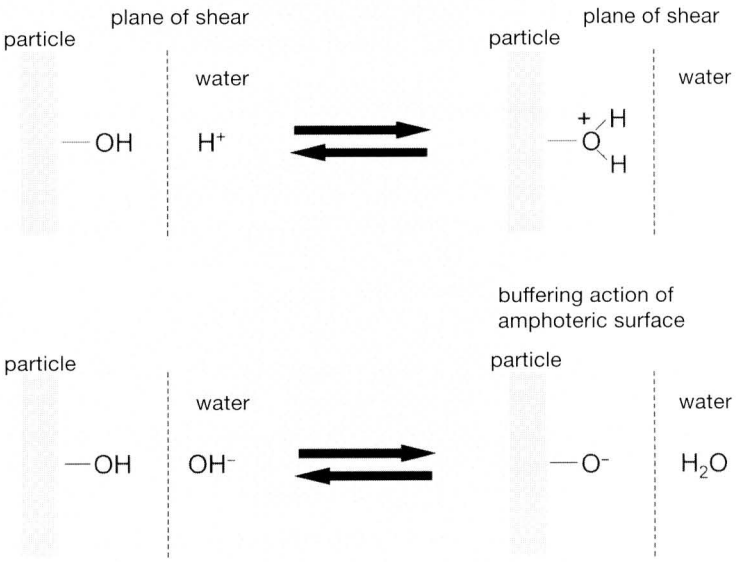

Fig. 6.6
Acid-base adsorption equilibria on amphoteric oxide surfaces

$$\text{Smoluchowski:} \qquad \zeta = \frac{\mu\varepsilon}{\eta} \tag{6.8}$$

$$\text{Hückel:} \qquad \zeta = \frac{3}{2} \cdot \frac{\mu\varepsilon}{\eta} \tag{6.9}$$

By definition, the zetapotential is the electrical potential at the shear plane of the solvate layer, which the particles carry with them when they migrate. It is assumed, that the shear plane is at a distance from the particle surface, where the potential has decayed to a value of 1/e of the surface potential Ψ_s. Following Guoy and Chapman (Literature cited in [15]), the course of the potential Ψ_x as a function of the distance x from the particle surface can be described by:

$$\Psi_x = \Psi_s \cdot e^{-\kappa x} \tag{6.10}$$

wherein κ is the "*inverse Debye length*". It carries that name because $\Psi_x = \zeta$ when the product of κ and x obtains the value of one. κ is linked to the *ionic strength* $\Sigma\, c_i \cdot z_i^2$ of the solution:

$$\kappa = \sqrt{\frac{8\pi \cdot e^2 \cdot \Sigma\, c_i \cdot z_i^2}{\varepsilon \cdot kT}} \qquad (6.11)$$

with

e = elementary charge (1.602×10^{-19} C)
k = Boltzmann constant (1.381×10^{-23} JK^{-1})
c_i = concentration of ions i (number per unit volume)
z_i = number of charges of ions i
T = temperature (K)

From equation 6.10, it is easily deducted that the potential drops steeper, the larger the ionic strength and therefore κ is. In that case, the London-van der Waals attraction can overwhelm, resulting in flocculation. The method of "*salting out*" suspended matter from water is based on this effect. This process is conceived as the addition of higher valency ions to electrostatically stabilized colloidal suspensions with the aim to initiate flocculation.

According to the "Schulze-Hardy rule", there is the following connection between the valency of the ions and their concentration at the onset of flocculation:

$Me^+ : Me^{2+} : Me^{3+} = 1^6 : 0.5^6 : 0.33^6$

This means that especially polyvalent counter ions are very detrimental in view of pigment stabilization. By experience, divalent ions flocculate 20 to 80 times more, and trivalent ions even 600 to 10,000 times more than monovalent ions. (Römpp Chemielexikon: search word "Kolloidchemie").

For this reason, titanium dioxide pigments are rinsed free of electrolytes to an extent that their "conductivity" (reciprocal value of the resistance of an aqueous extract following ISO 787, part 14, or ASTM D 2448; 20 g of pigment in 180 g of aqua dest.) is less than 100 $\mu S\,cm^{-1}$. This corresponds approximately to the conductivity of a 0.01% sodium chloride solution.

In aqueous systems, monovalent salts (e.g. NaCl, KNO_3 etc.) at concentrations of about a hundredth or a thousandth of a mole are sufficient to cause pigments to flocculate. Especially in electrodeposition paints for priming of metal parts, it is important that the pigments and fillers have low conductivities because, otherwise, electrolyte ions can accumulate and cause bath stability problems. In corrosion protection paints, low conductivities from adhering salts are also of importance, whereby chloride ions are especially disliked.

In figure 6.7, the principle dependence of the zetapotential of amphoteric colloids on the pH-value is shown. At low pH-values, they are charged positively, and at high pH-values negatively. In between, there is the "isoelectric point" (iep), at which the migration in an electric field ceases because the particles have the same

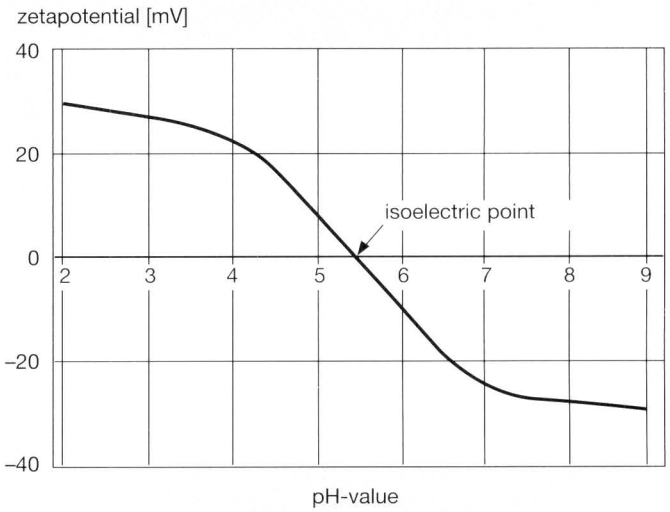

Fig. 6.7
Zetapotential as a function of the pH-value (schematically)

number of positive as negative charges within their planes of shear, so they appear to be uncharged[1] .

In the absence of potential determining ions, the location of the isoelectric point depends upon the polarization of the *...Me–OH* bond. If *Me* is strongly electron drawing, then the proton of the *...Me–OH* group acidifies and the dissociation into $...Me–O^-$ and H^+ occurs easily. Accordingly, in this case, the equilibrium is shifted to the undissociated state at lower pH-values.

Pure titanium dioxide has its iep at pH-values between 4.5 and 6.5. The iep of titanium dioxide from the chloride process (see chapter 3.3) lies at pH-values between 6.5 and 7, due to doping with rather appreciable amounts of Al_2O_3 that are partly on the surface of the particles. Sulfate grade titanium dioxide core particles have their iep somewhere between pH 1 and pH 3. This is caused by the phosphates that are used as annealing salts for calcination. These form acidic titanium phosphates on the surfaces of the particles. The *=PO–OH* group, that is very acidic, then becomes potential determining.

1 It makes sense to distinguish between the isoelectric point (iep) and the point of zero charge (pzc). Whereas the iep is defined as stated above, the pzc is defined as the pH value at which the adsorbed H^+ and OH^- ions compensate each other. The pzc is assessed by pH-titration (C.P. Huang, W. Stumm, J. Colloid Interface Sci., 43, No. 2 (1973) 409).

Modifying the pigment surface with inorganic layers of, for example, Al_2O_3, SiO_2, ZrO_2, and further TiO_2, phosphates of low solubility or mixed oxides, again changes the ieps.

Whereas, for example, Al_2O_3 (iep of $Al_2O_3 = 9$) shifts the iep to higher pH-values, other substances normally tend to reduce the iep to lower pH-values (iep of $SiO_2 = 2$, iep of $ZrO_2 = 4$).

In aqueous systems, the iep of a titanium dioxide pigment can have a considerable influence on the flocculation behavior. If two amphoteric pigments with different ieps are used, then, in the pH-range between their ieps, they have opposite charges (see figure 6.8). This leads to drastic flocculation, unless another stabilization mechanism becomes active (see below).

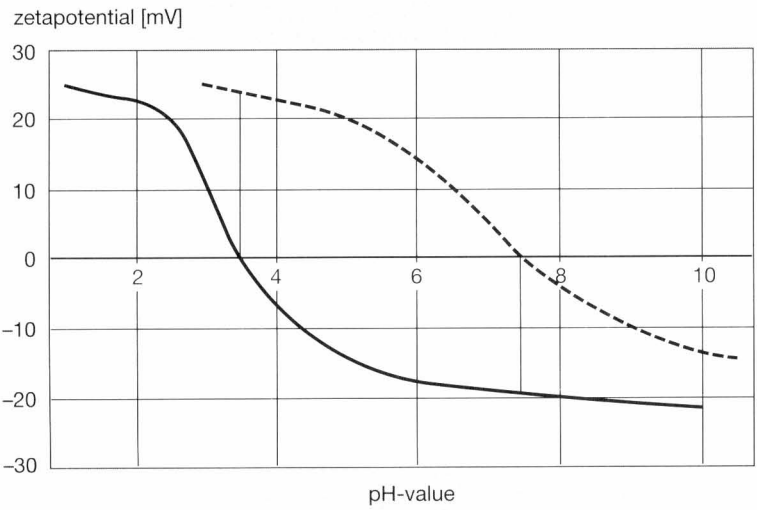

Fig. 6.8
Zetapotential curves of two pigments with different ieps (schematically)

Also fillers that, in a chemical sense, are mixed oxides, like talc [$Mg_3Si_4O_{10}(OH)_2$], kaolin [Al_2O_3 x 2 SiO_2 x 2 H_2O], mica [$KAl_2(AlSi_3O_{10})(OH)_2$] (= muscovite) and bentonite [$(NaCa)_{\cdot}(AlMg)_6(Si_4O_{10})_3(OH)_6$], etc., exhibit pH-dependent charging behavior. Contrarily, chalk [$CaCO_3$], dolomite [$CaMg(CO)_3$] and blanc fixe [$BaSO_4$], for example, have, irrespective of the pH, little to no charge in water.

This should be kept in mind when formulating aqueous systems with combinations of titanium dioxide pigments and fillers.

6.4.3 Stabilization by adsorption of polyelectrolytes

Polyelectrolytes are oligomers or polymeric materials that obtain ionic character in aqueous environments either by themselves, or by the reaction with an acid or a base.

Anionic and cationic polyelectrolytes are distinguished. Anionic polyelectrolytes, such as the salts of polyacrylic acid or salts of hexa meta phosphoric acid (e.g. the sodium salt: "calgon"), are negatively charged when dissociated. Cationic polyelectrolytes, for example polyacrylic amide, are molecules that obtain a positive charge in acidic environments.

By adsorbing on the pigment surfaces, polyelectrolytes determine their charge behavior and thereby stabilize them against flocculation [16]. In addition, they contribute to steric stabilization (see chapter 6.4.5).

Anionic polyelectrolytes are used in slightly alkaline pH-ranges (pH 7 to pH 8.5), whereas cationic polyelectrolytes are applicable under slightly acidic conditions (pH 5.5 to pH 7). Titanium dioxide pigments, that have a clearly negative zetapotential in the pH-range of the medium, cannot be stabilized by anionic polyelectrolytes because of their identical sign of charge. If the pigments are charged positively in the system, then cationic wetting agents fail. That is why anionic polyelectrolytes are not suited for stabilizing SiO_2-treated titania pigments, and cationic wetting agents only partially qualify in the case of titanias with basic surface treatments. For this type of stabilization, especially pigments whose ieps lie around pH 7 come into question, since neither in slightly acidic, nor in slightly alkaline media do they have such a high charge that they repel wetting agents. Likewise, uncharged fillers are advantageous under these conditions.

As said before, when a polyelectrolyte adsorbs, it becomes "*potential determining*". The iep is then governed by the dissociation equilibrium of the polyelectrolytes. For them to adsorb not only on oppositely charged surfaces, their solubility in water must be limited. Otherwise, at too good a solubility, they would not become "*surface active*".

If the polyelectrolytes fail to adsorb from aqueous media, then it is possible to overcome this problem by first dispersing the pigments with the non-neutralized polyelectrolyte, and then transform them into their ionic form by adding acid or base.

It is possible to hold titanium dioxide in aqueous suspension merely by adjusting the pH-value. This is normally the case if the system pH is approximately 4 units different from the iep, and if the ionic strength is not too high. Yet, following this strategy, poorer coating properties are achieved compared to when the pigment particles are surrounded by coats of wetting agents or resin molecules. The reason

for this is probably that, upon drying of the paint, the ionic strength in the media increases due to water evaporation and that, for that reason, the particle distribution is not maintained.

The first visible consequence is a poor gloss of the coatings. However, also other paint properties, such as mechanical strength, adhesion and protecting properties, can be negatively effected.

6.4.4 Adsorption of ions

Unlike in aqueous systems, pigments in organic media preferentially obtain charges by adsorption of small ions. Due to the poor solubility of ions in systems with low dielectric constants, the ionic strengths are low. Therefore, adsorbed ions are hardly shielded and, thus, can display far reaching potentials (compare equations 6.10 and 6.11). Only a few adsorbed ions may suffice to effectively prevent pigments from flocculating in these systems [17, 18].

Classical sources for ions in organic media are fatty acids of divalent and trivalent metals that are normally used as siccatives. Thus, calcium octoate [$Ca(Oct)_2$] easily dissociates into a calcium octoate cation [$CaOct$]$^+$ and an octoate anion [Oct]$^-$. The octoate anion, as the ion of the two with the higher charge density (because it is smaller), is less soluble in organic systems than the calcium octotate cation. Therefore, it absorbs preferentially and becomes potential determining [19].

A similar behavior is known from the salts of sulfosuccinic acid. But, under certain conditions, even purely inorganic salts like sodium sulfate can lead to a positive charging of pigment particles. This happens when one of the ions formed are stabilized by solvation and the other ion is preferentially adsorbed [20]. Again, this depends upon the charge density of the ions. The higher it is, the easier adsorption occurs.

Measuring electrostatic charges of pigments in organic systems is generally difficult because, compared to aqueous systems, the electrophoretic mobilities are very small due to the low dielectric constants. In table 6.1, the expected values of the

Substance	Equation of	ε_r	η / mPas	μ (μm/s)/(V/cm)
Water	Smoluchowski	80	1	1.42
1-Butanol	Hückel	17.8	2.95	0.07
Toluene	Hückel	2.3	0.58	0.05

Table 6.1
Estimation of electrophoretic mobilities of particles with a zeta-potential of 20 mV in water and organic solvents
ε_r = relative dielectric constant

electrophoretic mobilities of particles with a zetapotential of 20 mV in water and in 1-butanol or toluene, respectively, are compared. For calculating the electrophoretic mobilities in water, the Smoluchowski equation (equation 6.8) was used. For the organic solvent case, the Hückel equation (equation 6.9) was employed.

The electrophoretic mobilities in 1-butanol and toluene are approximately 20 to 30 times smaller than in water. In toluene, such a particle needs, for example at a field strength of 10 Vcm^{-1}, more than half an hour to cover a distance of 1 mm. At such low velocities, it used to be very difficult to measure electrophoretic mobilities, which probably accounts for the fact that, still today, there is a widespread notion that electrostatic charges do not play a role in organic systems. In the meantime, however, electroacoustic methods facilitate the measurements [20].

Titanium dioxide pigments, but also other pigments, can be indirectly stabilized by very small particles that themselves are charged by ion adsorption. The charged nano-particles attach to the pigment surface and thereby become potential determining [20]. This mechanism is more dependent upon the resins and solvents in the system, than on the nano-particles used.

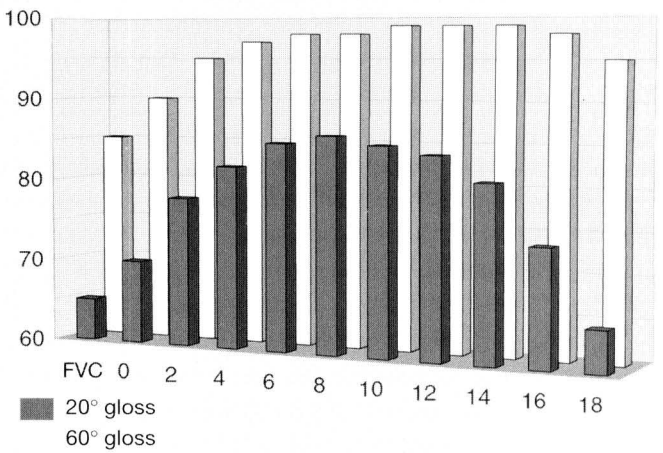

Fig. 6.9
Gloss improvements by electrostatic stabilization of titanium dioxide through nano-barium sulfate. (FVC= filler volume concentration)

In polyesters, for example, both nano-barium sulfates, as well as nano-titanium dioxides and nano-aluminum oxides act this way. Figure 6.9 shows the gloss values of such a coating with a titanium dioxide pigment volume concentration (PVC) of 25% and increasing amounts of an approximately 80 nm sized barium sulfate. At about 10 volume % addition of the nano-particles (total PVC there

= 35%), the best 20° angle gloss is achieved. However, the haze in this system was hardly improved in this experiment, as a consequence of diffuse light scattering of the TiO_2 pigment.

6.4.5 Steric (entropic) stabilization

Polymers in solution are present as solvent drenched, loosely packed tufts in the shape of rotational ellipsoides [21]. The polymer stays in solution as long as the interaction with the solvent molecules is more pronounced than the interaction of the different segments of the polymer with each other. Solvents that undergo much interaction and therefore are good solvents, are called "*thermodynamically favorable* solvents" for the polymer. Because of their conformation in solution, polymer molecules in these solvents take up more space (they have a larger hydrodynamic volume). Therefore, these solutions have a higher viscosity at the same concentration, compared with solutions with thermodynamically less favorable solvents.

In the thermodynamic equilibrium, all polymer molecules in a solution have approximately the same concentrations of solvents within the tufts. When two polymer molecules meet, they at first start to penetrate each other. In the overlapping region, the polymer concentration rises, which leads to an osmotic pressure of the solvent molecules. These then migrate into the higher concentrated region, thus separating the polymer molecules again. The osmotic pressure π_o that appears is – according to the van't Hoff equation – proportional to the polymer concentration c in the overlapping region and inversely proportional to the polymer's molecular weight M_n,

$$\pi_o = cRT \frac{1}{M_n} \tag{6.12}$$

whereby R is the universal gas constant and T the absolute temperature[2].

When, for example, linear polymers adsorb onto surfaces of solids, they change their conformation. They are then no longer in tuft conformation but – as shown in figure 6.10 – in a stretched form. Trains, tails and loops are distinguished. The polymers are adsorbed to the pigments by the anchor groups in the train sections of the polymers. The anchor groups are usually polar groups that often serve as functional groups; that is to say, they participate in curing reactions.

2 Equation 6.12 is valid for so called "theta solvents", in which the polymers are dissolved "free of strain". This means that the C-C-C binding angle is exactly the tetrahedron angle of an sp3-hybridized carbon atom. In the case of deviations from theta conditions, the concentration dependence of the osmotic pressure is traditionally described by a polynomial approach:

$$\pi = RT \left(\frac{1}{M} c + bc^2 + \ldots \right)$$

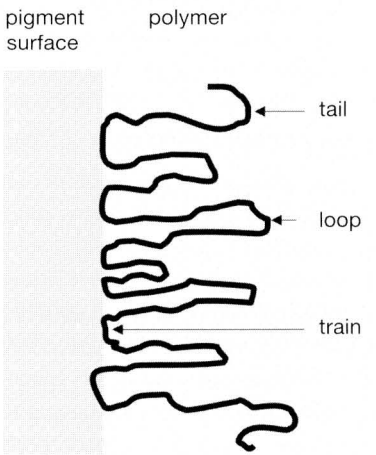

Fig. 6.10
Conformation of a linear polymer molecule adsorbed to a pigment surface

If highly polar solvents that are better able to interact with polar functional groups are used, then the, under these circumstances, less soluble non-polar, and therefore *lyophobic* (solvent repelling) parts of the polymer can anchor to the pigment surface, whereas the polar parts will sooner extend into the solution.

When two pigment particles with such adsorbed layers approach each other, then the loops and tails penetrate each other before the particles themselves meet. This again leads to an osmotic pressure of the solvents. Just as in the case of free polymers, the solvent migrates into the regions of higher polymer concentration between the particles and separates them in this way.

This steric stabilization is also called entropic stabilization, since one may argue that the adsorbed particles suffer a loss of mobility (loss of disorder) when the particles approach each other, which has a loss of entropy as a consequence. The first attempts to describe the stabilizing action of adsorbed polymers quantitatively indeed made use of models of statistical thermodynamics [22, 23].

Titanium dioxide pigments undergo strong polar interactions and especially hydrogen bonding with functional groups of polymers. Polymers with acidic groups in the molecules interact well with aluminum oxide modified surfaces. Silica treated titanium dioxides are, conversely, advantageous for use with amine group containing polymers.

Steric stabilization can come into effect either alone, or in combination with electrostatic stabilization. Examples for this are water soluble resins that carry

neutralized carboxyl groups. In that case, the negatively charged carboxyl groups extend into the solution instead of functioning as anchor groups.

But also cationic, water soluble resins that are, for example, used in cataphoretic primers, have both an electrostatic as well as a steric component of pigment stabilization.

No steric stabilization comes into effect in the case of dispersion resins (latex), however, since they do not consist of dissolved polymers, but of particles forming a separate phase, instead. It might be possible that the anionic latex particles arrange around slightly positively charged pigment particles and stabilize them similar to inorganic nano-particles [20]. An investigation dealing with this possible mechanism is, however, unknown to the author.

The free flow of coatings at high resin concentrations is often rendered possible by using low molecular weight resins ("high solids" or even "super solids"; properties: see table 6.2) in combination with thermodynamically poor solvents, so that the hydrodynamic volumes of the dissolved polymers are small.

Under these circumstances, polymers adsorbed to pigments, merely in consideration of their small size, do not extend far into the solution. Besides that, they form flat,

System name	Non-volatile content	Molecular weight
Conventional resins	25 weight-%	10^5 - 10^6 g/mol
High solids	50 weight-%	10^4 g/mol
Super solids	75 weight-%	10^3 g/mol

Table 6.2
Non-volatile contents and molecular weights of different resin classes

dense layers which have little or no stabilizing effect. Pigment flocculation may then occur. By formulating the coatings with larger portions of thermodynamically favorable solvents, stabilization can be achieved. Otherwise, high molecular weight dispersing additives have to be used.

6.5 Rub out effect and Benard cells

When, in a system containing only a colored pigment or a white pigment, flocculation takes place, this is often recognized only by a gloss reduction or maybe by the loss of mechanical properties of the material. If, however, either differently colored pigments or combinations of colored pigments with white pigments are used, then the color appearance changes upon flocculation. Flocculation is easily detected by rubbing the surface with a finger just before the paint solidifies due to solvent evaporation or the onset of the curing reaction. By

this, flocculates are dispersed once again, and the original pigment particle distribution is reestablished.

This method is called "rub out test". The rub out number is the quotient of the color strengths (see equation 4.21 in chapter 4.5) of the rubbed and non-rubbed surfaces. A positive rub out is when the color strength of the rubbed surface is enhanced. This is a sign that the color pigment was flocculated. In that case, a suitable wetting or dispersing agent should be utilized. A positive rub out is generally also found if both the color pigment as well as the white pigment is flocculated. In a negative rub out test, the white pigment was flocculated before rubbing. This can be remedied by either using an opportune dispersing agent or switching the TiO_2 grade.

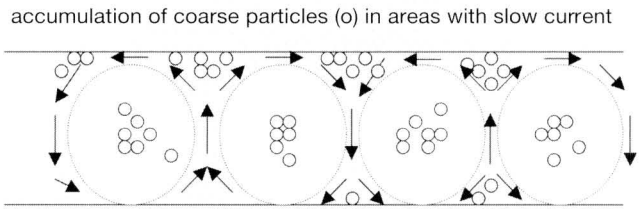

Fig. 6.11
Formation of Benard cells

Even when pigments don't flocculate, but are different in particle size, color differences can occur as a result of segregation due to convection. This leads to the formation of "Benard cells" on the surfaces of the coatings. Figure 6.11 clarifies their formation. When a solvent evaporates from a coating, a temperature gradient appears within the paint film due to the heat of evaporation that cools the surface. Liquid paint then starts to rise from the bottom to the top, so that a circulating current is formed. The larger of the two pigments, which is normally titanium dioxide, starts to accumulate in the areas of lower convection rates. On the paint's surface, a honeycomb pattern (see figure 6.12) of small, white specks appears. The centers of the six-membered rings is stronger in color, since the colored pigments are concentrated there. The appearance is exactly opposite if, normally due to flocculation, the colored pigments are larger and heavier than titanium dioxide.

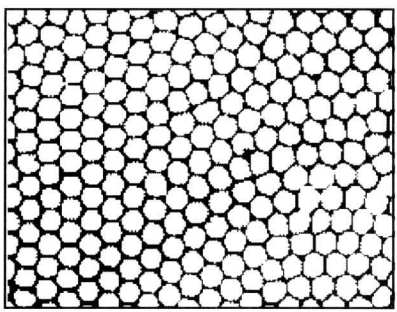

Fig. 6.12
View on Benard cells

6.6 Final remarks

Although, in principle, the influences on pigment dispersion and stabilization against flocculation are fairly well known, it is nevertheless hardly possible to forecast the behavior of a given formulation in advance. The value of the knowledge on the steps of

- wetting
- mechanical rupture of agglomerates and
- stabilization against flocculation

rather lies in the fact that models are available, so that, in the case of difficulties occurring, formulating alternatives can be pursued with strategy.

References

[1] D. P. Roloefsen, 20th FATIPEC Congress, Nice, (1990), Congress Book, p. 24

[2] T. C Patton, "Paint Flow and Pigment Dispersion", 2nd Edition, J. Wiley & Sons, New York, (1979), 290

[3] B. Schwegmann, FARBE&LACK 80 (1974) 311

[4] like [2], p. 326

[5] J. Winkler, FARBE&LACK 94 (1988) 108

[6] J. Winkler, FARBE&LACK 94 (1988) 263

[7] H.C. Hamaker, Physika, 4 (1937) 1058

[8] M.J. Vold, J. Colloid Sci. 16 (1961) 1

[9] J. Winkler, 19th FATIPEC Congress, Aachen, (1988), Congress Book, Vol. 3, p. 289

[10] J. Winkler, L. Dulog, FARBE&LACK 90 (1984) 355

[11] T. Rentschler, European Coatings J., 10 (1997) 939

[12] T. Rentschler, FARBE&LACK 106 (2000) 62

[13] J.A. Davies et al., J. Colloid Interface Sci. 63 (1978) 480

[14] U. Gesenhues, 19th FATIPEC Congress, Aachen, (1988), Congress Book Vol. 1, p. 237

[15] D.C. Grahame, Chem. Rev. 41 (1947) 441

[16] J. Winkler, 22nd FATIPEC Congress, Budapest, (1994), Congress Book. Vol. 2, p. 284

[17] G.D. Parfitt, J. Peacock, "Surface and Colloid Science", C.E Matijevic Ed., Vol 10, New York, (1978), p. 163

[18] J. Lyklema, Advan. Colloid Interface Sci. 2 (1968) 65

[19] J. Winkler, European Coatings J. 1-2 (1997) 38

[20] J. Winkler, FARBE&LACK, 97 (1991) 859

[21] B. Vollmert, "Grundriss der Makromolekularen Chemie", E. Vollmert Verlag, Karlsruhe, (1979), Vol. III, p. 34-39 and p. 136-166

[22] E. L. Mackor, J.H. van der Waals, J. Colloid Sci. 6 (1951) 492 and 7 (1952) 535

[23] E.J. Clayfield, E.C. Lumb, J. Colloid Interface Sci. 22 (1966) 269

[24] J. Winkler, W.-R. Karl, FARBE&LACK 100 (1994) 3

[25] P. Kresse, FARBE&LACK 72 (1966) 111

7 Nano titanium dioxide

7.1 Production of nano titanium dioxides

Nano titanium dioxides have mean particle sizes of less than 100 nm. They can be produced by different routes.

Common in the laboratory scale is the hydrolysis of titanium-IV-alkoxylates of ethanol or isopropanol, using acetic acid or nitric acid as catalysts. The titanium hydroxide gels that are formed first turn into anatase/rutile mixtures upon tempering. At temperatures exceeding 850 °C, the pure rutile structure is developed [1].

When neutralizing diluted titanylsulfate ($TiOSO_4$), a titanium oxy-hydrate precipitates, which turns into anatase at temperatures of around 350 °C [2].

By neutralization of titanium tetrachloride, for example with ammonia, a titanium oxy-hydrate appears, which turns into rutile at approximately 900 °C [3].

Gaseous titanium tetrachloride can be used in the "Aerosil process" [1] by reacting it with steam to obtain a fine particle sized TiO_2, which consists of a mixture of anatase and rutile.

In the production of nano rutiles from precursors of the sulfate process, freshly precipitated titanium oxy-hydrate ("metatitanic acid") from the hydrolysis is washed, reacted with sodium hydroxide to sodium titanate (Na_2TiO_3), and then "peptized" with hydrochloric acid, whereby again, a metatitanic acid evolves, which turns into rutile when it is heated.

Although nano scaled rutiles have improved photostability and weather resistance in comparison to anatase, their durability is by no means sufficient to protect materials without any further steps in production. The nano scaled core particles are therefore – similar to titanium dioxide pigments – further doped with foreign atoms such as aluminum.

However, other doping elements such as iron or manganese etc. also come into question, since absolute whiteness may not be an issue in all cases. In some applications, for example as a UV-absorber in glazes for wood protection, a certain buff color may even be desired, because the grain of the wood is optically intensified.

In addition, the nano particles are further inorganically surface treated in order to improve photostability and weather resistance. Figure 7.1 shows the results of the

1 Aerosil is a registered trade mark of Degussa. Hanau, Germany.

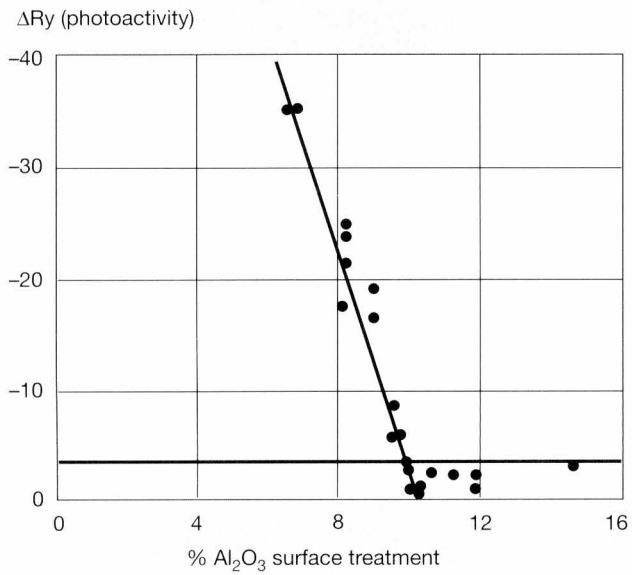

Fig. 7.1
Influence of the amount of inorganic surface treatment on the photoactivity of nano rutile

lead carbonate test [4] for UV-absorbers for cosmetics. It is seen that comparatively high loads of surface treatment are necessary to suppress photoactivity (for information on the test, see chapter 5.4). This is the consequence of the much higher specific surface area of nano titanium dioxide in comparison to titanium dioxide white pigments.

In order to improve dispersibility and compatibility in special systems, nano titanium dioxides, just like TiO_2 pigments, are further treated with organic substances.

7.2 Properties of titanium dioxide nano particles

As described earlier (see chapter 4.4), titanium dioxide with a mean particle size of approximately 0.3 µm (weight average) scatters visible light most efficiently. The scattering power of a single particle largely depends upon its size in relation to the wavelength of the incident light. Figure 7.2 shows calculated remissions of rutile nano particles in a hypothetical formulation with a PVC of 0.5 % and a film

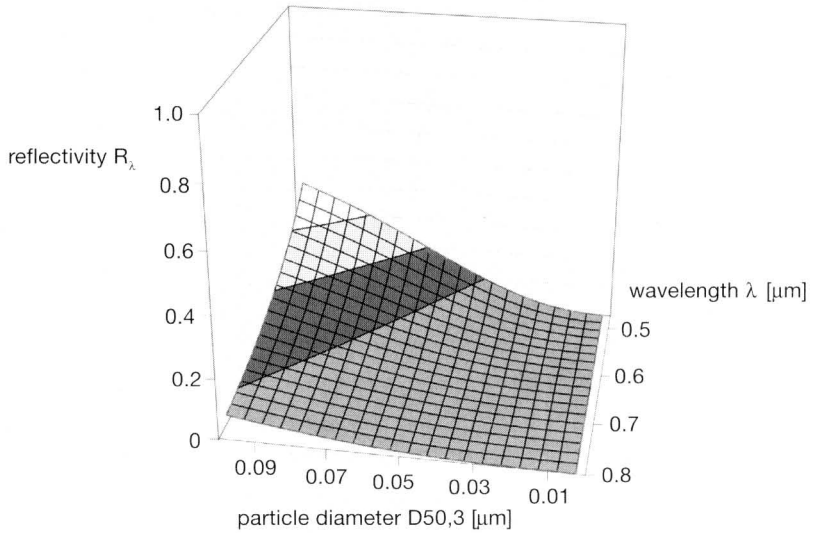

Fig. 7.2
Reflectivity of a coating with a nano rutile, with PVC of 0.5% (for further information, refer to text)

thickness of 50 µm. (Figure 7.2 is the extension of figure 4.12 from chapter 4.4 to smaller particle sizes.)

It is observed that particles with a diameter of approximately 20 nm already have a light scattering effectiveness that cannot be neglected. It is further seen, that light scattering is very wavelength dependent. Titanium dioxide nano particles preferentially scatter the short waved blue light. This serves as the basis for their use as effect pigments (see chapter 7.4).

A general feature of particles is that their specific surface areas grow with decreasing particle size. When the particles actually reach the size of a few nanometers, the large portion of atoms at or close to the surface have an influence on crystal properties. This leads to a short wave shift of the absorption edge.

In the case of colored materials such as cadmium sulfide, this results in a change in color. With titanium dioxide, where both anatase as well as rutile have their absorption edge in the UV-region to start with, the further shift into the UV-range has no color changes as a consequence. Yet, by this phenomenon, a certain plight arises in the relation between transparency and UV-protection. A, by virtue of its small particle size, completely transparent nano titanium dioxide would no longer have the desired UV-absorbing ability in the near UV.

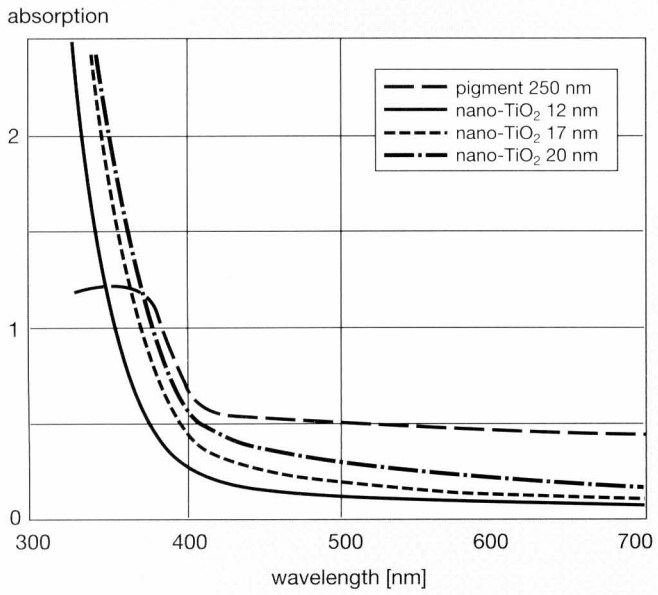

Fig. 7.3
Absorption spectra of nano rutiles with different particle sizes in comparison to titanium dioxide pigments

This is shown in figure 7.3, the UV-Vis spectra of a number of nano rutiles with different sizes. That's why one must compromise regarding transparency.

7.3 Nano titanium dioxides as UV-absorbers

The first generation of nano titanium dioxides consisted mainly of anatases, since these are blessed with a lower refractive index and are therefore per se more transparent. Yet on the other hand, they have the disadvantage of having their absorption edge farther in the UV region and, furthermore, having both lower photostability as well as weather resistance. Since UV-absorbers normally have a protective function, photocatalytic activity is detrimental.

In the meantime, however, nano rutile products are on the market with small particle sizes and a narrow size distribution, combined with acceptable dispersibility, so that they are sufficiently transparent. Nano anatases are therefore only seldomly used today. So consequently, nano rutiles are the UV-absorbers of choice.

In general, one can distinguish between substrate and matrix protection [5].
In the case of substrate protection, the UV-absorber is in a medium that is supposed

to protect the subsurface from UV-irradiation. An example for such a use is a transparent glaze for wood protection. Wood is not only harmed by UV-light, but is already attacked by the adjacent blue part of the spectrum. In the first step, it comes to a yellowing of the wood. Then, with the addition of moisture, the lignin is destroyed and the wood turns gray. The photochemical reactions in the end lead to a complete destruction of the wood, so that the coating can no longer adhere to it.

Naturally, a UV-absorber must be applied in a sufficient concentration in order to perform. If the wood is only stained with a formulation, the nano titanium dioxide particles cannot protect against the harmful UV-radiation. The disadvantage will rather come into effect that the liquid components will flash into the wood, whereas the nano particles will remain dry, and therefore light scattering active, on its surface. This is a common problem when dealing with porous substrates.

An optimal protection is therefore reached when a transparent primer (without nano TiO_2) is applied, followed by a top coat with UV-absorber. Provided a coating has a film thickness of approximately 30 to 40 µm, a nano rutile PVC of 0.3 to 0.5 % is sufficient to ensure UV-stability.

In matrix protection, the nano rutile protects either the resin or other ingredients of the formulation (such as sensitive colored pigments) from photochemically induced decay. For this, however, higher concentrations of nano rutile are necessary. The best results are obtained from PVC levels of 3 % onwards [6].

Organic UV-absorbers [7] like hydroxyphenyl-s-triazine, benzophenone or oxalanilide just begin to absorb light at about 380 nm wavelength, benzotriazole somewhat earlier at about 390 nm. In comparison, nano rutiles offer protection from longer wavelengths on, above 400 nm, by light scattering and, below 400 nm, by UV–light absorption (see figure 7.3). Furthermore, they don't migrate and therefore remain in the materials. In principle, nano rutiles can substitute organic UV-absorbers completely.

In many cases, a combination with organic radical scavengers has, however, proven to be the right choice. Radical scavengers transform free radicals in a material into less reactive radicals. In this context, especially sterically hindered amines (hindered amine light stabilizers; HALS) should be mentioned. HALS are almost exclusively derivatives of 2,2,6,6-tetramethyl pyridine. More information on the mechanism is found in [7].

7.4 Nano titanium dioxides as effect pigments

Until today, two different uses of nano rutiles as effect pigments are known. Both rely upon the selective blue light scattering of nano scaled titanium dioxides.

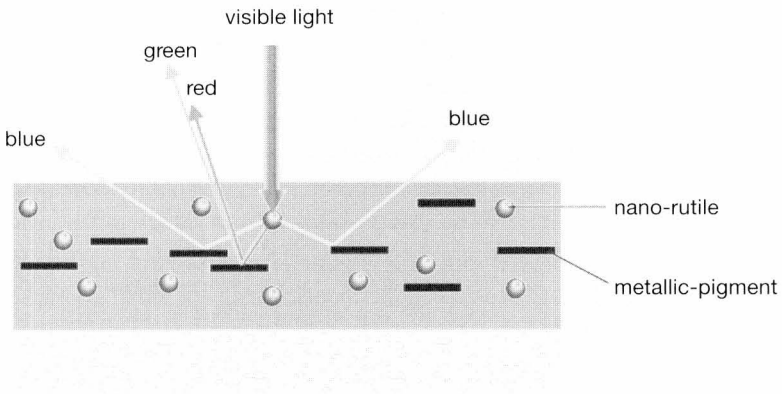

Fig. 7.4
The frost effect (see text)

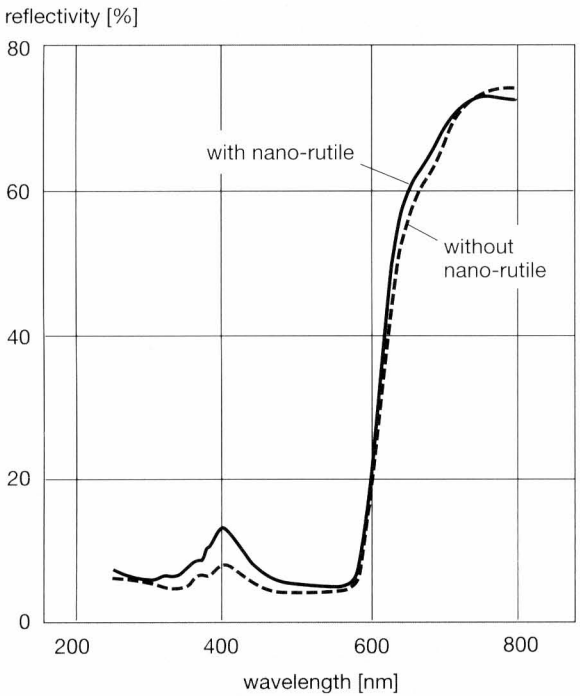

Fig. 7.5
Reflectivities of a quinacridone-pigmented coating (PVC 9.2 %) without and with nano rutile (PVC 7 %)

For the "frost effect" [8], nano rutile is used in metallic base coats. This is topped with the normal clear coats for metallics. When viewing these metallics from a facial angle, the coatings appear with a yellow tint, whereas from a slanting direction, a blue tint becomes visible. Figure 7.4 highlights these relations: the red and green parts of the visible spectrum are hardly scattered by nano rutile and are therefore reflected by the metallic pigments close to the angle of incidence. The blue wavelengths, however, are scattered and then reflected from the paint film at low angles.

This effect is also combined with "transparent", i.e. non-scattering, very fine sized color pigments, and with pearlescent pigments, which has led to a completely new class of effect coatings.

Contrary to this viewing angle dependent color impression, nano rutiles provoke a color shift in colored paints that does not depend upon the direction of observation [9]. In this way, for example, a red color is turned into magenta. With carbon black, a grayish-blue color is reached. Concerning this, figure 7.5 shows the comparison of the remission spectra of a red pigmented coating with and without nano rutile. In the latter case, from the wavelength of 475 nm downwards, an additional remission is found that is responsible for the color shift to magenta.

Since the change in color is not based on light absorption, but added reflection instead, the new color appears comparatively luminescent or brilliant. Due to the lack of lightening power of the nano rutiles, this effect is not comparable to the CBU effect of titanium dioxide pigments (see chapter 4.9).

References

[1] S. Music et al., Materials Science and Engineering B47 (1997) 33

[2] V. Ahmed Yasir, International J. Inorganic Materials 3 (2001) 593

[3] M. Vallet-Regi et al., Solid State Ionics 63-65 (1993) 201

[4] U. Gesenhues, FARBE&LACK 94 (1988) 184

[5] J. Winkler, W.-R. Karl, 23rd FATIPEC Congress, Brussels, (1996), Congress Book, Vol. B, p.195

[6] J. Winkler, B. Proft, FARBE&LACK 107, (2001) 28

[7] S. Zeren, Macromol. Symp. 187 (2002) 343

[8] Patent US 4753829, November 19, 1986

[9] Patent DE 4323372 C1, July 13, 1993

8 Titanium dioxide in catalysis

Only since a relatively short time has titanium dioxide gained some importance in catalysis. It is used either as a catalyst itself, or as a carrier for catalysts. Compared to classical carriers such as aluminum oxide, steatite (magnesium silicate) or cordierite (2 MgO x 2 Al_2O_3 x 5 SiO_2), titanium dioxide has the benefit of being practically insoluble at any pH-value. Another property that is favorable for TiO_2 is that the adsorption of sulfate ions or the reaction to a sulfate, respectively, is reversible at temperatures of approximately 500 °C. Opposed to this is the disadvantage of a mostly smaller specific surface area.

Generally, in the field of catalysis, heterogeneous and homogeneous catalysts are distinguished. In homogeneous catalysis, the catalyst itself is dissolved in the reaction medium, whereas in heterogeneous catalysis, the catalyst is present as a solid, separate phase during the reaction.

The element titanium plays an important role in homogeneous catalysis as a component of the "Ziegler-Natta" catalysts. These consist of mixtures of titanium tetrachloride or titanium trichloride and aluminum alkyl chlorides [1]. They catalyze the polymerization of alkenes, such as ethene, to polyethylene and are useful for achieving a certain tacticity[1], for example in the reaction of propene to polypropylene or of vinyls to polyvinyl polymers.

Titanium dioxide itself is always a heterogeneous catalyst. The advantage of heterogeneous catalysts is that they can be removed from the reaction mixture after the reaction is completed. Their disadvantage is that *they may have to be* taken out of the mixture afterwards. For use in gas phase reactions, titanium dioxide has to be immobilized in some way.

Anatase is definitely preferred in catalysis over of rutile [2]. No application of rutile as a catalyst is known to the author, although there are some investigations in which rutiles gave similar results to anatase [3]. Although rutile photocatalysts can be imagined, anatase has advantages in this field, also. Titanium dioxide *pigments* are absolutely useless as catalysts.

From all this, it can be concluded that no serviceable products for heterogeneous catalysis are generated from the chloride process of TiO_2 pigment manufacturing.

1 From Greek: taxis = arrangement. The word tacticity describes the regularity with which monomers are built into a polymer chain with regard to "head-tail" arrangement and stereoregularity.

Only the sulfate process generates intermediates that, when correctly handled, can lead to qualified materials for this type of catalysis. Normally, the metatitanic acid from the hydrolysis of anatase (approximate composition $TiO(OH)_2$) is used as the starting material. Typical steps in catalyst production involve rinsing, doping with other elements, calcining or hydrothermal treatment, depending upon the particular field of use.

For gas phase reactions, titanium dioxide must be brought into the form of stabile, ceramic bricks. This is usually accomplished by adding binders, such as aluminum oxide or silicium dioxide, in the ceramic's production prior to calcining. Lately, pure TiO_2 ceramics are also commercially available [4].

The general catalytic properties of titanium dioxide are versatile. First, titanium dioxide with surface bound phosphate [15, 16] or sulfate [17] act as solid acids and can catalyze reactions that are facilitated in the presence of acids. Examples for such reactions are the formation of esters, amides and transamidation reactions.

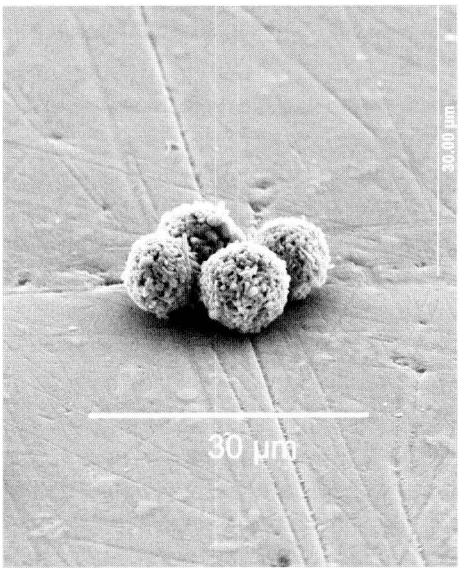

Fig. 8.1
Titanium dioxide catalyst particles with wide pores (2000 Å pore diameter)

Compared with zeolites that are also used as "solid acids", titanium dioxides have the advantage that they can be obtained with larger pore volumes, into which larger reactants can migrate. Figure 8.1 is a scanning electron microscopic picture of such a material.

Second, titanium dioxides are suitable as oxidation catalysts as well as catalysts for comproportio-nation reactions. The use of titanium dioxide as a rearrangement catalyst in the production of camphor has been known for a long time [12]. In addition, titanium dioxide is a main component of catalysts for the purification of diesel engine exhausts from non-combusted fuel. In this application, it has the further function of reducing the emission of nitrogen oxides. Table 8.1 gives an overview of some applications of titanium dioxide in catalysis.

Finally, the photoactivity of titanium dioxide is the starting point for a number of research activities which have the goal to clean surfaces from dirt, to avoid the condensation of moisture in the form of droplets onto surfaces, to clean water, to

Reaction	Usage	Literature	Typical catalyst composition (active component)
Comproportionation	Denitrification of off gases of incinerators		TiO_2/V_2O_5
	Denitrification of diesel engine tail gases		TiO_2/Rh/Pt/Pd
Selective oxidation	Conversion of benzene to maleic acid anhydride	[5]	TiO_2/V_2O_5
	Conversion of butadiene to maleic acid anhydride	[6]	TiO_2/V_2O_5
	Conversion of butene to acetic acid and acetaldehyde	[7]	TiO_2/V_2O_5
	Conversion of methanol to formaldehyde	[8]	TiO_2/V_2O_5
	Conversion of o-xylene to phthalic acid anhydride	[9]	TiO_2/V_2O_5
	Conversion of 3-methyl pyridine to 3-carboxy pyridine		TiO_2/V_2O_5
	Conversion of CO to CO_2	[10]	TiO_2/Pt; TiO_2/Ru
	Conversion of H_2S to sulfur	[10]	TiO_2/MoO_3
Epoxidizing	Conversion of propene to propane oxide		TiO_2/Ag
Hydrogenation	Carbon liquifaction	[11]	TiO_2/MoO_3
	Conversion of thiophene to H_2S and butane	[10]	
Isomerization	Conversion of alpha-pinene to camphene	[12]	TiO_2
	Conversion of butane to isobutane	[13]	TiO_2
Aldole reaction	Reaction of acetaldehyde to 2-butenaldehyde	[14]	TiO_2

Table 8.1
Uses of titanium dioxide in catalysis

kill bacteria or even to remedy tumors specifically. That the potential for titanium dioxide in catalysis is only now beginning to be explored is probably due to the fact that the TiO_2 pigment producers, who have access to the chemical precursors, have not invested too much research and development efforts into this field as yet.

Of the applications presented in table 8.1, only the DeNOx and the diesel exhaust gas purification are of commercial relevance today. Therefore, the discussion will be limited to these and photocatalysis, as the use with the probably next highest economical potential.

8.1 DeNOx catalysts

Titanium dioxide is the active component in so called DeNOx catalysts for the reduction of different nitrogen oxides (NO_x) in the tail gases of power plants and incinerators.

The precursor in the manufacturing of these catalysts is the hydrolysate of anatase from the sulfate process. Its surface is impregnated with vanadium pentoxide and/ or tungsten trioxide as further active components, and then, ceramic honeycomb catalysts are manufactured. With these SCR catalysts (selective catalytic reduction), the reduction of nitrogen oxides to molecular nitrogen takes place in a comproportionation reaction with ammonia or urea, respectively, that is fed into the offgas stream.

A typical reaction scheme would be:

$$N_2O_3 + 2\,NH_3 \longrightarrow 2\,N_2 + 3\,H_2O$$

Common conversions reach values of about 90 %. Working temperatures are between 120 °C [18] and 500 °C. Typical lifetimes are a number of years. The spent catalysts are brought to landfill, although it would be ecologically better to either recycle them [19], or make use of them in blast furnaces to regenerate the insulating fire bricks [20].

Since SO_2 is always present in the tail gases, the conversion of SO_2 to SO_3 plays a role. SO_3 can form ammonium sulfate with vapor and ammonia, which then settles on the catalyst's surface and deactivates it. That's why the gases are often prepared by alkaline gas scrubbing first.

8.2 Diesel catalysts

Diesel engines are run with a lean mixture, that is with an oxygen surplus. This leads to a more complete combustion of the propellant and thus to about 30 % higher energy efficiency, when compared to Otto engines. Under these circumstances, contrary to Otto motors, only little CO and hydrocarbons are found in the exhaust, but instead more nitrogen oxides (mainly NO) as a result of the reaction of N_2 with O_2 – both coming from the air. Simultaneously, SO_2 is in the vehicle tail gas, which would deactivate catalysts based only on Al_2O_3 irreversibly in no time.

Momentarily, commercially available diesel catalysts for car engines consist of cordierite ceramics (see figure 8.2) that are treated with a so called "wash coat" [21]. These are 25 to 50 µm thick layers of a temperature stable Al_2O_3 and further

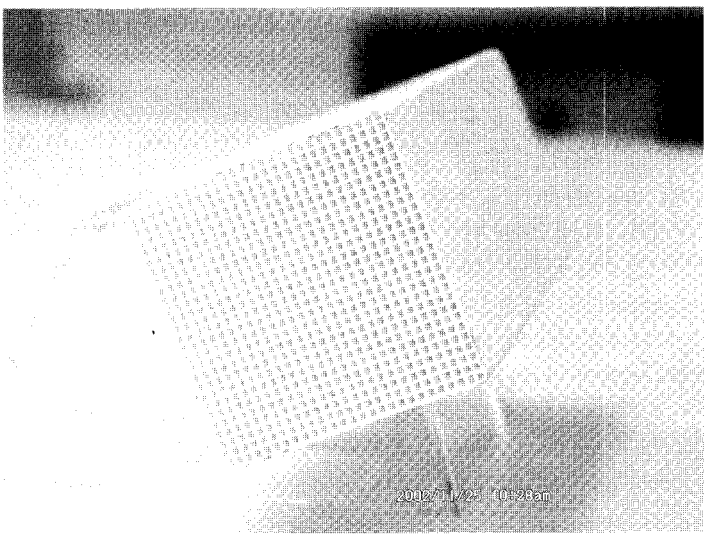

Fig. 8.2
Cordierite honeycomb catalyst support

oxides, as well as 0.1 to 0.15% of the noble metals platinum, palladium and/or rhodium.

For catalysts that contain titanium dioxide, tungsten impregnated anatase is used. The tungsten trioxide prevents sintering that would otherwise take place at the working temperature of the catalyst. Since the year 2000, a product is also on the market that is sufficiently temperature stable even without tungsten.

Contrary to the DeNOx process, no reducing agent is additionally incorporated to react with the NO_x, though. Instead, simultaneously emerging CO and any non-combusted hydrocarbons are utilized as reduction agents ("three way catalysts"). In the operation of these, the air to fuel ratio is preset in such a way that exactly enough CO and hydrocarbons are present in the exhaust gas, so that the NO_x can be reduced (almost) quantitatively.

An optimized process consists of alternately running the engine with a surplus of oxygen (for better fuel utilization), followed by a cycle run with a lack of oxygen (for NO_x reduction). In this case, the NO_x has to be stored intermediately, which works well with barium carbonate [21] or with barium oxide, on which it adsorbs, but especially well with Pt-Rh/TiO_2/Al_2O_3 catalysts [22]. These have the advantage of far better rigidity against sulfur oxides, compared to the catalysts containing barium.

8.3 Titanium dioxide in photocatalysis

In the preceeding chapter 5, the reasons for the photoactivity of titanium dioxide were already explained and also, which measures are taken to reduce the photoactivity of titanium dioxide pigments.

In order to use titanium dioxide as a photocatalyst, however, naturally every measure should be avoided that suppresses its photoactivity. For that reason pure anatase without any lattice doping or inorganic surface treatment is normally used.

Like in other catalytic applications, the surface area which is available for reactions plays a part in photocatalysis also. Furthermore, the supply of photons must be guaranteed. On the other hand, the catalyst must be immobilized (in gas phase reactions) or be removable (in liquid reactions).

When immobilizing the catalyst, care must be taken that the catalyst surface is not shielded by the embedding medium. In principle, the following possibilities exist:

- The catalyst is employed as a ceramic body. Favorable is the high resistance to wear in combination with an only small pressure drop in the gas stream. Less favorable is the low specific surface area and the limited supply of photons.
- Embedding of the catalyst in a polymer. In this case, as little amount of polymer as possible should be used, since otherwise the catalyst surface would not be available. The polymer itself is inevitably degraded. Even poorly degradable polymers like polytetrafluorethylene or polyvinylidenefluoride are attacked and are more or less sacrificed in the course of time. Apart from that, all the limitations already listed for ceramic bodies apply.
- Adsorption of the catalyst to a carrier. Here, the application of titanium dioxide particles on fiber glass is worth mentioning. Beneficial in this case is the relatively high catalyst surface achievable and the unhindered light access. Detrimental is that high flow rates of gas may not be possible, due to low mechanical stability, even if photocatalysis normally doesn't proceed so fast that that might play an important role.

The utilization of titanium dioxide as a photocatalyst for "self-cleaning surfaces" finds widespread interest. With the help of inorganic binders such as water glass (Na_2SiO_3), coatings can be formulated [23] that degrade dirt (including fouling) with the help of UV-light. (In the widest sense, dirt is a matter at a place, where it's not supposed to be.) The role of the photocatalyst is to decompose organic components, such as fats, that allow the dirt to cling to surfaces in the first place. Inorganic material is not attacked by titanium dioxide.

Less favorable for such coatings is their lack of gloss, which derives from the high loading of the photocatalyst and, furthermore, their relatively low mechanical stability, which also has to do with the high concentration.

Especially for self-cleaning surfaces, the covering of substrates with titanium dioxide from titanium dioxide sols may play an important role [24]. Titania sols consist of colloidal solutions of nano crystalline titanium dioxide particles. They may be applied to surfaces where, after drying – and maybe heating – a photocatalytically active film remains that, under certain conditions, exhibits "superhydrophilicity" [25].

On superhydrophilic surfaces, the free surface energy of the layer is so high that water does not condense in the form of droplets, but spreads instead (see chapter 6.2). It is assumed [25] that this superhydrophilicity is due to a loss of oxygen atoms at the surface of the TiO_2 film upon irradiation with UV-light. The effect remains for a longer period of time – even in the dark – if water attracting substances like silica are added.

One commercial use for such sols is the treatment of automobile rear view mirrors for the outside that then do not fog (or are not supposed to fog). Such titania layers are in principle able to prevent fouling of outdoor (and indoor) construction parts by algae, tresses and fungi. One might consider facades and roofs in this context. A condition for a long lasting protection is, however, also in this case a mechanically stabile and durable film. Much development work is being invested in trying to find connecting layers, such as silanes, that assist in meeting these demands.

In sanitary ceramics, coatings with titanium dioxide photocatalysts have antimicrobial properties. Titanium dioxide photocatalysts are definitely bactericidal [26, 27].

As far as the utilization of photocatalysis is concerned, there seems to be no limit to imagination. From Japan comes the idea to coat houses with titanium dioxide in order to improve the quality of the air [28]. In the opinion of the author, though, this approach doesn't seem all too promising in view of the relation of the amount of air to the available surface area. (It's difficult to sanitize nature.)

Considerable efforts were already made to photocatalytically mineralize (to turn into CO_2 and H_2O) pollutants in waste waters. In general, it shows that the photocatalytic activities of different titanium dioxides vary from case to case. This suggests that every problem calls for a specific catalyst for optimum results. According to findings in our own house (Sachtleben, Duisburg, Germany), the rate of photocatalytic degradation is limited by the rates of adsorption and desorption. Because in order to be mineralized, a molecule must first adsorb to the catalyst's surface. If the pollutant is too well soluble in water, or if it is even ionic

with the same sign of charge as the catalyst (see chapter 6.4.2), then it won't go there. Furthermore, if the degradation of the molecule proceeds via ionic intermediate stages, then it is desorbed instead of being further desintegrated.

In both cases, it is possible to influence the charge of the catalyst by pH adjustment. Yet, this leads to an increased salt freight in the purified water, which cannot be tolerated in all cases.

Photocatalytic processes can be powered by sunlight, but for example, in order to treat a waste water, a sufficiently large area has to be available to install a trickling reactor [29]. There, the polluted water flows as a film over slanted catalyst surfaces that are exposed to sunlight. Even in dull weather, there is enough UV-light to let the process take place.

Photocatalysis using natural light is more economical than the use of artificial irradiation. Especially for kinetically slow degradation reactions, the use of UV-lamps soon becomes inefficient and is only justified if alternative methods fail.

In suspension reactors, in which the photocatalyst (as the name says) is present as a suspension of small particles, there is a need to separate the catalyst later on. If this is done by filtration, then further costs are generated. Therefore, it would generally be preferable to run the reactors with immobilized catalysts.

Although the quantum yield – defined as the quotient between the degradation rate of the pollutant and the photon flux, both expressed in *moles per liter and second* – can reach almost 100 %, this is true only for low photon fluxes [30]. This is probably the consequence of a diffusion controlled reaction.

Halogenated hydrocarbons and other halogenated species like, for example, insecticides, that often present an ecological problem, are unfortunately not easily attacked photocatalytically. Quantum yields between 0.3 and 4 % were measured here [31].

In an overview article [32] with 414 (!) literature citations, many specific examples of photocatalytic purification of waste waters with TiO_2 are described. And yet, until today, photocatalytic processing of effluents or service waters has not achieved a breakthrough. Actually, alternative methods, like the adsorption on to charcoal that is later incinerated or brought to landfill, have an economical advantage, at least as long as no legal requirements make these less attractive.

Likewise, efforts to utilize the photoactivity of titanium dioxide for chemical synthesis are still in an experimental stage. Some examples of reactions that can be performed are the generation of methanol from CO_2 and water, the cyclization of dicarboxylic acids, hydrozones and 1,5 diamino pimelic acid as well as the hydroalkylation of olefins [34, 35]. Also known are the synthesis of amino acids from CH_4, N_2 and water [36] and the formation of peptides from glycine [37].

Titanium dioxide photocatalysts also attack cultivated tumor cells [33, 34]. It is still being exploited if this effect can be used to fight tumors in living organisms also by bringing it in contact with the tumor and irradiating it with UV-light by an optical fiber. There is evidence that the photo-genotoxicity of TiO_2 is based on DNA destruction and thereby chromosome aberration, and not on it causing genetic defects. It is helpful for these uses that titanium dioxide for itself is an nonpoisonous substance that leaves no damage to an organism even when swallowed [38] or brought under the skin [39] (see chapter 2.3).

References

[1] B. Vollmert, Grundriss der Makromolekularen Chemie, E. Vollmert Verlag, Karlsruhe (1979), Vol. I, p. 221

[2] K. I. Hadjiivanov, D. G. Klissurski, Chem. Soc. Rev. 25 (1996) 61

[3] P. Härter, H.-J. Eberle, Bayerischer Forschungsverbund Katalyse (FORKAT II), 2. Statusbericht zum Teilprojekt A4, April 1999 to March 2000); p. 31

[4] www.sachtleben.de

[5] Y. Murakami et al., Proc. 7th Int. Cong. Catalysis, Tokyo (1980), B (1981) 1344

[6] G. C. Bond et al., J. Catalysis 57 (1979) 476

[7] W. E. Slinkard, P. B. Degroot, J. Catalysis 68 (1981) 423

[8] F. Roozeboom et al., J. Catalysis 68 (1981) 464

[9] D. Vanhove, M. Blanchard, J. Catalysis 36 (1975) 6

[10] S. Matsuda, A. Kato, Applied Catalysis 8 (1983) 149

[11] K. Tanabe, H. Hattori, Energy Shigen (Rexsourdes), 2 (1981) 570

[12] R. Onoshi et al. Z. Phys. Chem. Neue Folge 130 (1982) 205

[13] H. Hattari et al., Applied Catalysis 50 (1989) L11

[14] Patent US 4316990

[15] A. Krzywicki, M. Marczewski, J. Chem. Soc. Faraday Trans. 1: 16 (1980) 1311

[16] G. Busca, G. Ramis et al., Langmuir 5 (1989) 911 and Langmuir 5 (1989) 917

[17] T. Jin et al. J. Phys. Chem. 90 (1986) 4794

[18] P. G. Smirniotis et al., Angew. Chem. 113, No. 13 (2001) 2537

[19] M. Foguennes et al. Trans. Instn. Min. Metall., Sect. C: Minerals Process. Extr. Metall. 106, Jan.-Apr. (1997) C9

[20] Patent DE 44 37 548 C1, October 20, 1944

[21] M. Jacoby, C&EN, January 25 (1999) 36

[22] H. Y. Huang et al., Applied Catalysis B: Environmental 33 (2001) 127

[23] J. Winkler, Macromolecular Symposia, 187 (2002), 317

[24] A. Fujishima, K. Hashimoto, T. Watanabe, "TiO_2 Photocatalysis", Bkc Inc., Tokyo, 1999, p. 130

[25] like [24], p. 66-73

[26] C. Wei et al., Environ. Sci. Technol. 28 (1994) 934

[27] H. N. Pham et al., J. Environ. Sci. Health A30 (3) (1995) 627

[28] like [24], p. 99-101

[29] D. W. Bahnemann et al., Solar Energy, Vol. 56, No. 5 (1996) 455

[30] D. W. Bahnemann et al., "Solar Engineering", W. B. Stine, T. Tanake, D. E. Claridge Editors, Book No. H0932A (1995) 399

[31] D. W. Bahnemann et al., Lecture held at the international Conference: "Oxidation Technologies for Water and Wastewater Treatment", Goslar, May 12–15, (1996)

[32] M. R. Hoffmann, D. W. Bahnemann et al., Chemical Reviews, 95, No. 1 (1995) 69

[33] H. Yamashita et al., Catalysis Today 45 (1998) 221

[34] H. Kisch, W. Lindner, Chemie in unserer Zeit, 35 (2001) 250

[35] H. Kisch, "Advances in Photochemistry", Volume 26, D.C. Neckers, G. v. Bünau, W. S. Jenks Ed., J. Wiley & Sons, 2001, p. 93

[36] H. Reiche, A. J. Bard, J. Am. Chem. Soc. 101 (1979) 3127

[37] J. Onoe, T. Kawai, S. Kawai, Chem. Lett. (1985) 1667

[38] R. Cai et al. Cancer Res. 52 (1992) 2346

[39] Y. Kubota et al., Br. J. Cancer 70 (1994) 1107

[40] B. K. Bernard et al., J. Toxicol. Environ. Health 28 (1989) 415

[41] F. Bischoff, G. Bryson, Res. Commun. Chem. Pathol. Pharmacol. 38 (1982) 279

9 Titanium dioxide in photovoltaic cells

Solar cells convert the energy of light into electrical energy. State of the art silicium cells have, depending upon their design, an efficiency (the relation between delivered electrical power and the power of the incident light; physical dimension of both: Watt) of 10 to 22 %, in general about 15 %. The construction of silicium solar cells is, however, somewhat expensive because of the high purity of the silicium necessary, which is ensured by zone refining. In this process, the silicium raw crystal is drawn as a strand through a zone oven. The impurities collect in the melted front and are discarded before the purified material is processed.

The so called "energetic payback time", that is the time in operation that a solar cell needs in order to regenerate the energy that was necessary for its production, is about seven years.

High hopes were therefore laid into inexpensive solar cells that were first introduced by Grätzel (ETH Lausanne, Switzerland) [1]. They were supposed to cost only one tenth of the silicium based solar cells at a comparable performance.

Their construction principle is shown in figure 9.1. The minus electrode consists of fluorine-doped tin dioxide on which a layer of TiO_2 nano particles is sintered. This porous, approximately 10 µm thick layer has a internal surface of about a thousand times higher than the projected surface area of the electrode. The titanium dioxide is covered with a dye whose highest occupied molecular orbital (HOMO) lies at a lower energy level than the conduction band of the TiO_2, whereas its

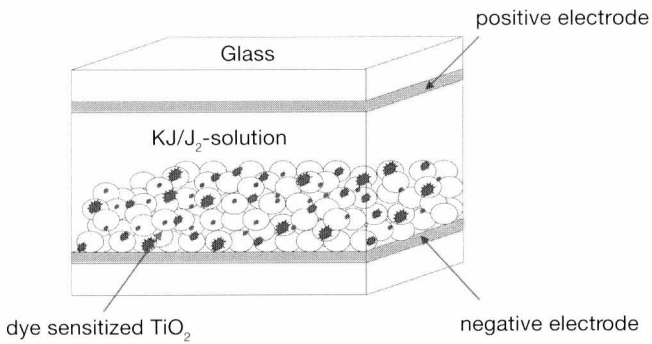

Fig. 9.1
Principle construction of a Grätzel cell

lowest unoccupied molecular orbital (LUMO) lies higher. Next comes an iodine/potassium iodide solution. The transparent positive electrode that is applied to glass also consists of fluorine-doped tin dioxide, but it is metallized by a small amount of platinum.

Figure 9.2 shows the redox reactions that occur when the cell is operated. The light enters the cell through the positive electrode. The working principle is not based upon the generation of excitons in the titanium dioxide, as one might first assume, but rather on the transfer of an electron from the HOMO of the dye to the

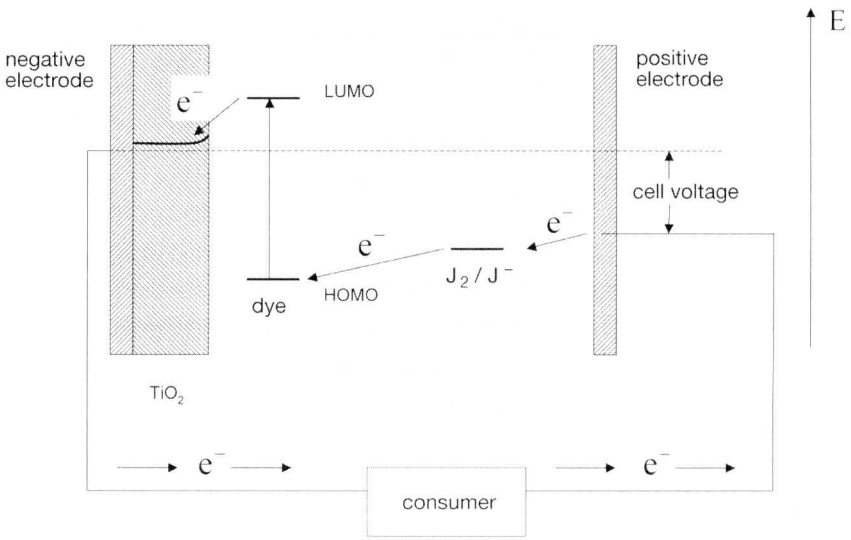

Fig. 9.2
Redox reactions taking place in a Grätzel cell

LUMO. Since the dye is adsorbed on the TiO_2, the electron can pass over into the conduction band of the TiO_2 and, from there, flow to the fluorine-doped tin dioxide layer of the minus electrode.

The electron travels through an external consumer ("sink") in the circuit to the positive electrode, where tri-iodide ions (J_3^-) are reduced to three iodide ions ($3J^-$) by the uptake of two electrons. The iodide ions finally pass their electrons on to the dye molecules, thereby compensating the charges that were lost by them in the initial reaction. Thus, the electric circuit is closed.

Useful dyes are complexes of ruthenium and osmium with 2,2'-bipyridine [3]. Although naturally occurring dyes, such as chlorophyll or the dye of blackberries, can be used, they are less stable. The durability of the dye is however crucial with

regard to the service life of "Grätzel cells". If an operation term of twenty years is aspired, then approximately one hundred million redox transactions would have to be endured. The technical limit today is about half of that amount.

A further, material related problem arises from the corrosiveness of the electrolyte solution that makes a long termed hermetic sealing of cells difficult. One way to solve the problem would be to find a substitute for the electrolyte solution [4, 5].

Still, research is optimistic in this area and hopefully, the next decade will bring a breakthrough in the design of photovoltaic cells based on that principle.

References

[1] B. O'Regan, M. Grätzel, Nature 353 (1991) 737

[2] A. Kay, M. Grätzel, J. Phys. Chem. 97 (1993) 6272

[3] W. Kaim et al., Chemie in unserer Zeit 21, No. 2 (1987) 50

[4] M. Thelakkat, C. Schmitz, H.-W. Schmidt, Adv. Mater. 14, No. 8 (2002) 577

[5] O. A Ileperuma, M. A. K. L. Dissanayake, S. Somasundaram, Electrochimica Acta, 47 (2002) 2801

Index

B

C

D

I

K

L

M

N

Dr. Jochen Winkler studied chemistry at the University of Stuttgart. From 1980 to 1985 he worked with the German Paint Research Institute „Forschungsinstitut für Pigmente und Lacke“ in Stuttgart, where he studied pigment flocculation and performed work on the energy balancing of dispersion equipment. Since 1985 he is with Sachtleben Chemie in Duisburg, Germany, where he is currently responsible for Research and Development.

ISBN 3-87870-148-9

VINCENTZ
Providing Professional Information